Altair Engineering

Light Truck Frame Joint Stiffness Study

July 25, 2001

Altair Report No.:   A/SP-005-1

Prepared For:

Auto/Steel Partnership

2000 Town Center, Suite 320

Southfield, MI 48075-1123

Prepared By:

Katy Lewis, Project Engineer
Christian Spencer, Project Engineer
Michael White, Engineering Manager

PREFACE

The Light Truck Frame Project Group entrusted Altair Engineering Inc. to conduct the Light Truck Frame Joint Stiffness Study. This report comprises the results of Phase 1, the modeling and testing of five joints typically used in light truck frames. Subsequent, similar phases to study additional frame joints are planned by the Light Truck Frame Project Group. The study results are presented in two documents. This document describes the study and its results. The other document, an Excel Spreadsheet, is an interactive tool that frame designers may use to determine the stiffness for variations of the five joints in Phase 1. This tool will help designers reduce the weight of light truck frames.

EXECUTIVE SUMMARY

Background

There is little published information available to frame designers on the relative stiffness of the joints in a light truck frame. A survey of current production frames found that most frames used joint styles from a group of approximately 15 joints. Many joints had obvious packaging or manufacturing-driven constraints, but the relative merits of each joint type is not well documented or available in a form useful for frame designers. The A/SP Light Truck Frame committee felt that a study to determine relative stiffness of the joints, along with a tool to communicate the results of the study to frame designers, would allow better decisions to be made at the concept design phase and would facilitate lighter weight frame design.

Project Goals

The goal of this program is to provide the frame designers with data and tools to facilitate early concept choices for frame joints that promote more efficient, and lighter weight steel designs. The Frame Joint Toolbox resulting from this program takes the form of an interactive worksheet a designer can use to investigate the choices of different joint designs, and varying parameters within a design.

In order to achieve the goal, the scope of the project involves the following steps:

- Research and organize existing information available on joint stiffness
- Develop methods to characterize joint stiffness and evaluate analytically using finite element analysis
- Perform physical tests on multiple (three) samples of five joint types
- Correlate the physical testing and finite element analysis
- Evaluate the sensitivity of the joint stiffness to the various joint parameters
- Create the Frame Joint Toolbox that incorporate design rules and the sensitivity analysis

Project Results

Based on the literature search, and newly developed methods, a process was developed to evaluate the stiffness of a side rail to crossmember joint, and an interactive Frame Joint Toolbox was developed to document the program results, and provide a mechanism for frame designers to utilize the data in the design process. The joint stiffnesses varied from 0.116 KNm/deg to 50.429 KNm/deg and the mass of the joints ranged from 4.68 kg to 7.01kg. The Toolbox is based on an interactive spreadsheet. The spreadsheet allows the designer or engineer to modify the geometric and gage properties of the joint members, and calculates joint stiffness and relative mass based on the new properties.

ACKNOWLEDGEMENTS

TABLE OF CONTENTS

INTRODUCTION

Currently, there is no standardized reference manual or process for frame designers to employ when developing new frame architecture. At the request of the Auto Steel Partnership, Altair Engineering Inc. has performed a literature search, finite element analysis, physical joint testing, and sensitivity analysis of five common crossmember to side rail joints in order to provide designers with a "Joint Stiffness Toolbox." The purpose of this report is to present the results of Altair's research and analysis and provide design rules and guidelines for joint stiffness, which will help designers implement robust, yet lightweight, frame designs.

LITERATURE SEARCH

Introduction

A literature search was performed to identify previous published papers on testing, finite element analysis and design guidelines for steel joints. The research is summarized below. Abstracts of the 43 articles that we identified as relevant and read, along with 12 additional articles that we judged not relevant and did not pursue, are included in the appendix.

Two papers contained information on light truck frames and frame stiffness. The articles were written on a van frame structural evaluation (Hull, 1979) and an idealized truck frame design (Michejda, 1971). Both articles mentioned joint stiffness but provided very little detailed information about joint design or analysis. Much of the available automotive research focused on body joint design. There were many papers on welded joints used in construction trusses and offshore oil platforms (tube through tube joints) which provided valuable information on joint measurement and test fixtures.

Defining the Joint

Studies from civil engineering structures focused extensively on structural (non-automotive) frames and joint stiffness and stress testing. These studies, however, included pertinent information regarding specimen size, constraints, loading and instrumentation. The length of the structure surrounding the joint interface should be sufficiently long to minimize the influence of the end conditions (Chiew, 1996), and sufficiently small to keep the surrounding structure from affecting the stiffness. The joint dimensions we used were based on the work of Rao et. al. 1983 and adhered to the following guidelines:

- The test joints contained a finite amount of surrounding structure
- All unique characteristics of the joints were included (i.e. local reinforcements, extended flanges, access and lighting holes)
- Inclusion of surrounding structure was minimized to prevent joint stiffness value contamination
- Standard dimensions containing identical amounts of structure were used, when possible, for comparison across joint types
- Joint samples were removed from the frame structure to isolate their performance. To facilitate testing, joint boundaries were developed in the plane of the cross section of the crossmember and rail
- Load and support plates were welded to the ends of the joint specimen for load application and restraint

Our test samples adhered to the guidelines in the following manner:

- Joints were tested to evaluate the optimum length to incorporate the unique characteristics of the joint
- We established boundaries 150mm from the joint interface to be used in all joint samples
- The joints were removed from the surrounding frame structure at the established boundaries
- ¾-inch end plates were welded to the joint for the constraining and load application fixture

LITERATURE SEARCH

Testing

The joint testing literature we reviewed was composed of fixturing, setup, instrumentation and test methods. Because we were looking to evaluate the stiffness of the joint type, for a comparison to other types, the fixturing and testing methods were critical to adequately evaluate the joint stiffness. In the literature search, the following testing methods were noted:

- The test fixture (rig) is designed to ensure that the deflection of the rig is an order of magnitude lower than that of the specimen (Yeoh S-k et al., 1995)
- When setting up the joints for testing, the specimen should be first subjected to an incremental static load (Yeoh, 1995). Shanmugam, 1995, specifies that pre-load should be 5% of the expected ultimate load to help remove residual stresses and ensure the rigidity of the test fixture.
- The end loading conditions, either bolted to a bedplate via an end plate welded to the flange beam (Korol et al, 1977) or simply supported (Shanmugam et al, 1995), were based on the joint configuration and loading
- The load should be applied "in increments of about 10% of the expected branch member's working capacity" (Koral, 1979)

Different loading techniques were investigated due to the geometric variance of the structure surrounding the joints. These geometric variations in the joints include height and section changes in the side rail and crossmember. Superposition versus direct loading was considered as an option to remove unwanted additional loads due to height variation inducing a moment in the joint. Yeoh et al., 1996, reported good correlation between test and analysis with this comparison, where the two different loads were applied at the same time and then individually and the results combined. Another method for removing the induced moment was found by applying the load at the shear center of the crossmember.

Instrumentation of the joint deflection was consistent throughout the researched papers, focusing on obtaining comprehensive information relating to joint deformation. Tests involved the use of dial indicators, including redundant measurement devices on the joint to evaluate non-linearity in the deflection (Korol et al., 1977). Another measurement set-up allowed both the rotation of the crossmember to side rail interface as a whole, and the contributions of the individual components to be obtained (Bernuzzi et al., 1996). Overall, although the experimentation reviewed in literature pertained mostly to large building type frame joints, the methods could still be applied in the evaluation of smaller-scale truck frames because the same static analysis principles are present.

Finite Element Analysis

The finite element modeling technique was researched based on model element types, constraints, and assumptions. Different modeling techniques have been applied with good success. Van Wingerde, 1992, modeled the weld with "solid elements to allow for a clear definition of the weld toe." This was done because "simple FE models without modeling of the corner radii and weld that might be used for the analysis of the static behavior of the joints will not be satisfactory for fatigue analysis"(van Wingerde, 1992). In van Wingerde's analysis, "all FE analyses carried out are linear elastic."

Another area of focus in the analysis is spot weld modeling. Garro et al., 1986, "simulated spot welds by beam elements having a section equal to the width of one of the spots and a length equal to the distance between the mean surfaces of the two welded plate edges." In all of the research papers, the member sections were simulated with shell elements.

LITERATURE SEARCH

Joint Stiffness

The research evaluation of joint stiffness and rotation focused on the definition of joint stiffness and where to calculate it. Different methods of measuring stiffness were employed based on where and how to measure the deflection in order to calculate the rotation. Liew defined their method to measure the rotation based on the "deformation of the connection elements, not deformation of the column and beam members" (Liew et al. 1997). Some assumptions were made analyzing the joints and calculating stiffness: the material is linear elastic, in-plane deformations are negligible, and the deformations are small and mainly due to bending. With these assumptions, the stiffness is calculated as $K=M/\theta$. The rotation θ and applied moment M are based on the instantaneous center of rotation (Rao et. al, 1983).

For the sensitivity study of the joint, the joint parameters, member thickness and shape are varied to measure how sensitive the joint is to a particular parameter. Although actual stiffness prediction experiments were not found in the literature, relevant information was found regarding stress concentration factors (SCF). "From the raw SCF numerical values, parametric equations were obtained at the six critical locations for the three load cases under consideration. The parametric equations were obtained using MATLAB, which is capable of performing a non-linear data fitting by using different least square methods" (Chiew et al.,1996). For the stiffness analysis, a similar technique of finding the critical locations can be used for data fitting parametric equations to the joint stiffness. The parametric equation for the joint sensitivity can also be calculated analytically through a design of experiments.

Lessons Learned

Joint Definition:

- The length of the structure surrounding the joint interface should be sufficiently long to minimize the influence of the end conditions (Chiew, 1996)
- Joints should contain all the unique characteristics (i.e. local reinforcements, extended flanges, access and lightening holes), minimize the inclusion of surround structure, and have boundaries defined in plane of the crosssection of the beam member (Rao et al., 1983)
- The joint stiffness has a large effect on system dynamic performance (offshore platform) (Chen & Zhang, 1996). Joints must be well discretized to measure the stiffness using dynamic methods (Becker et al., 1999)
- Joint stiffness has a greater effect on system stiffness when the joint stiffness is decreased than when it is increased, suggesting that current body joints are designed near a "threshold" value (Chen, 1998)

Fixture/Test Setup:

- Designing the rig's stiffness to ensure that the deflection of the rig when the specimen is loaded is an order of magnitude lower than that of the specimen (Yeoh S-k et al. 1995)
- Bolt torque and weld quality are critical in measuring maximum capacity of the joint (Davison et al., 1987)

Test Procedure and Load Cases:

- The specimen should first be subjected to an incremental static loading on one axis, and the strains checked for linearity and zero drift to indicate shake-down of residual stresses (Yeoh et al., 1995)

Measurements:

- To evaluate the initial stiffness of the connection, the following assumptions are made: the material is linear elastic, the deformations are small and mainly due to bending and in-plane deformations are negligible (Korol et al., 1996)
- Measurement should be set up allowing for both the rotations of the connections as a whole and the contributions of the various components to be obtained (Bernuzzi et al., 1996)

FE Model:

- All nodes lying on the cut surfaces of the model should be subjected to an imposed boundary condition in which displacements normal to the plane of symmetry and rotations about that plane are restrained (Chiew et al., 1996)
- For closer correlation with experimental measurements, it is necessary to model the variation of thickness in the cross-section of the rail and crossmember and the corner radii as realistically as possible (Van Wingerde, 1992)

Conclusions

Valuable information in testing, FEA joint stiffness and sensitivity studies provided a basis of information to initiate the light truck frame joint stiffness study and the development of guidelines for improving joint stiffness. Ultimately, the literature search revealed that no current studies are available in open publications specifically evaluating truck frame joint stiffness and parameterizing those values that affect joint stiffness.

Introduction

Finite element analysis was used to evaluate the stiffness of five different light truck frame joints. Using information from the literature search and fundamental finite element techniques, the joints were post-processed to understand model and joint behavior, and to compare FEA results to physical test data. The study included defining the joint, modeling, determining the loading conditions and evaluating the stiffness of the joints. A picture of each joint and a brief description are shown in Figures 1 through 5.
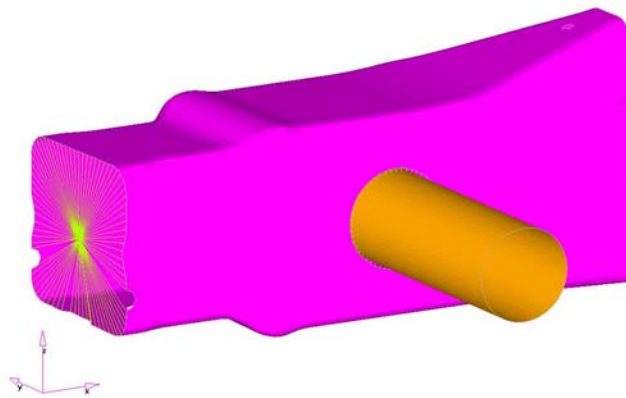
Figure 1: Joint 1: Tube-Through-Tube (welded to both webs)
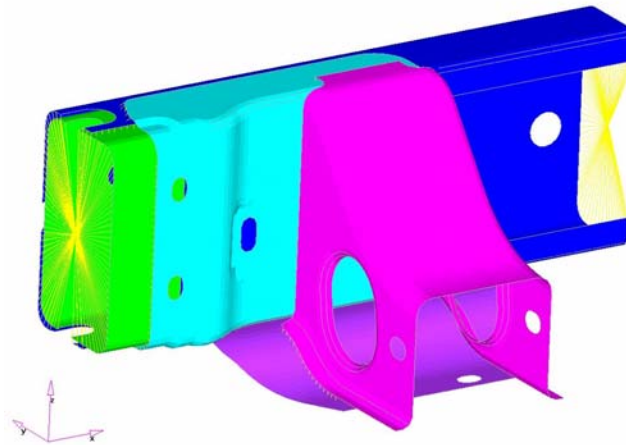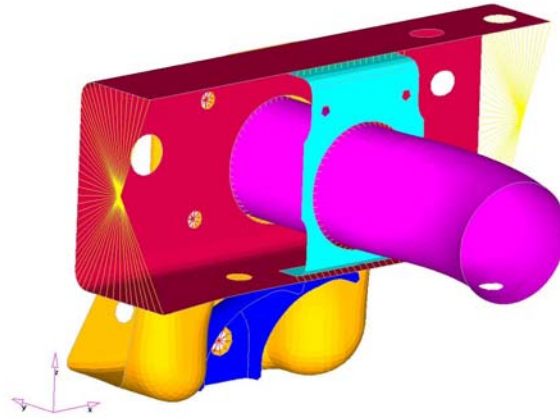

Figure 2: Joint 2: Box to Lipped Channel

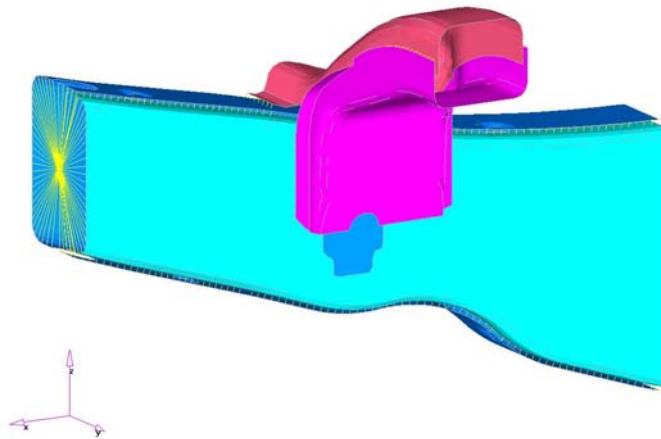**Figure 3: Joint 3: Tube Through Partially Boxed Section (welded on both sides)**

Figure 4: Joint 4: Alligator to Box Section (welded to both flanges)
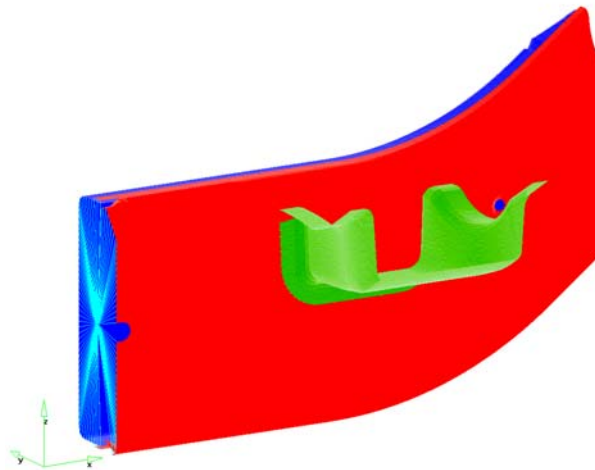

Figure 5: Joint 5: Hat Section to Box Section (welded around outer flange perimeter only)

FINITE ELEMENT ANALYSIS

Defining the Joints

The joint definition incorporated the ideas of keeping the distance from the end plate to the center of the joint at a length long enough to minimize the effect of end conditions (Chiew, 1996) and small enough to minimize the influence of the surrounding structure (Rao, et al., 1983). The joint dimensions were defined to contain all unique characteristics of the joint and minimize the inclusion of the surrounding structure. An experiment was performed to understand the effects of sidebar and crossmember length. Four different lengths of crossmember and side member were simulated. Plots of stiffness and crossmember length of approximately 150mm gave maximum member deflection while not affecting the deflected shape of the joint. All joints were simulated and physical tests were performed with specimens cut 150mm from the edge of the joint. These dimensions are shown in Figure 6.
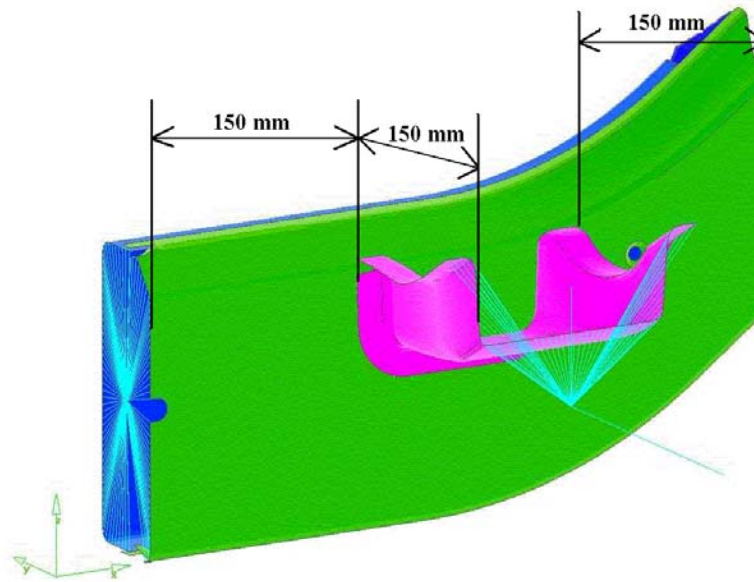

Figure 6: Joint Definition, Length of Structure Surrounding the Joint

Finite Element Analysis Model

The finite element models of the joints were developed from CAD data supplied by the Auto/Steel Partnership. The mid-plane surfaces of the joints were modeled with shell quad and tri elements with an average size of 5mm. The welds were modeled with rigid elements perpendicular to the surfaces welded. The entire loading fixture, composed of two steel end plates with a steel tube welded between them, was also modeled. An example FEA model is shown in Figure 7, with a more detailed picture of the loading fixture in Figure 8. The overall length of the loading fixture was 200mm and had two additional bars welded to it. These bars were non-load-bearing members welded to the base plate of the fixture, and were used to measure the deflection of the joint. This fixture is bolted, modeled with rigid spiders, to a plate welded onto the end of the crossmember.
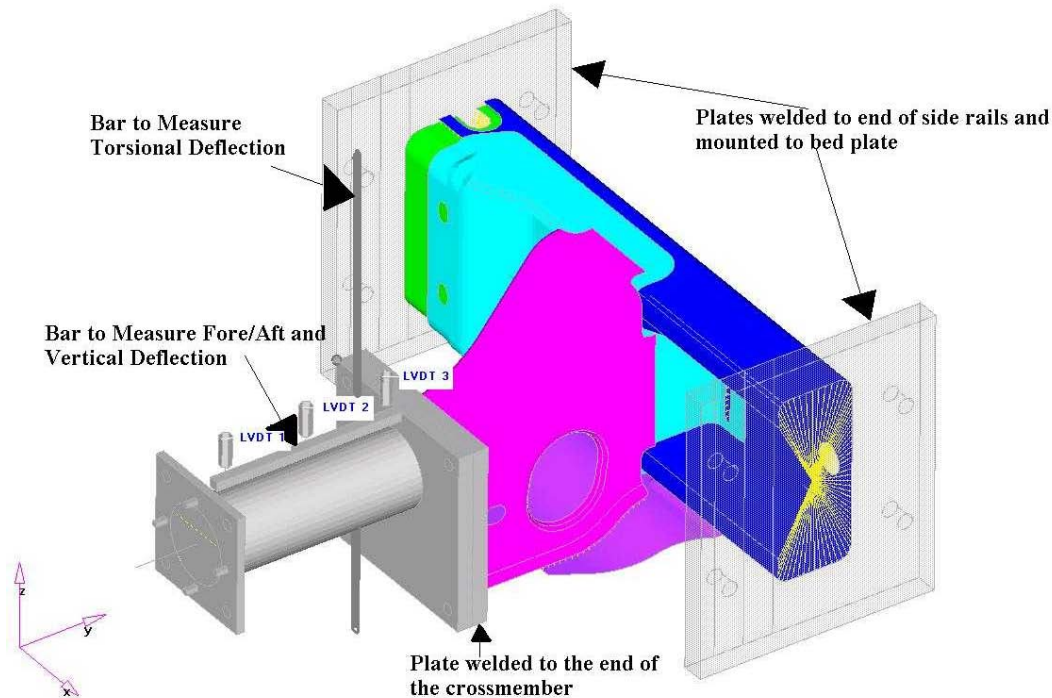
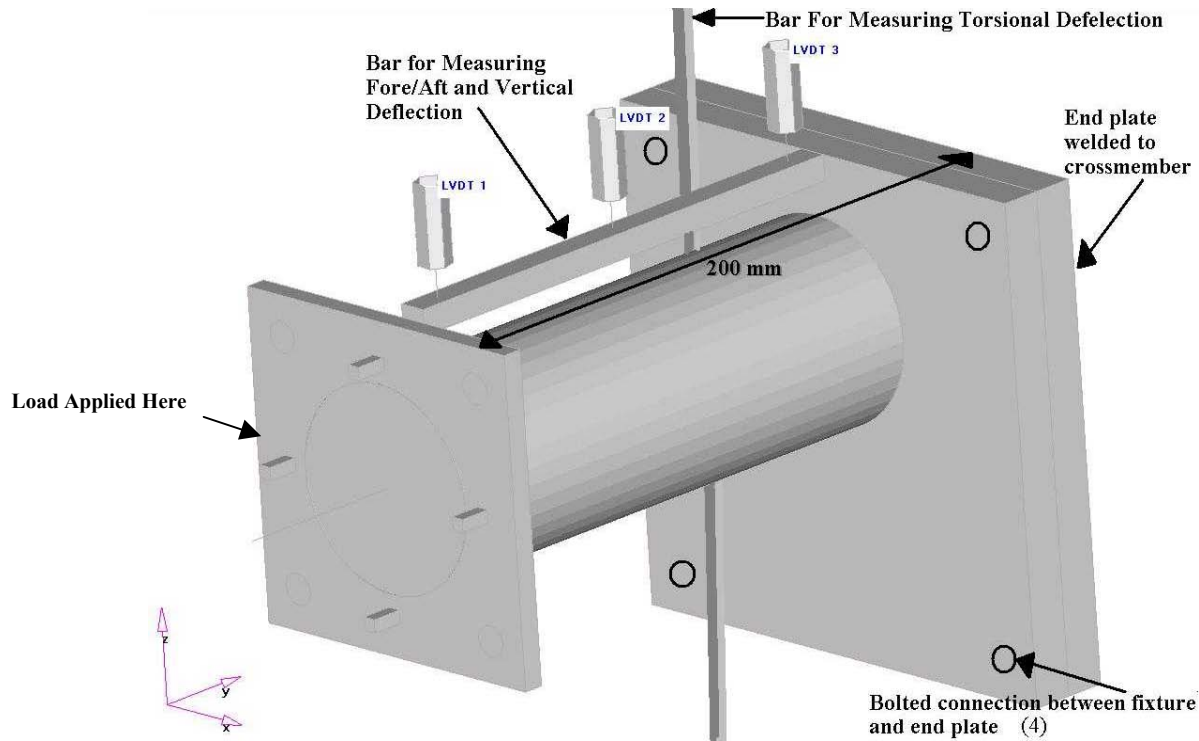**Figure 7: Example of FEA Model with Loading Fixture**

FINITE ELEMENT ANALYSIS

Figure 8: Close Up Picture of Loading Fixture

Loading Conditions

The three stiffnesses, K_x, K_y, and K_z are the rotations of the crossmember relative to the side rail. K_x is obtained by applying a vertical load (+/- Z) at the end of the crossmember and measuring the rotation from the vertical deflection of the non-load-bearing bar on the fixture. K_y is obtained by applying a torsional load (+/- Y) along the crossmember and measuring the rotation from the fore/aft deflection of a bar attached to the base of the fixture. For K_z, a fore/aft load (+/- X) is applied at the cross member and the rotation from the fore/aft deflection of the non-load-bearing bar on the fixture is measured. Each load was applied at the end of the loading fixture. The fixture was used to increase applied moment, permitting lower loading forces and measurable deflections during test. The loading was adjusted for each joint so the peak stress was 200MPa, permitting the maximum deflection without the risk of yielding the joint. The model was constrained at the two ends of the side rails with rigid spiders to the center of the section. The center node was then constrained in all six degrees of freedom. The deflections were measured off a non-load-bearing bar that was attached to the base plate of the loading fixture. This assured that the deflections measured would be that of the deformed joint, and not include deformation of the fixture.

FINITE ELEMENT ANALYSIS

Stiffness Calculations

The joint stiffness is based on the load and deflection of the joint. It is calculated using the instantaneous center of rotation (Rao, 1983) to measure the applied moment. The center of rotation is calculated from the deflection of the joint members. The distance from the applied load to the center of rotation is the length the load is applied over. This is significant in that it changes calculated applied moment. The stiffness equation is:

$$K = \frac{M}{\theta}$$

where M is the applied moment and θ is the resulting rotation. Since the moment is the applied force times the distance, and the distance is from the loading point, to the center of rotation, the stiffness equation becomes:

$$K = \frac{F(L + a)}{\theta}$$

where F is the applied force, L is the distance between the two measured defections (δ_2 and δ_1) and a is the length to the center of rotation. The equation for a, the distance to the center of rotation is:

$$a = \frac{L\delta_1}{\delta_2 - \delta_1}$$

The rotation (θ) of the joint is:

$$\theta = a\tan\left(\frac{\delta_2 - \delta_1}{L}\right)$$

For the stiffnesses Kx and Kz the loads are applied as a force at the end of the loading fixture. To calculate the moment, the distance to the center of rotation is included in the calculation. These equations are illustrated in Figures 9 and 10.

FINITE ELEMENT ANALYSIS

$$K_z = \frac{F_x(L+a)}{\theta}$$
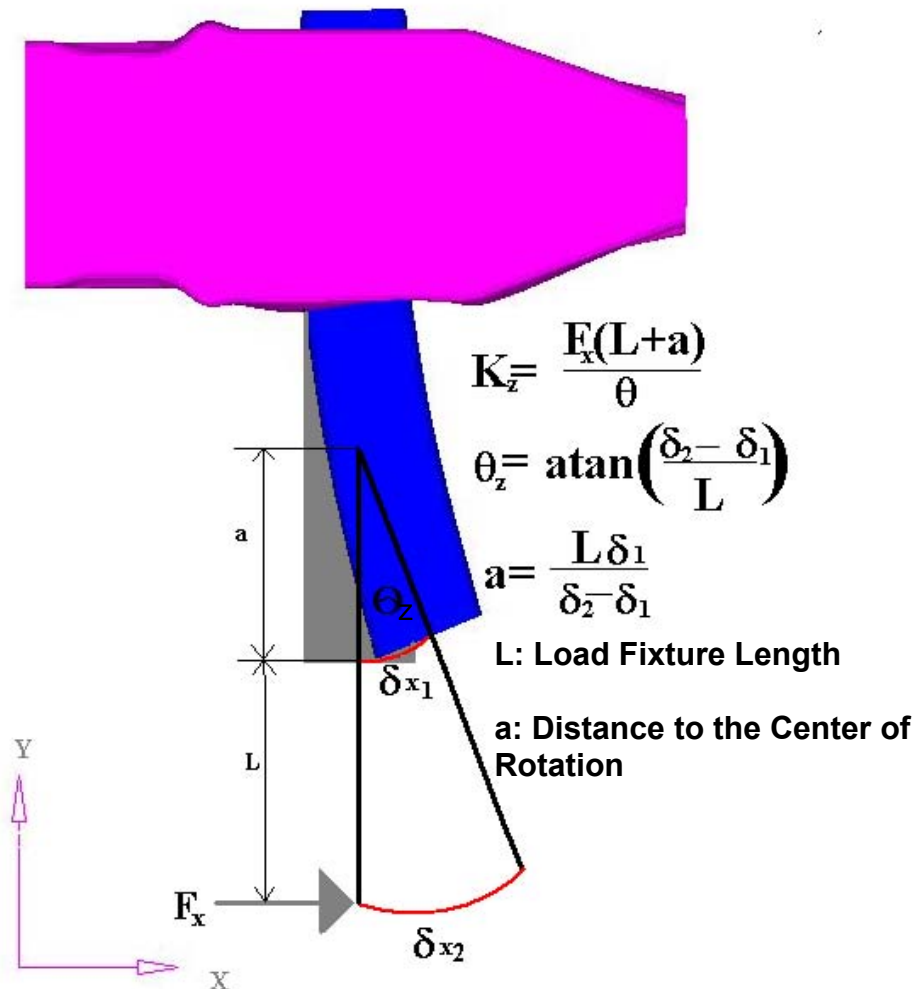
$$\theta_z = \text{atan}\left(\frac{\delta_2 - \delta_1}{L}\right)$$

$$a = \frac{L\delta_1}{\delta_2 - \delta_1}$$

L: Load Fixture Length

a: Distance to the Center of Rotation

Figure 9: Joint Stiffness Calculation Kz

$$K_{\overline{x}} = \frac{F_z(L+a)}{\theta}$$

$$\theta_{\overline{x}} = atan\left(\frac{\delta_2 - \delta_1}{L}\right)$$

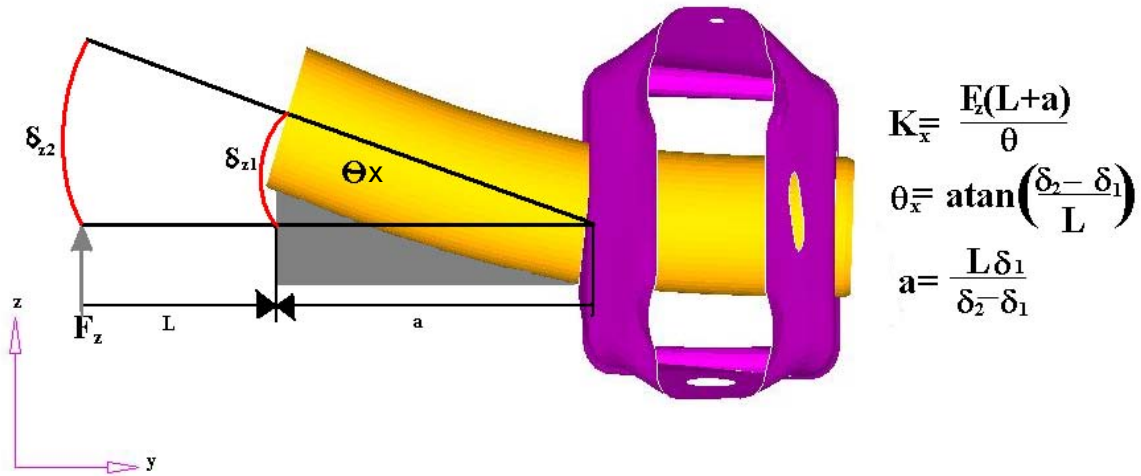$$a = \frac{L\delta_1}{\delta_2 - \delta_1}$$

Figure 10: Joint Stiffness Calculation Kx

For the stiffness Ky, the load was applied as a moment. The equation simplifies, not needing to include the additional length to the center of rotation, and is shown in Figure 11.
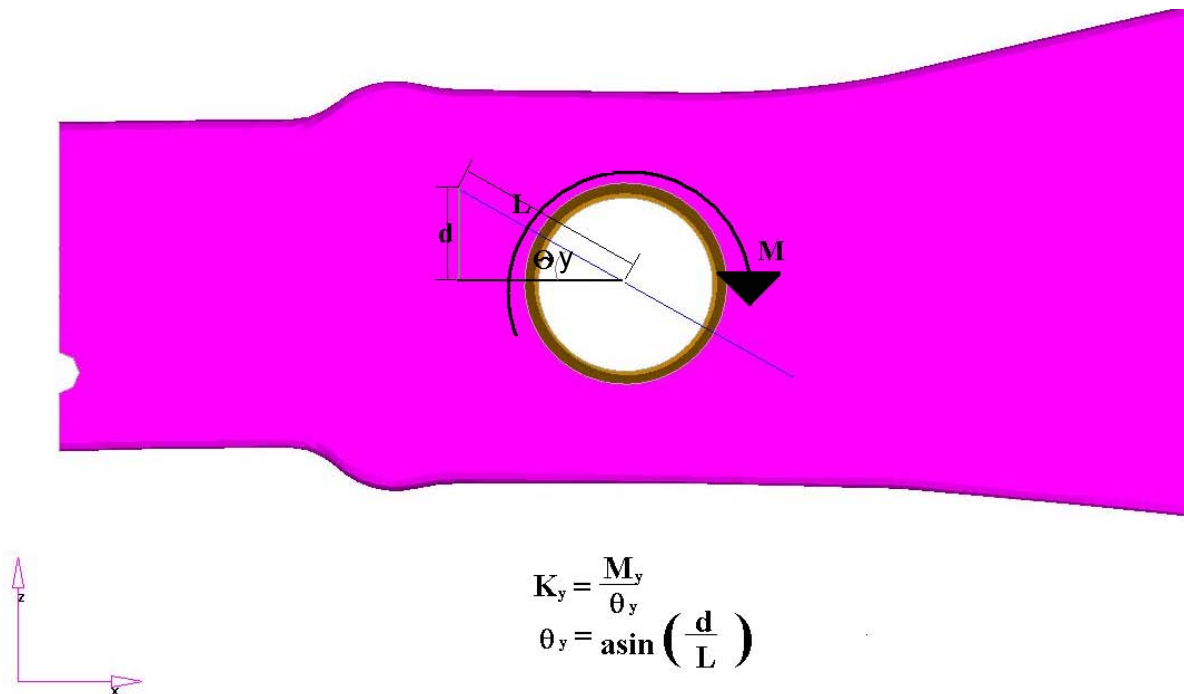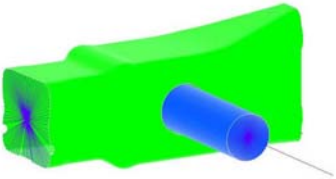

$$K_y = \frac{M_y}{\theta_y}$$

$$\theta_y = asin\left(\frac{d}{L}\right)$$
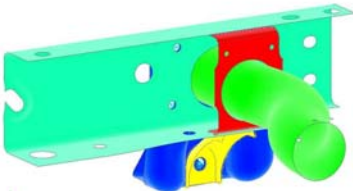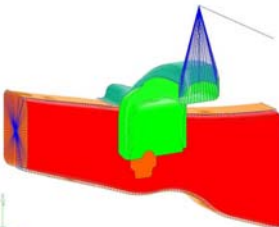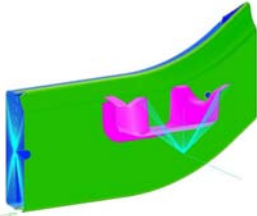
Figure 11: Joint Stiffness Calculation Ky

The calculated stiffness for the five joints is listed in Table 1.

FINITE ELEMENT ANALYSIS

Table 1: Analysis Stiffness Summary

	Kx	Ky	Kz
Joint 1: Tube- Through-Tube (welded at both ends)	2.102 KNm/deg	3.059 KNm/deg	2.513 KNm/deg
Joint 2: Box to Lipped Channel	9.006 KNm/deg	5.117 KNm/deg	40.994 KNm/deg
Joint 3: Tube Through Partially Boxed Section (welded on both sides)	1.899 KNm/deg	5.567 KNm/deg	3.102 KNm/deg
Joint 4: Alligator to Box Section (welded to both flanges)	0.543 KNm/deg	1.413 KNm/deg	1.016 KNm/deg
Joint 5: Hat Section to Box Section (welded all around)	0.100 KNm/deg	0.202 KNm/deg	0.202 KNm/deg

TESTING PROCEDURE

Introduction

The five joints were tested under the same loading conditions as the finite element in order to later correlate the data. Three samples of each of the five joints were tested to identify the effect sample variation. A written procedure and a pictorial procedure, included below, were used for testing. This pictorial procedure, containing the joint preparation, fixturing and test setup is included for each of the five joints and can be found on pages 21-43. The test results are summarized in Stiffness Table 2.

Joint Preparation

The test joints and the surrounding frame material were removed with a plasma cutter from the frames containing the test joints. These rough-cuts were made at a distance far enough from the joint area to avoid changing the material properties of the steel from the high heat. Final cuts at the required distance (usually 150mm from the joint) were performed on a band saw.

Joint Fixturing

All joints were equipped with steel plates on each end of the side rail and on the end of the crossmember. These plates were welded to the member ends. During test setup each joint was oriented with the side rail positioned parallel to the ground and the crossmember perpendicular. Longitudinal end plates were bolted to angle brackets that were in turn bolted to a bedplate. This proved to be a sufficiently stiff fixturing method verified by a dial indicator during testing. A steel tube sandwiched between two steel plates was bolted to the crossmember end plate. This allowed force application at a distance away from the joint, increasing deflection to a measurable level while keeping the applied loads to a reasonable level. This fixture is shown in Appendix D.

Deflection Measurement

Deflection was measured using five Linear Variable Displacement Transducers (LVDTs). Two transducers were placed on the side rail surface positioned parallel to the crossmember. The remaining three LVDTs monitored lateral frame rail displacement and were positioned relative to the direction of force being applied. Contact points for these three LVDTs were on additional surfaces not receiving any of the applied loads. A diagram of the loading and measurement locations are shown in Appendix D.

Force Application

Based on the required loading, two different load application methods were employed. Joint 5, the Hat Section to Box Section, had low loading requirements and a pulley/hanging weight system was used to apply the necessary force. This was chosen because of its simplicity to set up and run and its relatively low cost. For each load case (X, Z, and torsion) loads were increased to the desired value, reduced back to zero load, and then repeated in the opposite direction. This procedure was repeated three times for each of the three samples. For all other joints, air cylinders were implemented to apply the force. The air cylinders were chosen to provide increased force that would have been impractical to implement with weights. Measurements were taken as force was increased to maximum, decreased back to zero, increased to maximum in the opposite direction and then decreased back to zero to provide a continuous hysterisis loop.

Test Repeatability

Each joint was tested multiple times to ensure repeatability. Three separate samples of each joint were tested three times in each of the loading directions. In all, a total of 15 were tested.

TESTING PROCEDURE

Joints 1 - 4 Joint Preparation and Fixturing
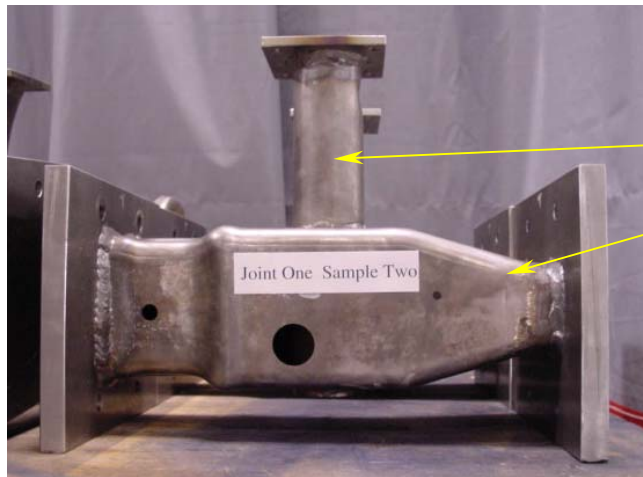
Crossmember
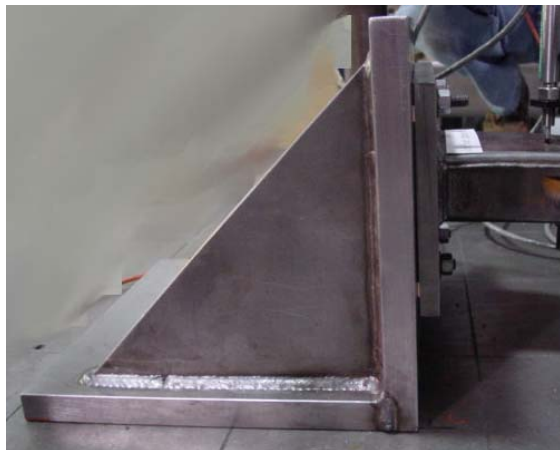
Side Rail

Frame sample with welded endplates

Endplate/angle bracket bolt connection

Dial indicator monitoring endplate movement

Bed plate/angle bracket bolt connection
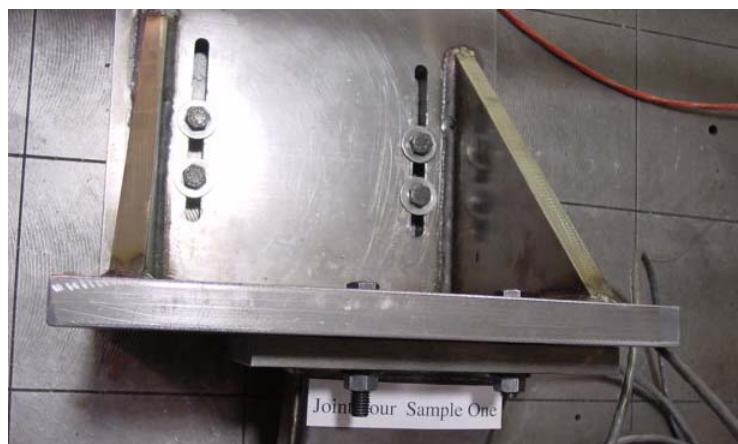
TESTING PROCEDURE

Joints 1 - 4 Pneumatic Cylinder Setup
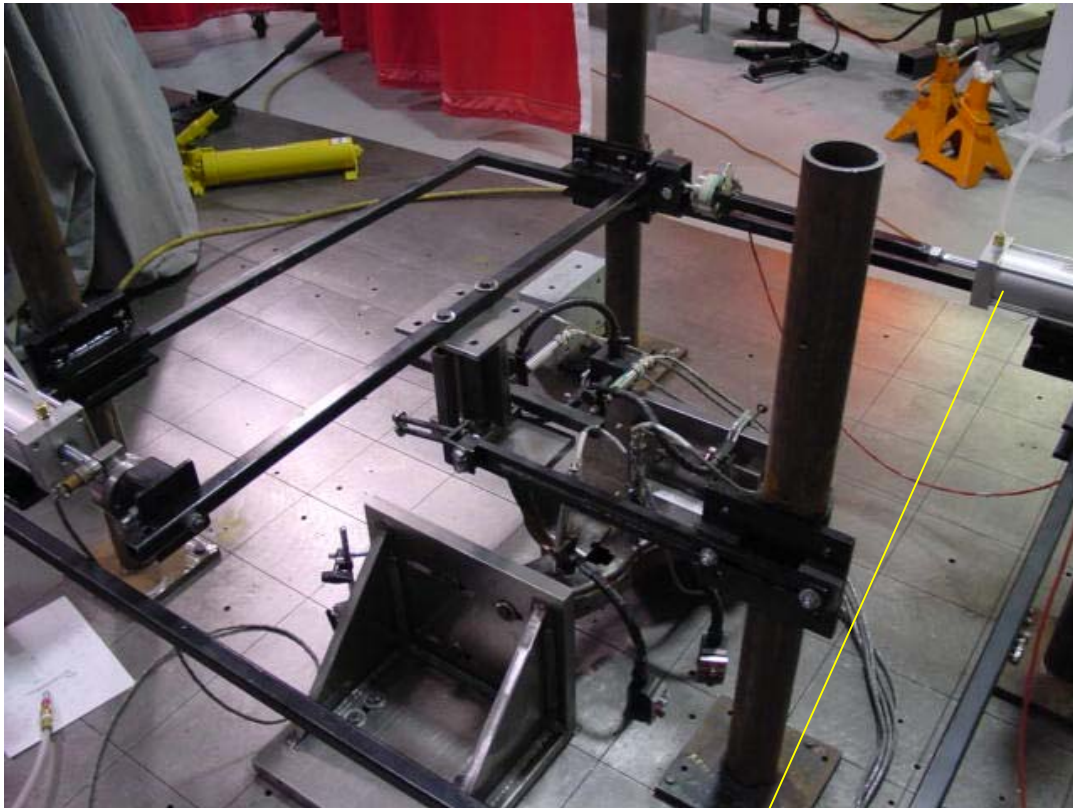
7" Stroke pneumatic cylinder with load cell and heim joint connections
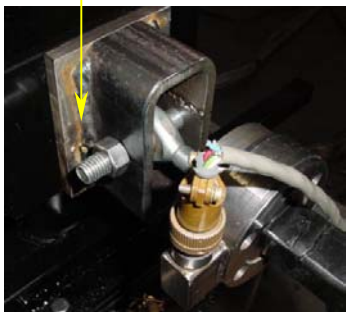
Joint end connection

Pneumatic regulator
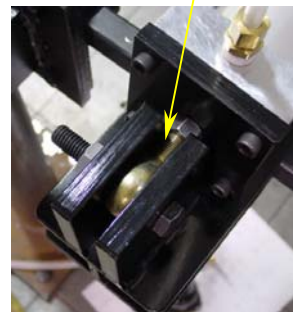
Cylinder end connection

TESTING PROCEDURE

Joint 1 - Joint Sample and Test Setup

Side View

Top View

Bottom View

TESTING PROCEDURE

Joint 1 - X Direction Test Setup

X direction test setup including LVDT positioning

Crossmember displacement measurement

Side rail displacement measurement

TESTING PROCEDURE

Joint 1 - Z Direction Test Setup

Z Direction test setup including LVDT positioning

Crossmember displacement measurement

Side rail displacement

TESTING PROCEDURE

Joint 1 - Torsion (Y) Test Setup

Torsion test setup including
LVDT placement

Crossmember displacement

Side rail displacement

TESTING PROCEDURE

Joint 2 - Joint Sample and Test Setup

Side View

Top View

Bottom View

TESTING PROCEDURE

Joint 2 - X Direction Test Setup

X direction test setup including LVDT positioning

Crossmember displacement
measurement

Side rail displacement measurement

TESTING PROCEDURE

Joint 2 - Z Direction Test Setup

Z Direction test setup including LVDT placement

Z Direction test setup including LVDT placement
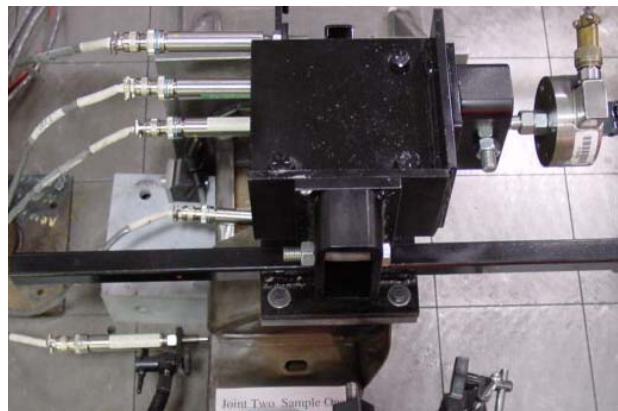
Side rail displacement measurement

TESTING PROCEDURE

Joint 2 - Torsion (Y) Test Setup

Torsion test setup including LVDT placement

Crossmember displacement measurement

Side rail displacement measurement
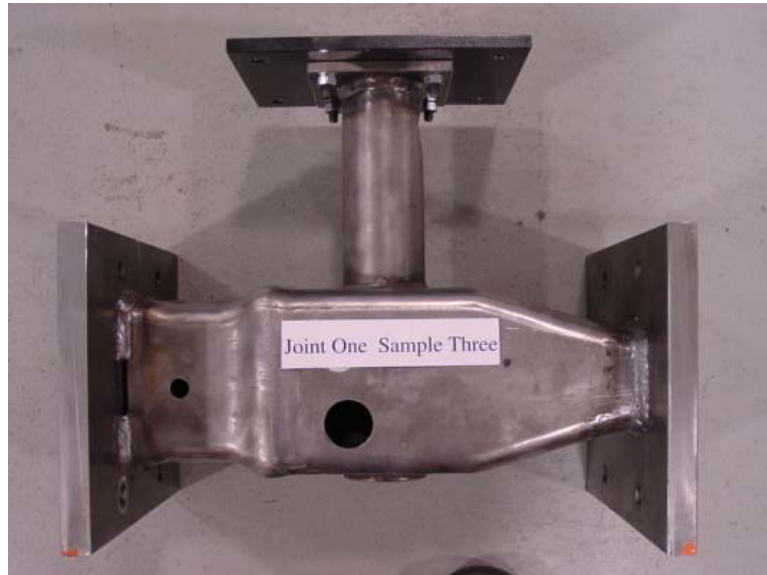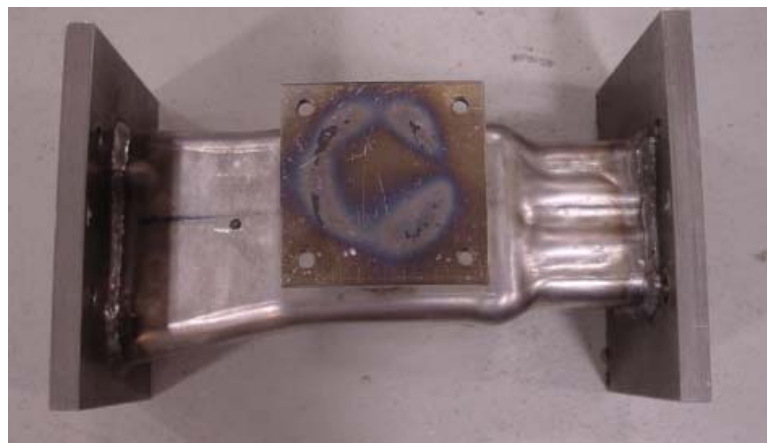
TESTING PROCEDURE

Joint 3 - Joint Sample and Test Setup

Side View
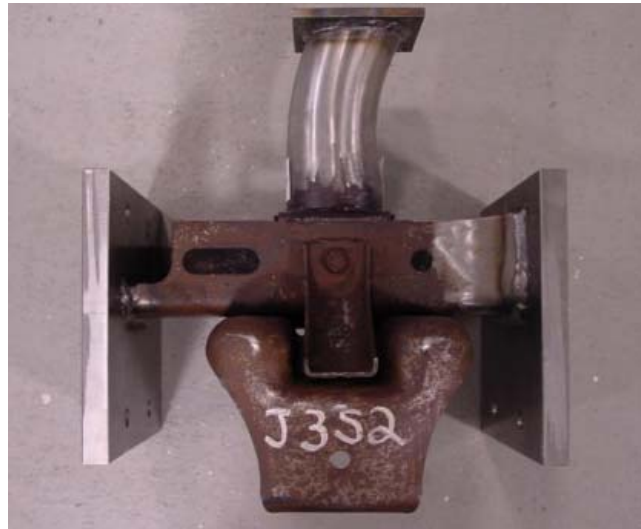
Top View
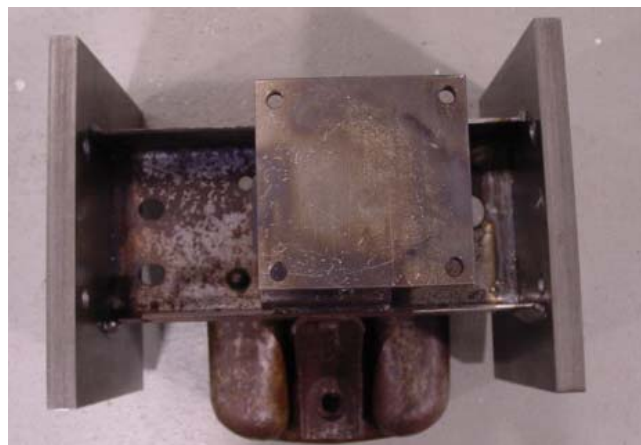
Bottom View
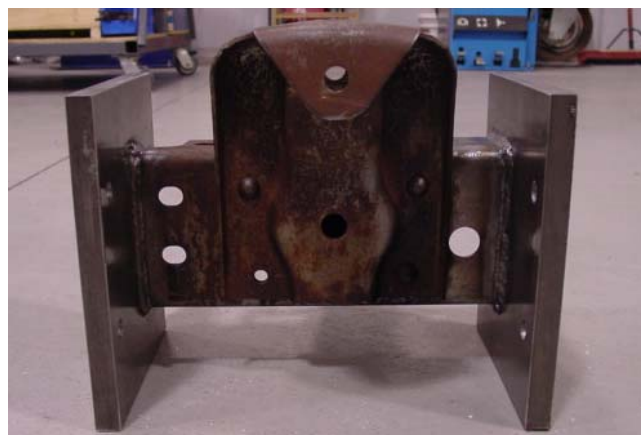
TESTING PROCEDURE

Joint 3 - X Direction Test Setup

Overview of X-direction setup including LVDT placement
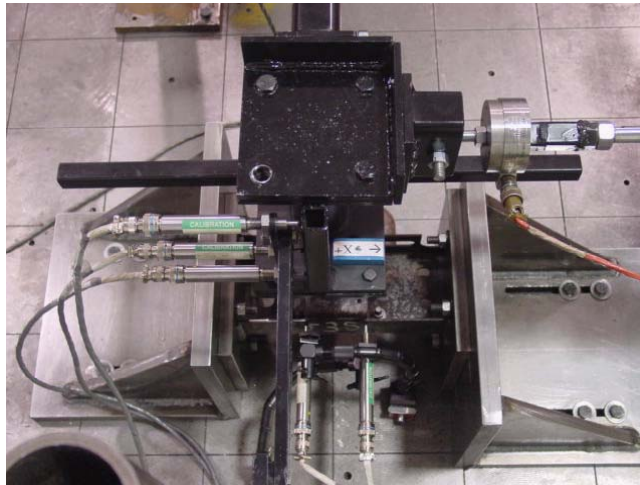
Crossmember rail displacement

Side rail displacement showing positive X direction
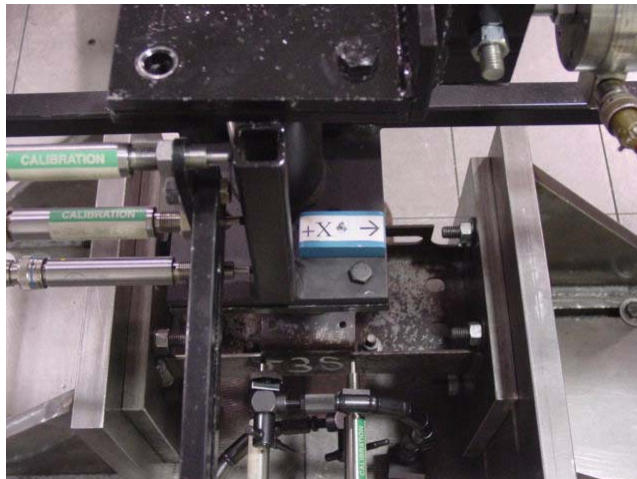
TESTING PROCEDURE

Joint 3 - Z Direction Test Setup
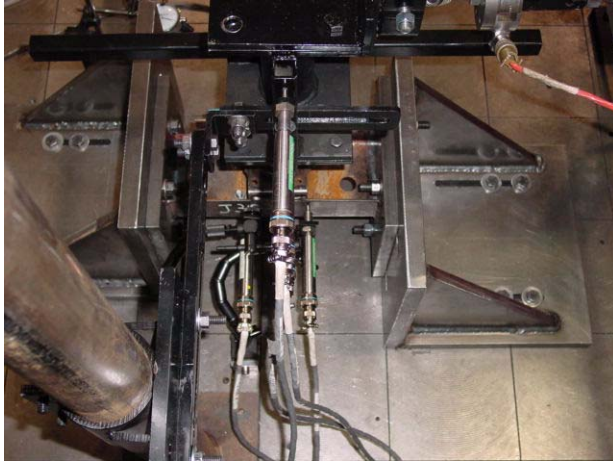
Crossmember and Side rail displacements
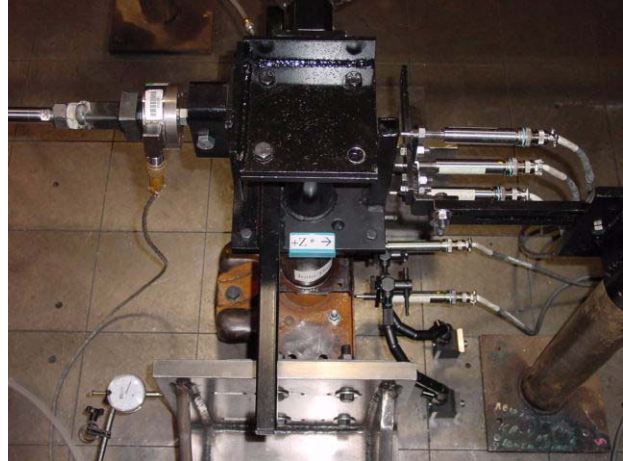
Z-Direction test setup including LVDT placement
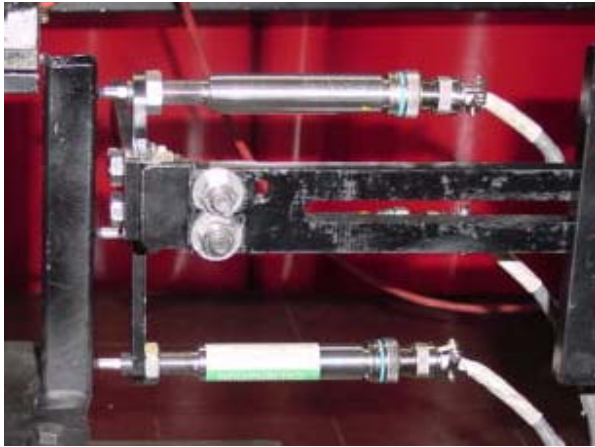
Crossmember displacement

Side rail displacements
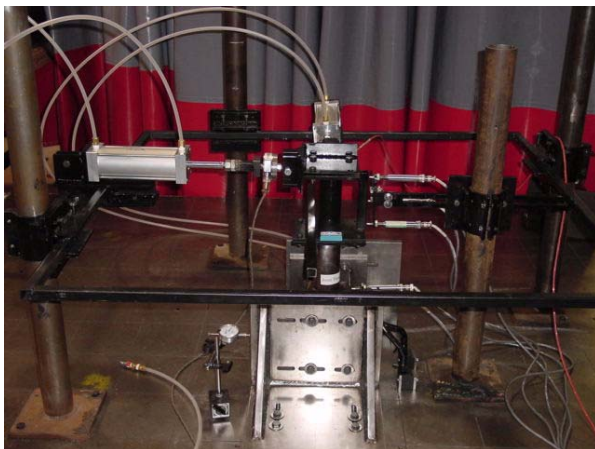
Z-Direction test setup

TESTING PROCEDURE

Joint 3 - Torsion (Y) Test Setup

Overview of torsion setup
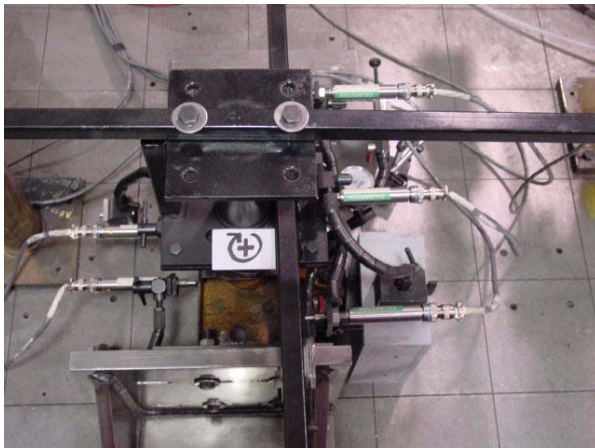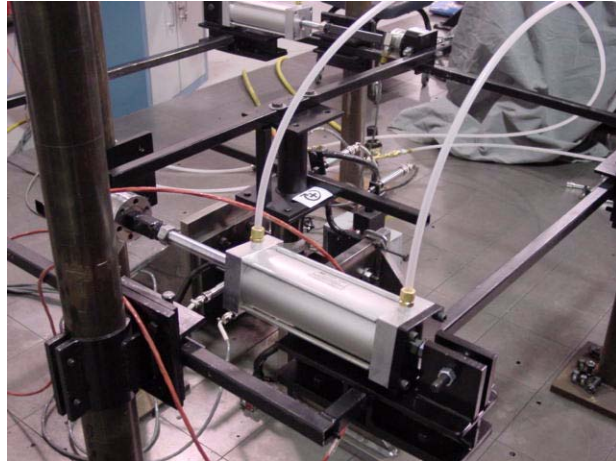
Torsion test setup including LVDT placement
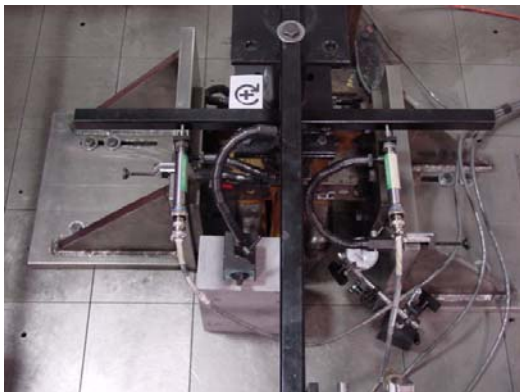
Side rail displacement
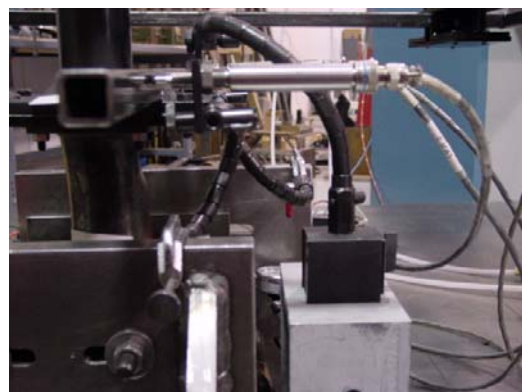
Crossmember displacement

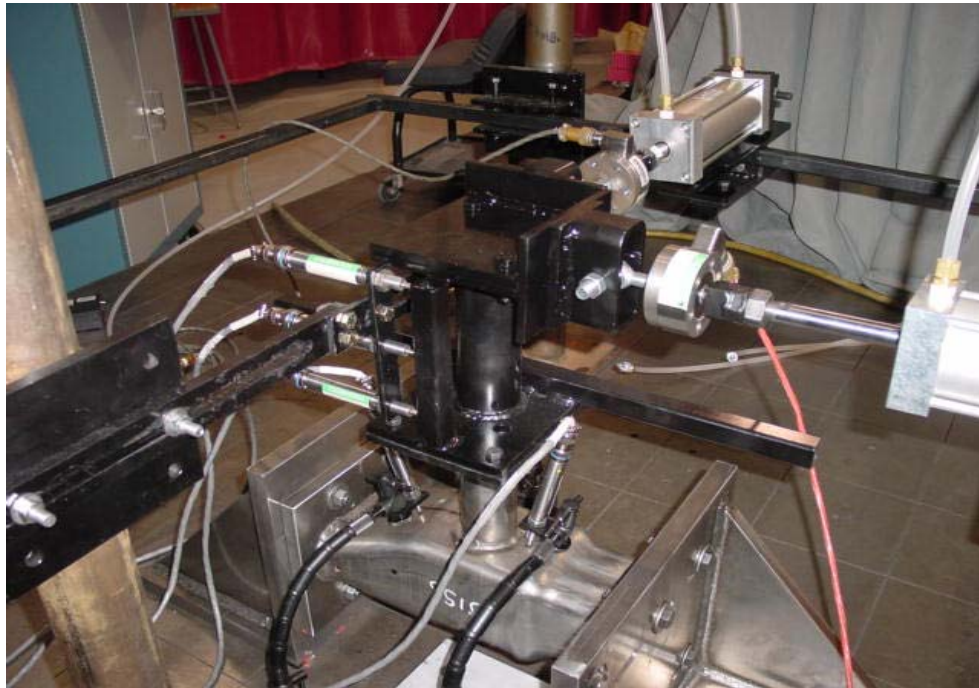## Joint 4 - Joint Sample and Test Setup

Side View
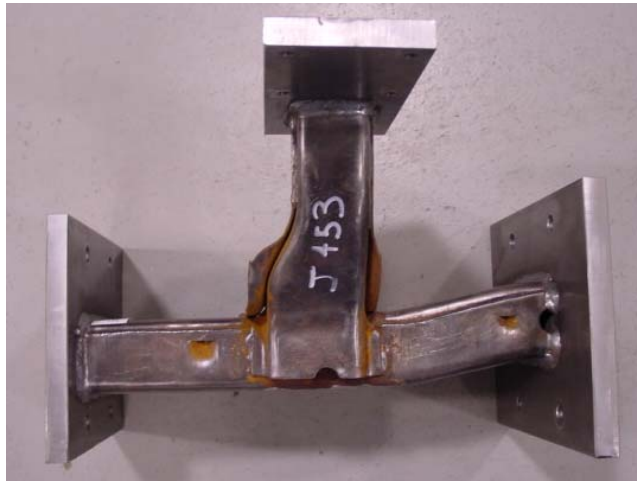
Top View
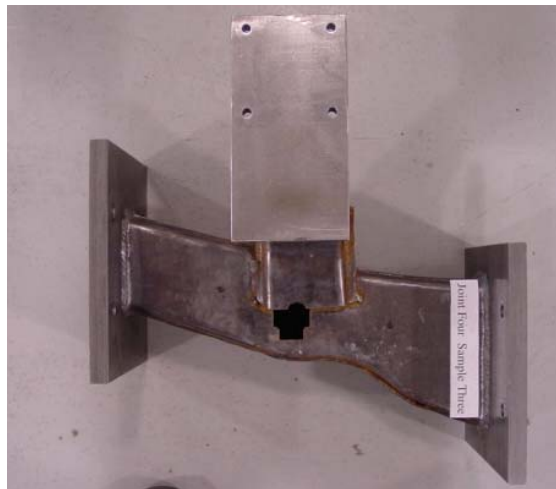
Bottom View

TESTING PROCEDURE

Joint 4 - X Direction Test Setup

X direction test including LVDT placement
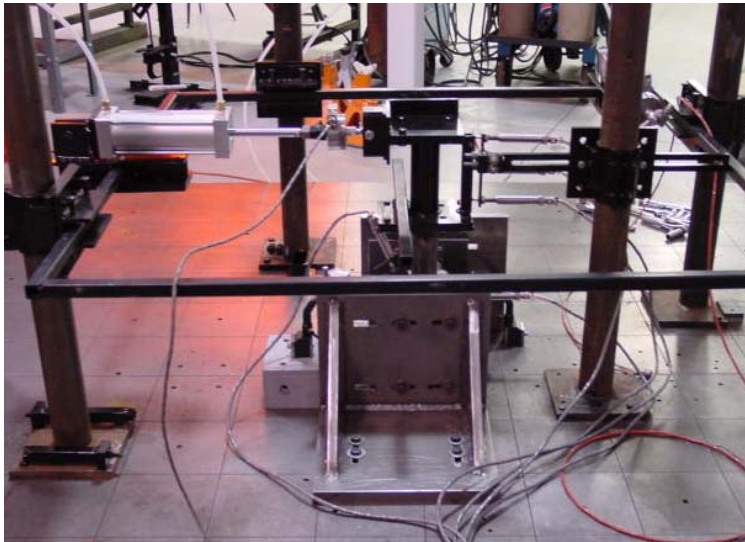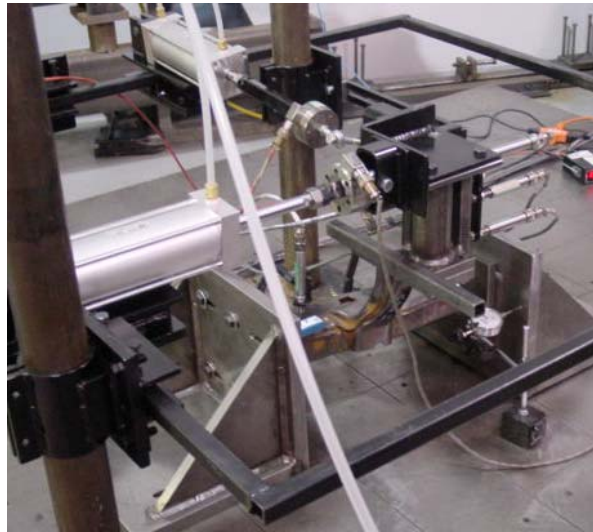

Crossmember displacement measurement
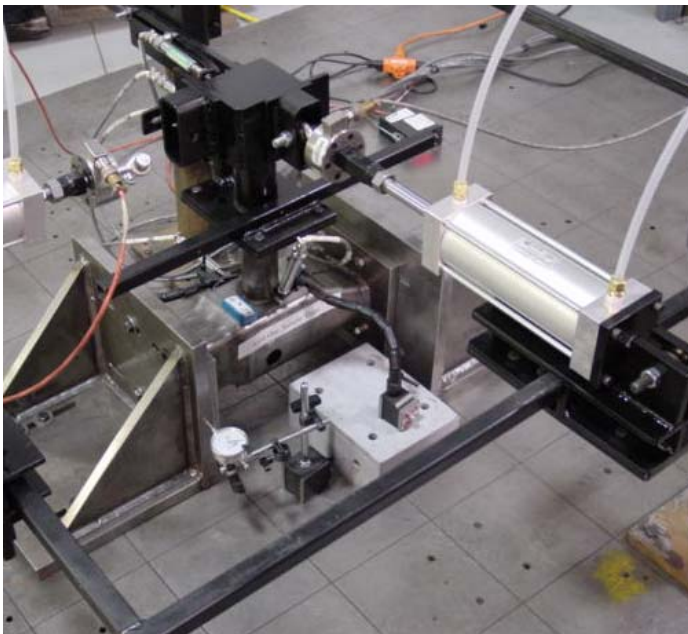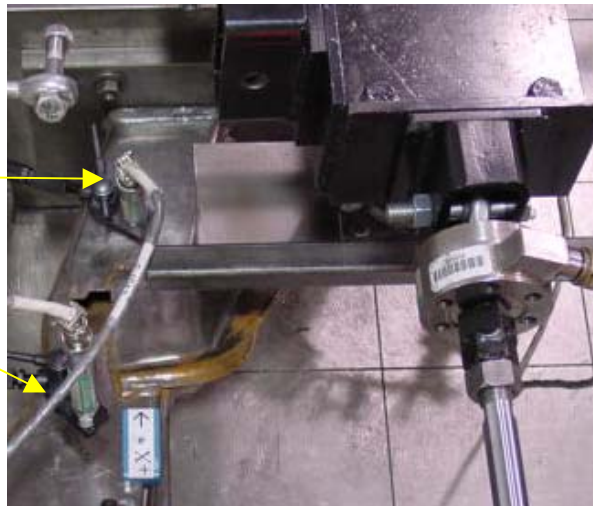

Side rail displacement measurement
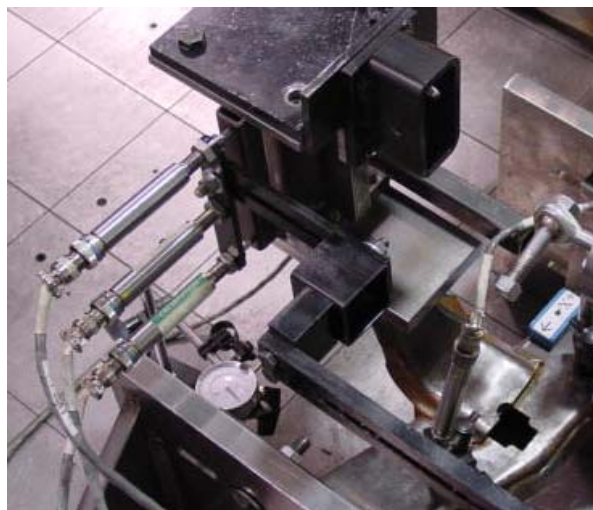
TESTING PROCEDURE

Joint 4 - Z Direction Test

Z direction test setup including LVDT placement
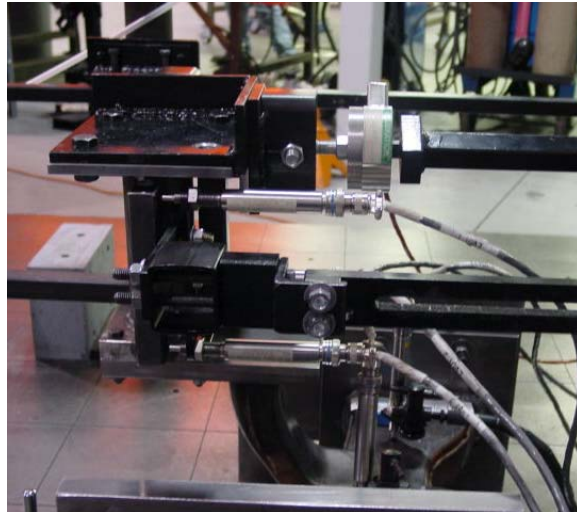
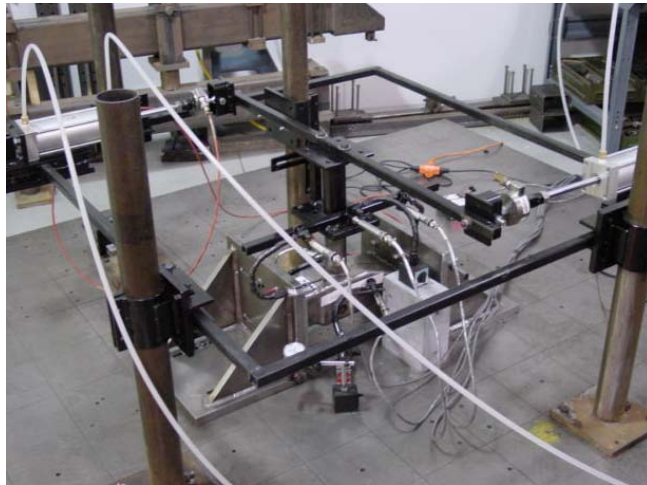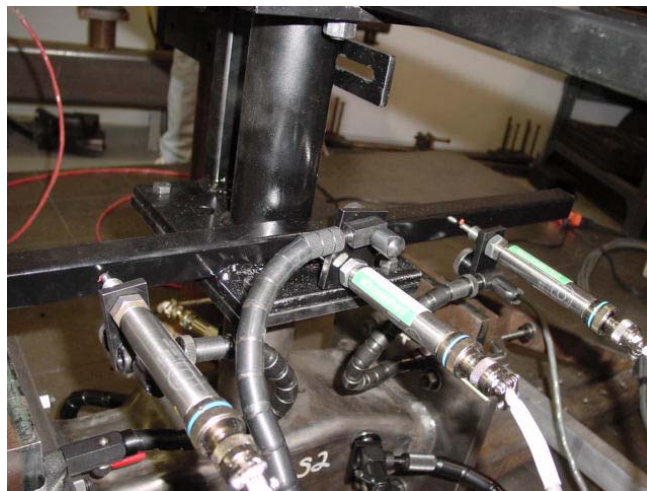Crossmember displacement measurement
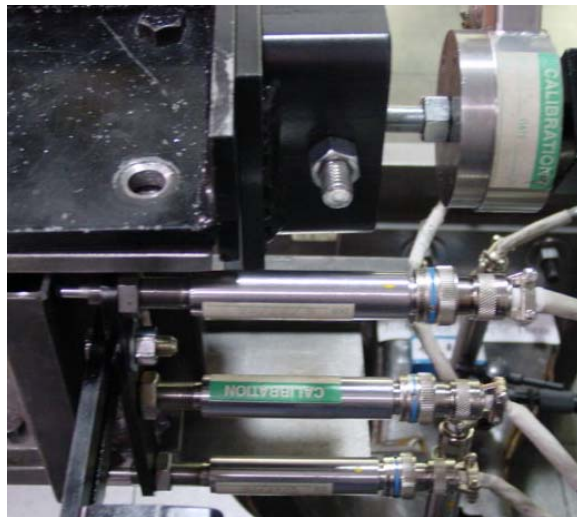
Side rail displacement measurement
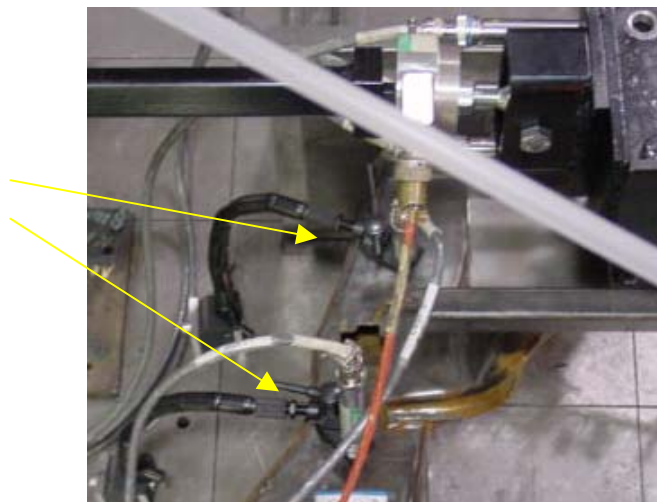
TESTING PROCEDURE

Joint 4 - Torsion (Y) Test

Torsion test setup including LVDT placement
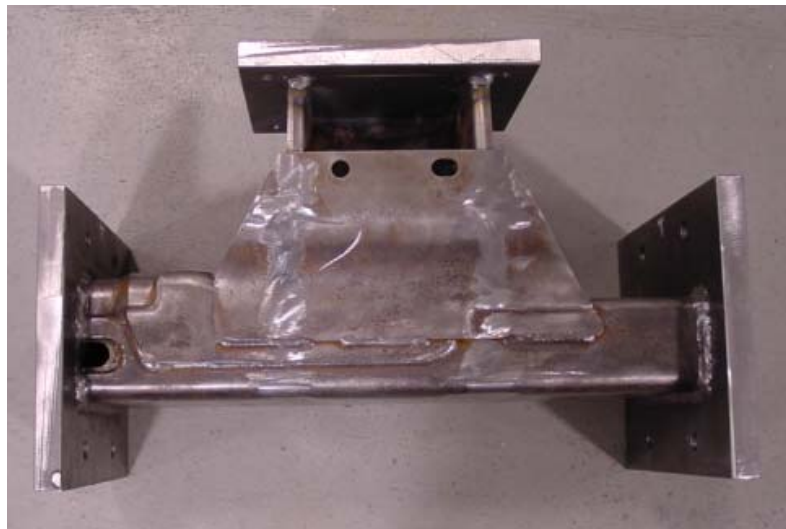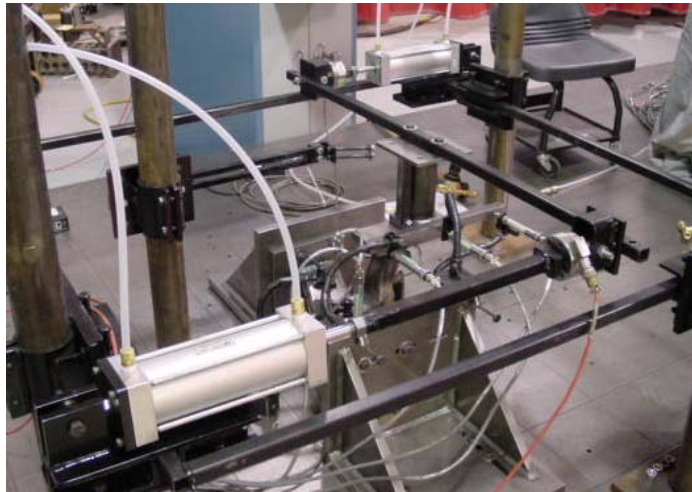

Crossmember displacement measurement
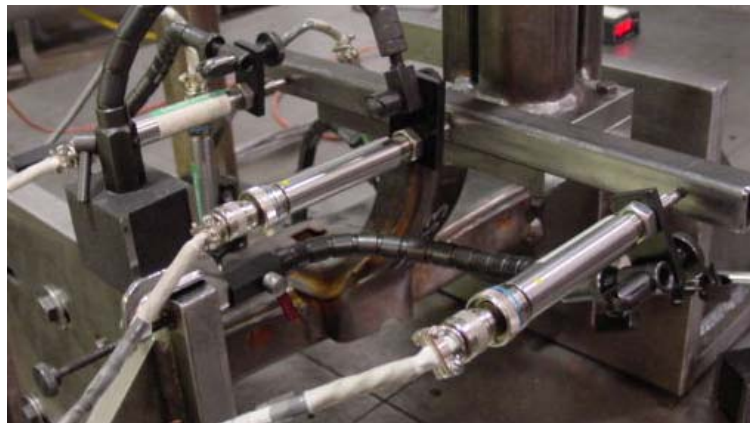
Side rail displacement measurement

TESTING PROCEDURE

Joint 5 Preparation-Joint Fixturing

Crossmember

Side rail

Frame sample with welded endplates

Endplate/Angle bracket bolt connection

Dial indicator monitoring endplate movement

Bed plate/ angle bracket bolt connection
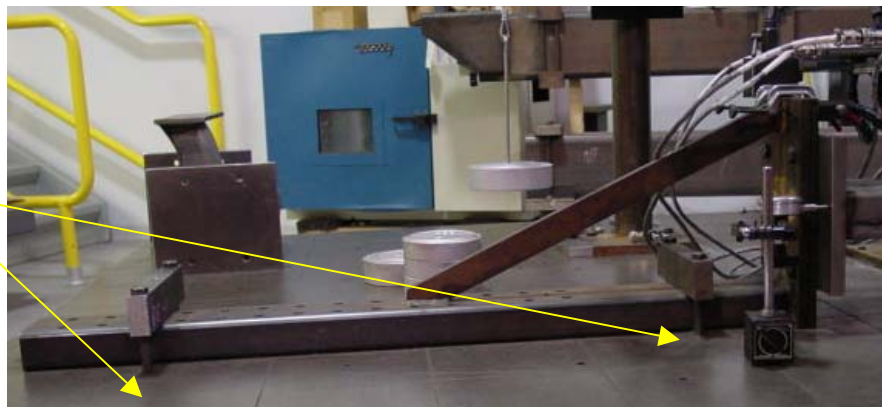
TESTING PROCEDURE

Joint 5 - Hanging Weight Setup
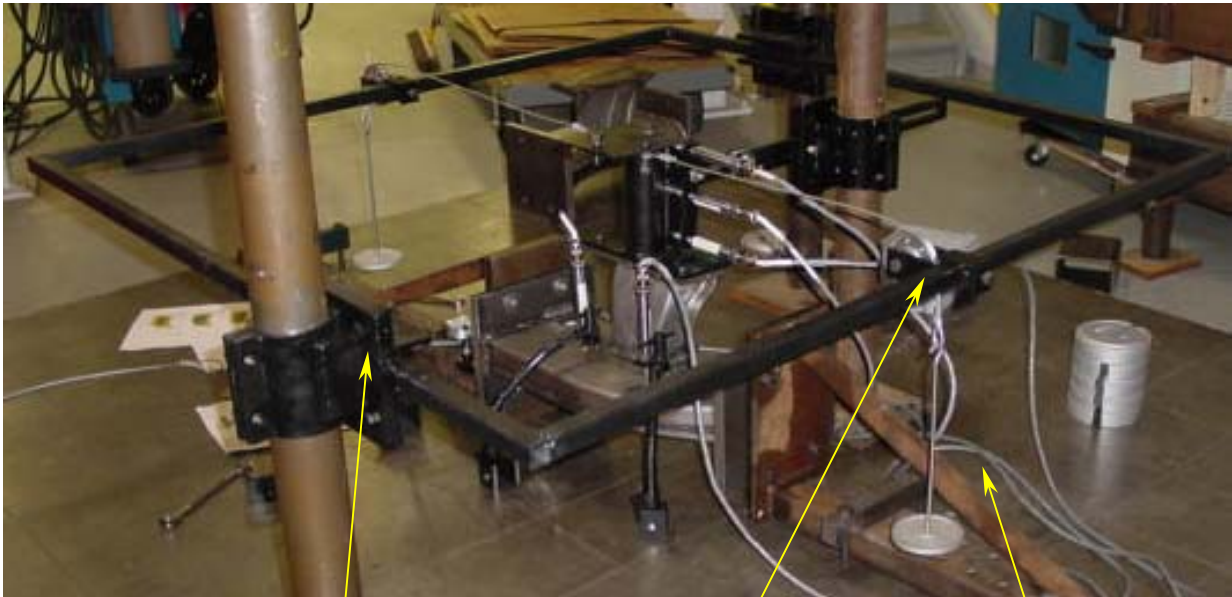
Hanging weight setup (joint 5 only)
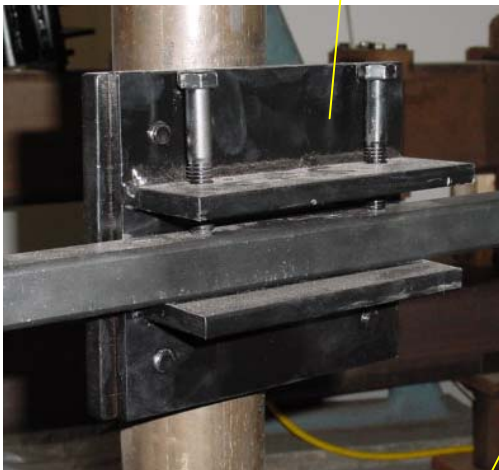
Frame fixture-mounting clamp

Fixture pulley

Calibrated 1lb weight hanger
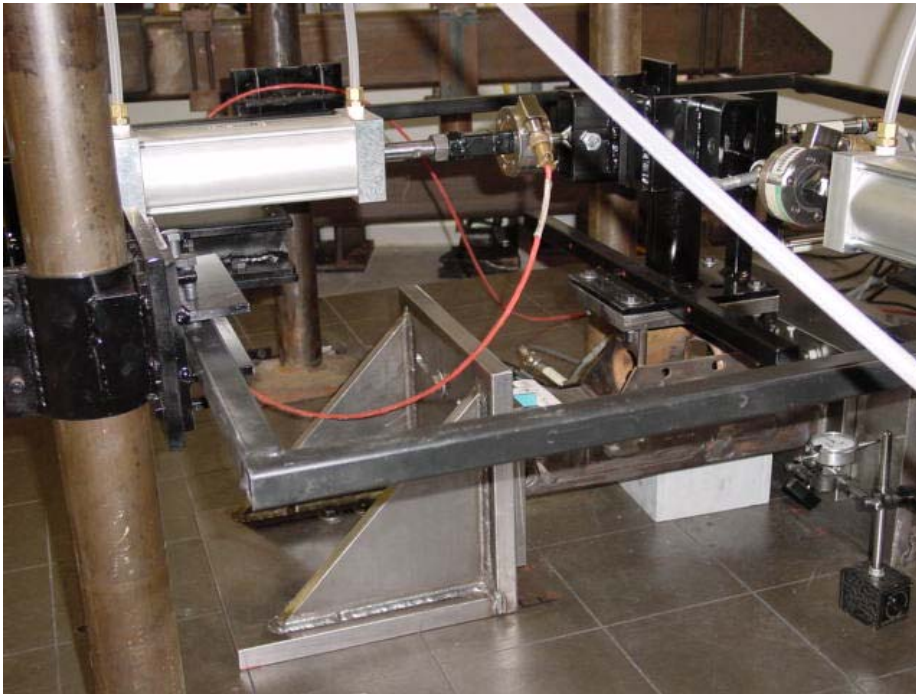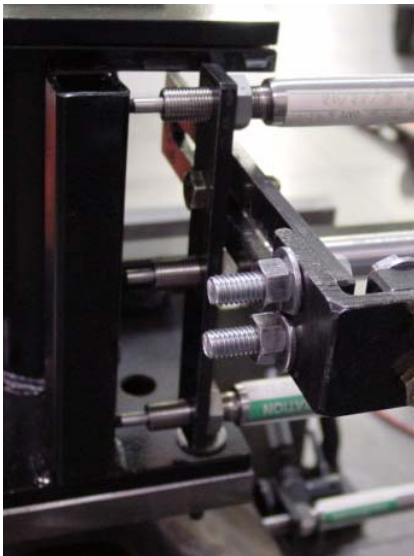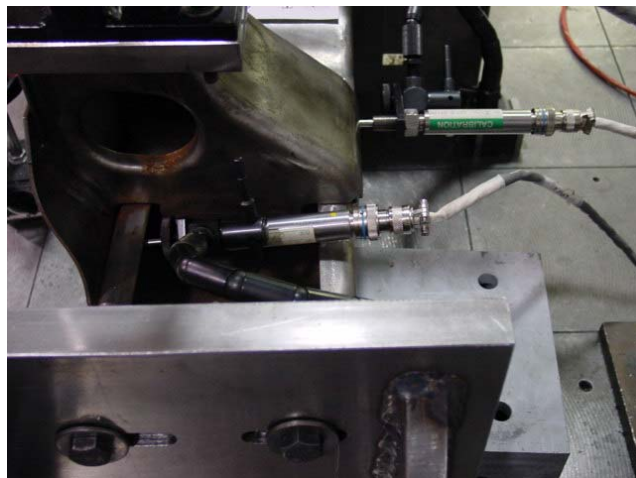
TESTING PROCEDURE

Joint 5 - X Direction Test Setup
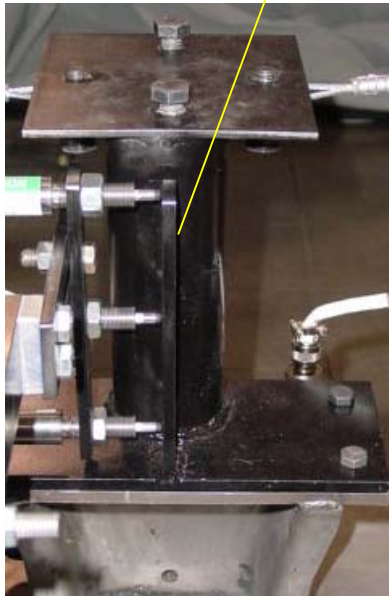
X direction test setup including LVDT positioning

Crossmember displacement
measurement

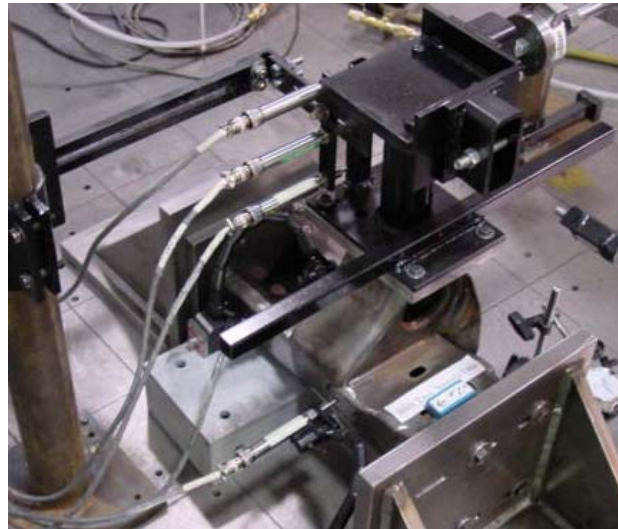
Side rail displacement measurement

TESTING PROCEDURE

Joint 5 - Z Direction Test Setup
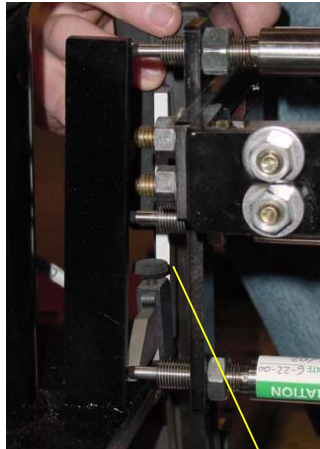
Crossmember displacement measurements
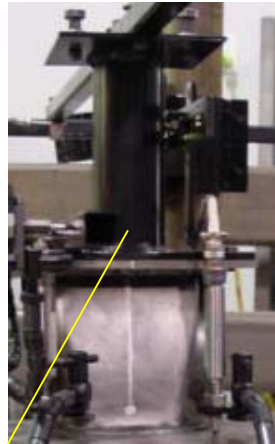
Force actuation tube
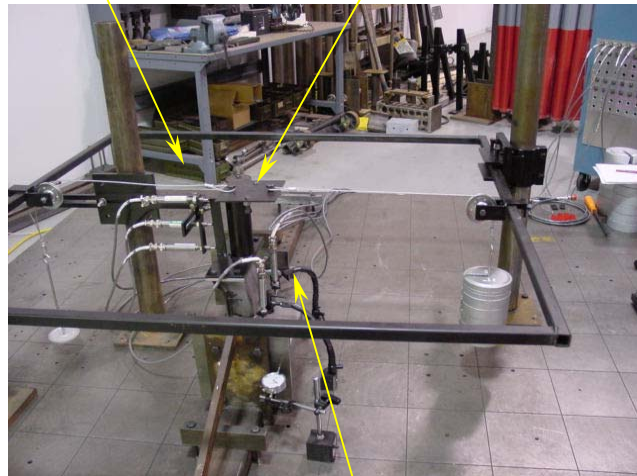
Direction test setup including LVDT positioning

Side rail displacement measurement

TESTING PROCEDURE

Joint 5-Torsion (Y) Test Setup

Torsion test setup including
LVDT placement

Crossmember displacement
measurement

Side rail displacement
measurement

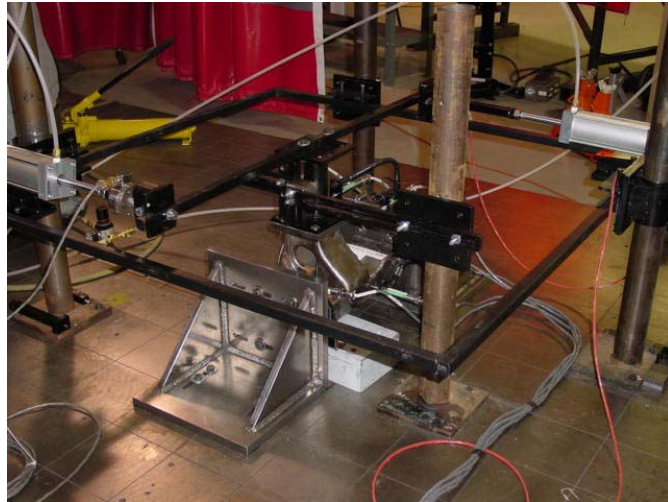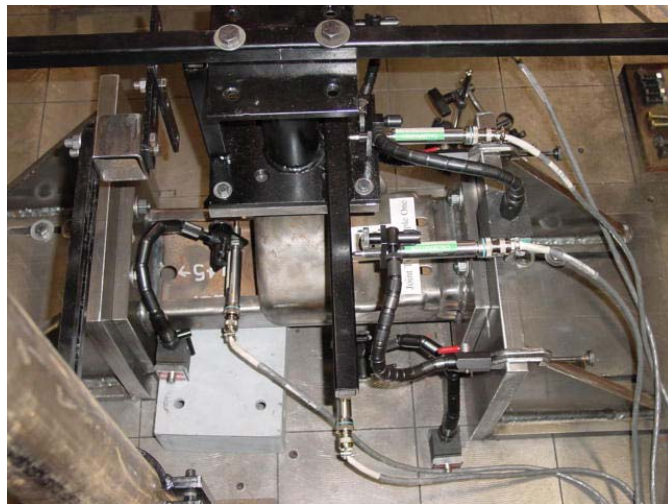# TESTING PROCEDURE

Joint Stiffness Summary

A total of 135 tests were conducted. For each joint, three samples were tested three times in each direction. The load applied and the resulting deflections were measured.

Data

The deflection for each test was measured at increments as the joint was cyclically loaded and unloaded. The average slope of the measured deflections was fit and used to calculate the joint stiffness. An explanation and example of these results is shown below.

The test results were evaluated for repeatability. Figure 12 compares the test results with the curve fit for the Fore/Aft loadcase of Joint 1. Three samples of Joint 1 were tested. Three tests were conducted on each sample. The curve fit for each sample, using the data from all three tests on the sample, was averaged.
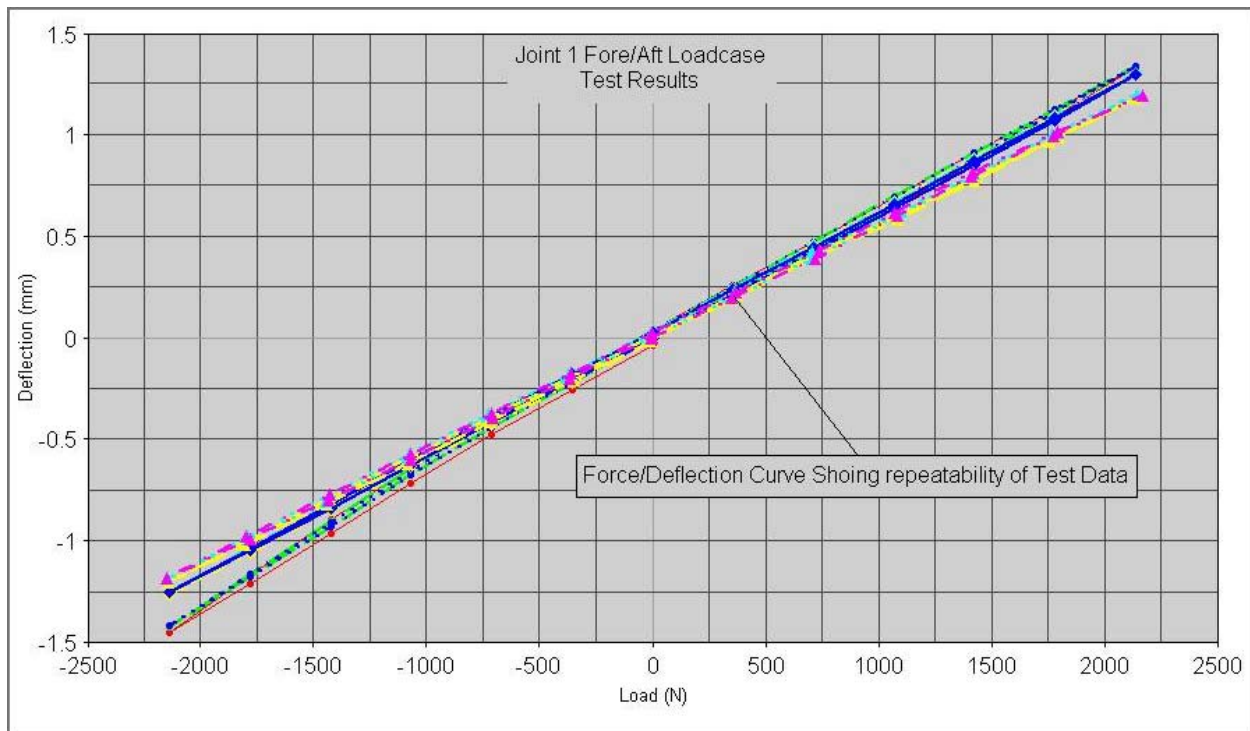
Figure 12: Comparison of Joint 1 Fore/Aft Test Results For Joint 1 (3 samples, 3 tests each)

The average of the nine tests for each joint (three tests on each of the three samples) was found and fit with a linear equation. The test fit average (based on nine tests) was used for comparison to the analytical results (Figure 13). These results are shown in Appendix C. The slope of the test fit average is the test stiffness of the joint. The test joint stiffnesses are tabulated in Table 2.
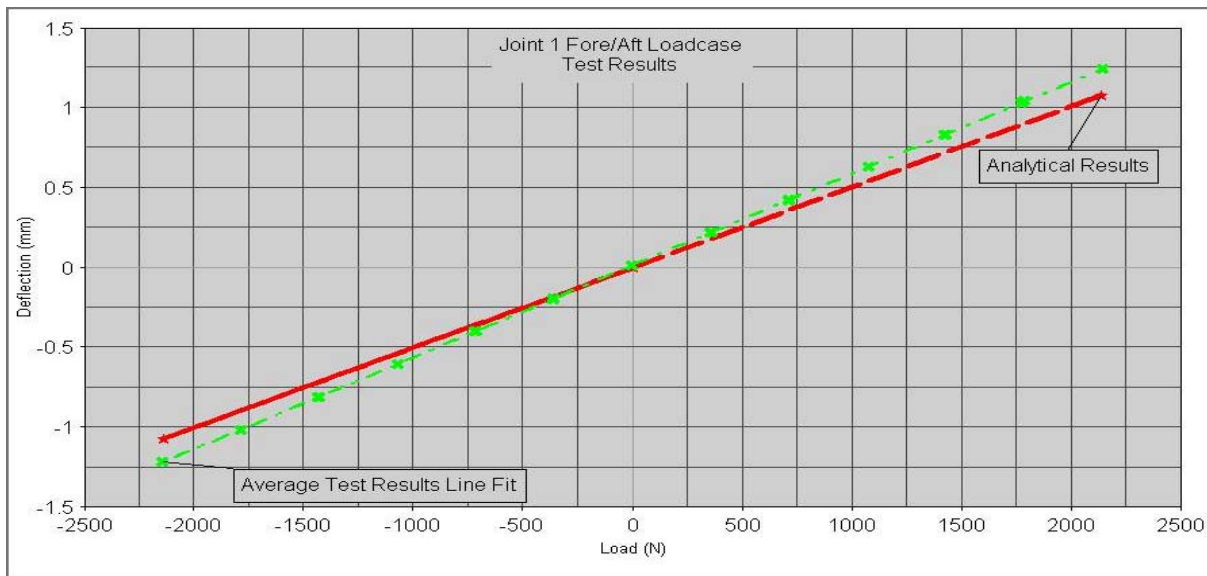
Figure 13: Force Deflection Curve of Joint 1 Evaluating Correlation of Test Data to Analytical Results
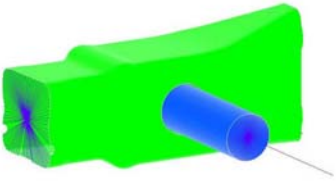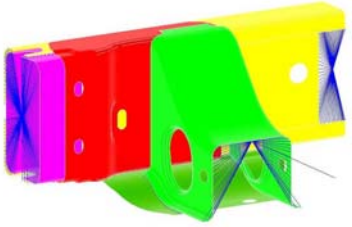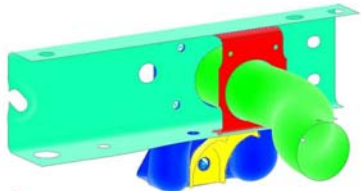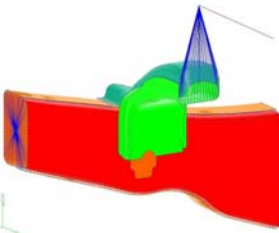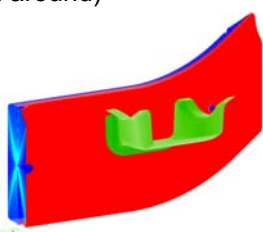
The torsional loadcases were evaluated in the same manner. The plots in these tests have a crossed pattern due to the positive and negative applied torque (Figure 14).
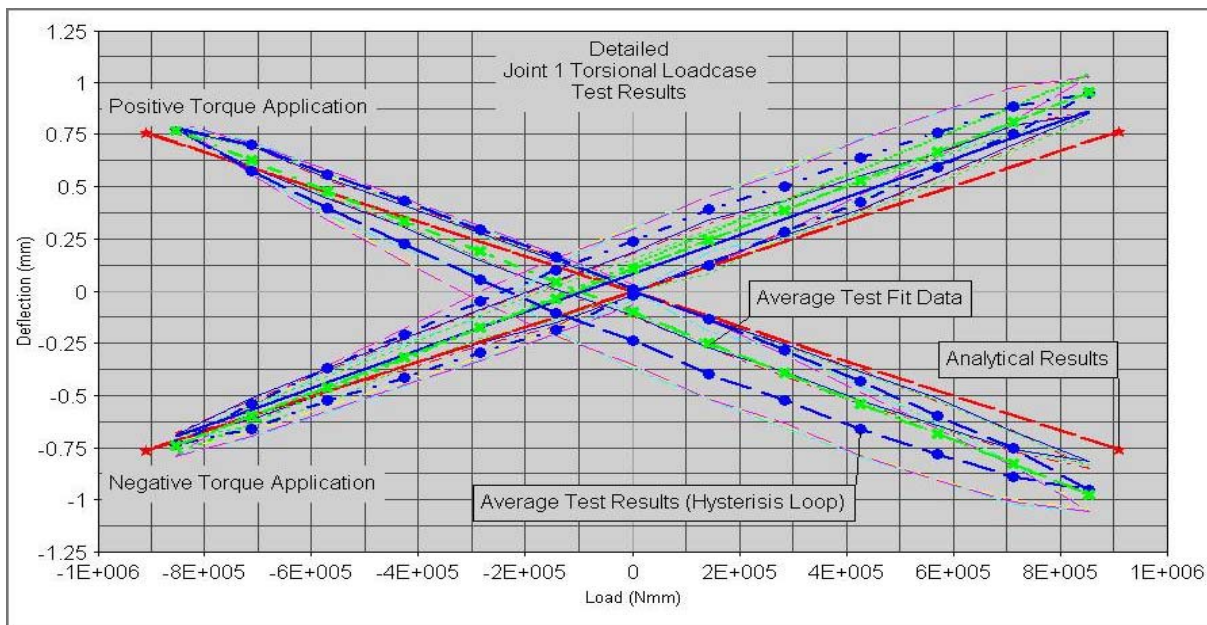
Figure 14: Force Deflection Curve Comparing Torsional Test Results

TESTING PROCEDURE

Table 2: Test Joint Stiffness Summary

	Kx	Ky	Kz
Joint 1: Tube- Through-Tube (welded at both ends)	2.563 KNm/deg	2.372 KNm/deg	2.573 KNm/deg
Joint 2: Box to Lipped Channel	8.415 KNm/deg	3.909 KNm/deg	50.429 KNm/deg
Joint 3: Tube Through Partially Boxed Section (welded on both sides)	1.940 KNm/deg	4.211 KNm/deg	2.979 KNm/deg
Joint 4: Alligator to box Section (welded to both flanges)	0.452 KNm/deg	1.081 KNm/deg	0.816 KNm/deg
Joint 5: Hat Section to Box Section (welded all around)	0.116 KNm/deg	0.180 KNm/deg	0.494 KNm/deg

CORRELATION

Introduction

Correlating the test and analysis results required multiple iterations. In the literature search, 15-30% was the average range of deviation between test and analysis. This average percent came from a combination of papers, including Fragoso, 1993. The joint stiffness study deviation between test and analysis is well within that range.
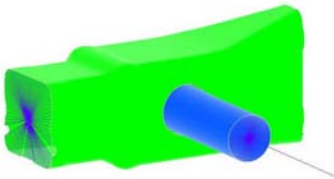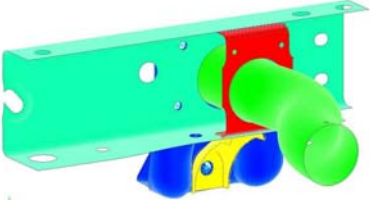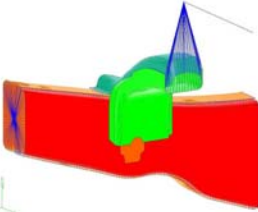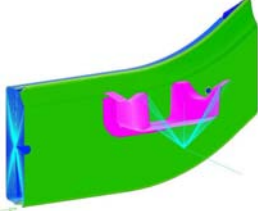
Correlating the Test and Analysis Data

Initially, the fixtures were modeled with rigid elements due to the assumed rigidity of the loading fixture, and the deflections were measured using similar triangles. This meant that the location, and in some cases, the direction of the deflections measured between test and analysis, were not the same. But through geometry, the same rotations and thus stiffness could be calculated. The problem with this approach is that because of out of plane rotations in the joint and a slight influence of the loading fixture on the deflection of the crossmember, the finite element model did not correlate well.

By including the fixture in the finite element model the deflections were measured at the same point as in the test. This proved to be critical for accurate test/analysis correlation and lowered our deviations by providing a more representative model of the physical test. The main deviation between the model and test occurred from not modeling surface contact at fixture interfaces, resulting in local deflection in the finite element model of the loading fixture base plate. Increasing plate thickness from 3/8 to 3/4 inch in both test and analysis and retesting resulted in good correlation between the two. The test data had not changed but the finite element analysis results were brought into the same range as the test results. The final percent difference between the test and analysis results is shown in Table 3. Graphs of each loadcase for the five joints, comparing the test and analytical results can be found in the appendix.

CORRELATION

Table 3: Test and Analysis Joint Stiffness Correlation Summary

	% Deviation Between Test and Analysis Joint Stiffness		
	Kx	Ky	Kz
Joint 1: Tube-Through-Tube (welded at both ends)	21.92%	-22.46%	2.39%
Joint 2: Box to Lipped Channel	-6.56%	-23.62%	23.32%
Joint 3: Tube Through Partially Boxed Section (welded on both sides)	2.12%	-24.36%	-3.96%
Joint 4: Alligator to Box Section (welded to both flanges)	-16.63%	-23.50%	-19.65%
Joint 5: Hat Section to Box Section (welded all around)	15.44%	-11.25%	5.79%

* The negative indicates analytical results lower than test

Introduction

An important requirement of the study was to establish a set of frame joint design rules. By using FEA, we were able to establish guidelines for the five joint types included in the study. The designer will be able to use the design rules to predict the stiffness of a joint that is similar to one of the five types in the study.

Study Model

To normalize the joints for the sensitivity study, the joint models needed to be modified. Geometric factors of the joint's surrounding structure were removed to eliminate its influence on the joint stiffness. These changes included straightening out the crossmember and side rail. Figure 8 shows the modified joint geometry compared to the original.
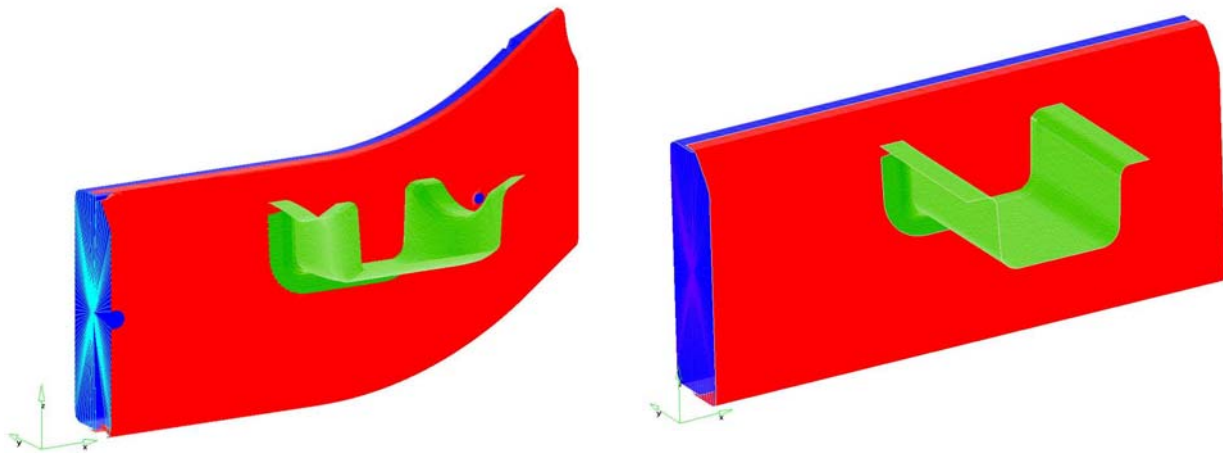
Figure 15: Example of Original Joint Geometry (left) vs. Modified Joint Geometry for Study (right)

Joint Parameters

The joint parameter variables are component thickness and shape. The thickness of each of the joint components is allowed to vary within a range of 2 to 4mm. The shape variables include:

- Side rail height
- Side rail width
- Crossmember height
- Crossmember width
- Flange width

The influence of the joint parameter on the stiffness of each load case is shown in Figures 16 through 30. For each plot, the Y-axis shows the relative stiffness. The X-axis, for each component listed, shows how the stiffness varied over the range of values allowed for each component. For example, the point furthest left of a parameter's plotted line would be the minimal allowed value for that parameter, and the point furthest right of the line would be the stiffness at the upper value for the specified parameter. (i.e. For the crossmember thickness in Figure 16, the stiffness is 2.5 when the crossmember thickness is lowest at 2mm and the stiffness of the joint is 4.8 when the crossmember thickness is 4mm).

Crossmember Thickness	Side Rail Thickness	Crossmember Tube Diameter	Side Rail Height	Side Rail Width
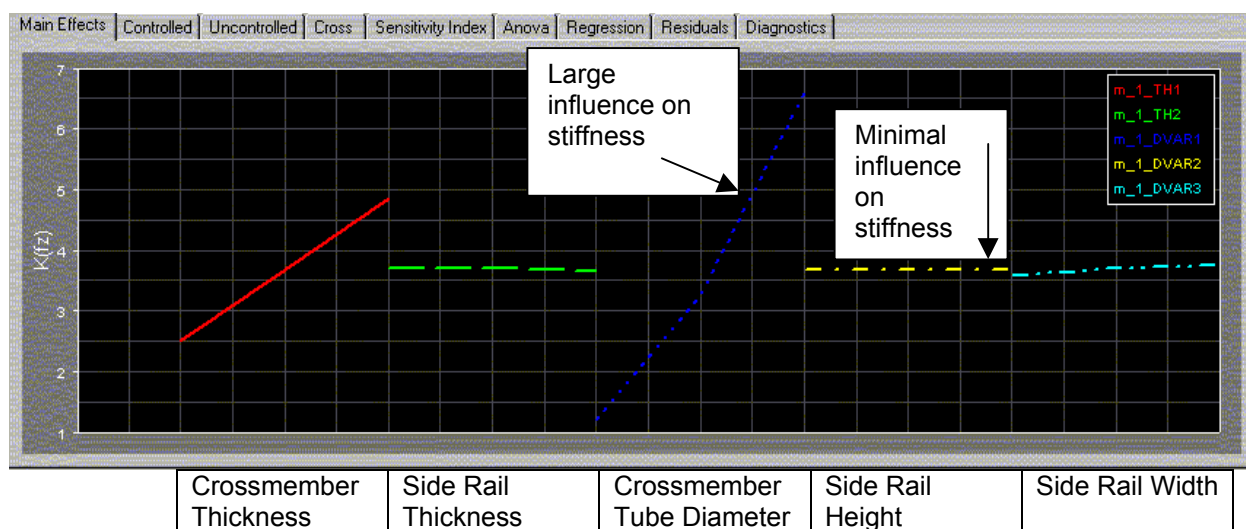
Figure 16: Main Effect Plot for Joint 1: Tube-Through-Tube Vertical Bending Stiffness $K_{\theta x}$

Crossmember Thickness	Side Rail Thickness	Crossmember Tube Diameter	Side Rail Height	Side Rail Width
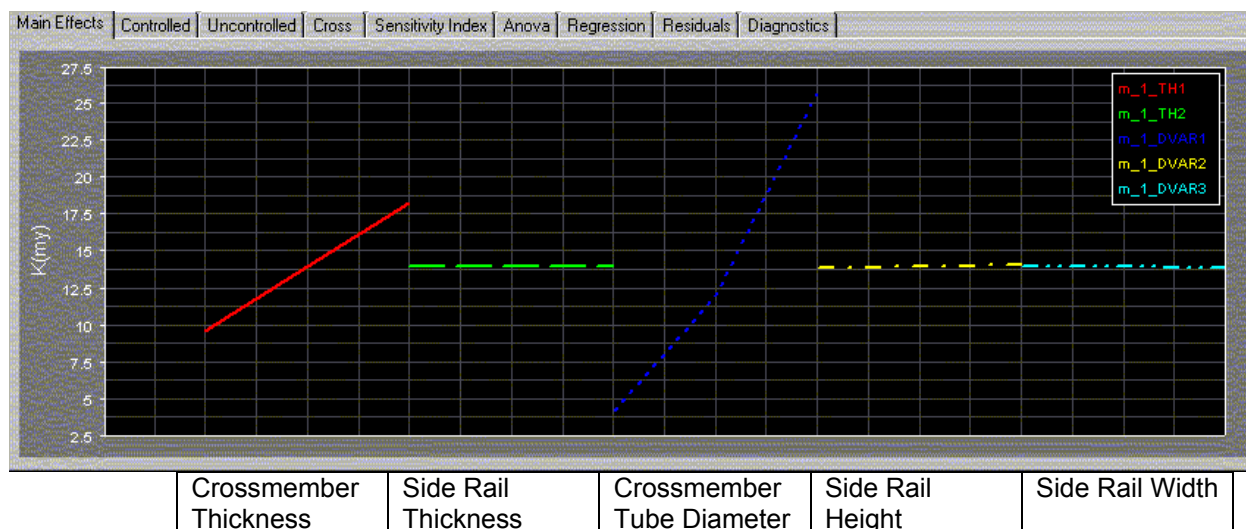
Figure 17: Main Effect Plot for Joint 1: Tube-Through-Tube Bending Stiffness $K_{\theta y}$

SENSITIVITY STUDY

Crossmember Thickness	Side Rail Thickness	Crossmember Tube Diameter	Side Rail Height	Side Rail Width
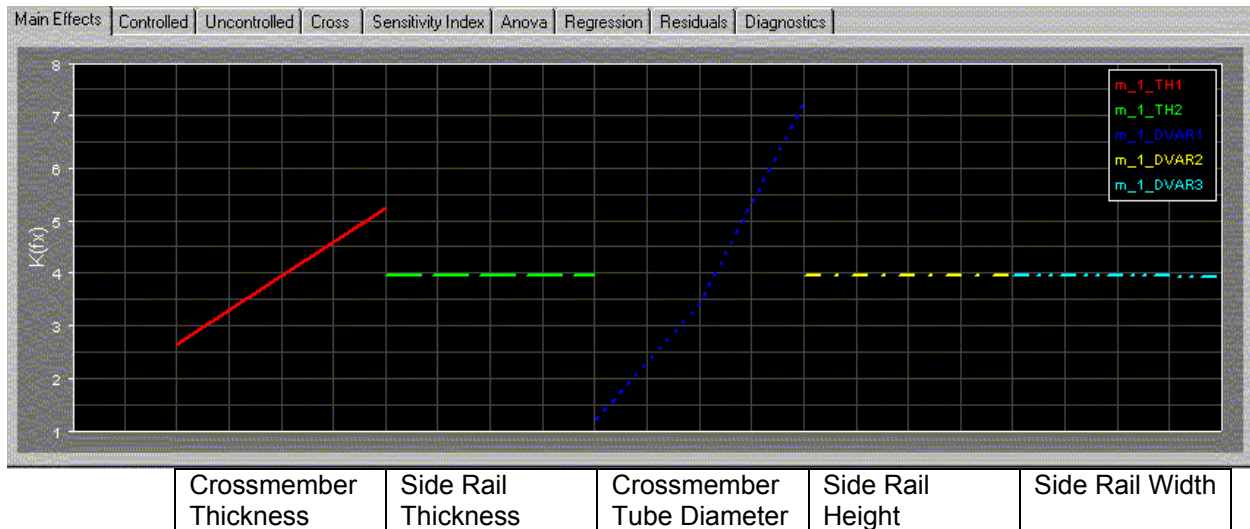
Figure 18: Main Effects Plot for Joint 1: Tube-Through-tube Fore/Aft Bending Stiffness $K_{\theta z}$

C-Channel Gage	Cross-member Gage	Cross-member Plate Gage	End Square Gage	Inner Rail Gage	Cross-member Width	Rail Width	Flange Width	Rail Height	Cross-member Height
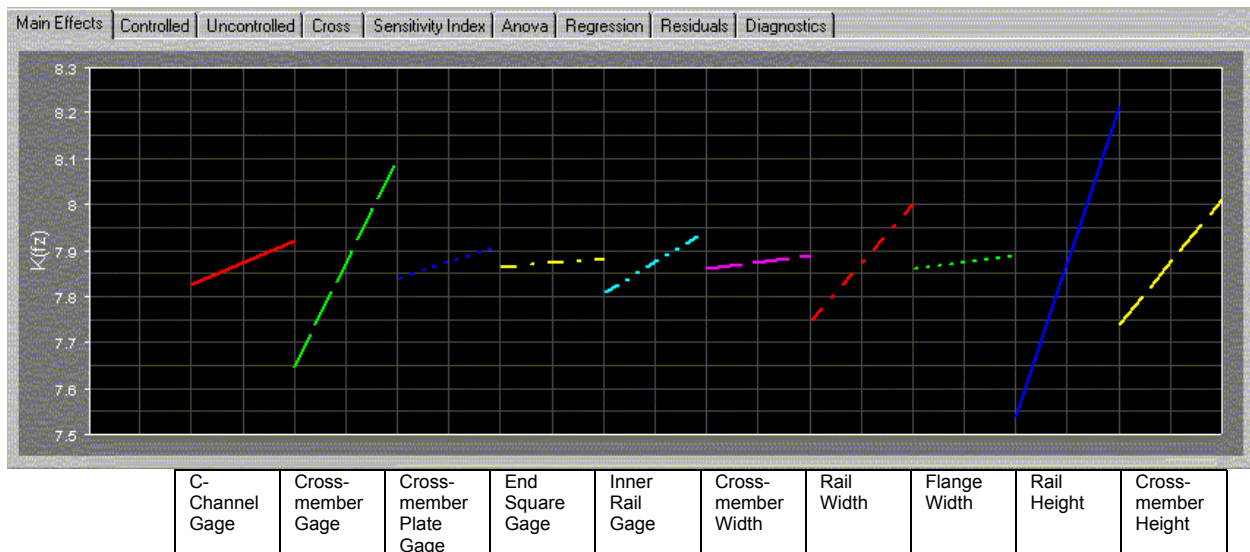
Figure 19: Main Effects Plot for Joint 2: Box to Lipped Channel Vertical Bending Stiffness $K_{\theta x}$

Altair Engineering
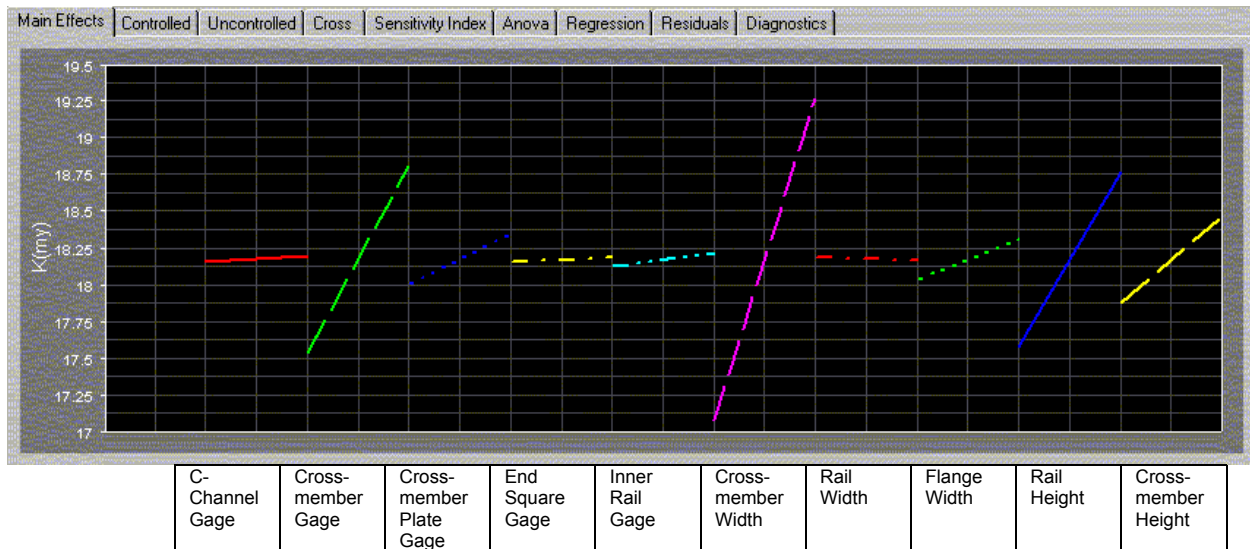
SENSITIVITY STUDY

Figure 20: Main Effects Plot for Joint 2: Box to Lipped Channel Bending Stiffness $K_{\theta y}$
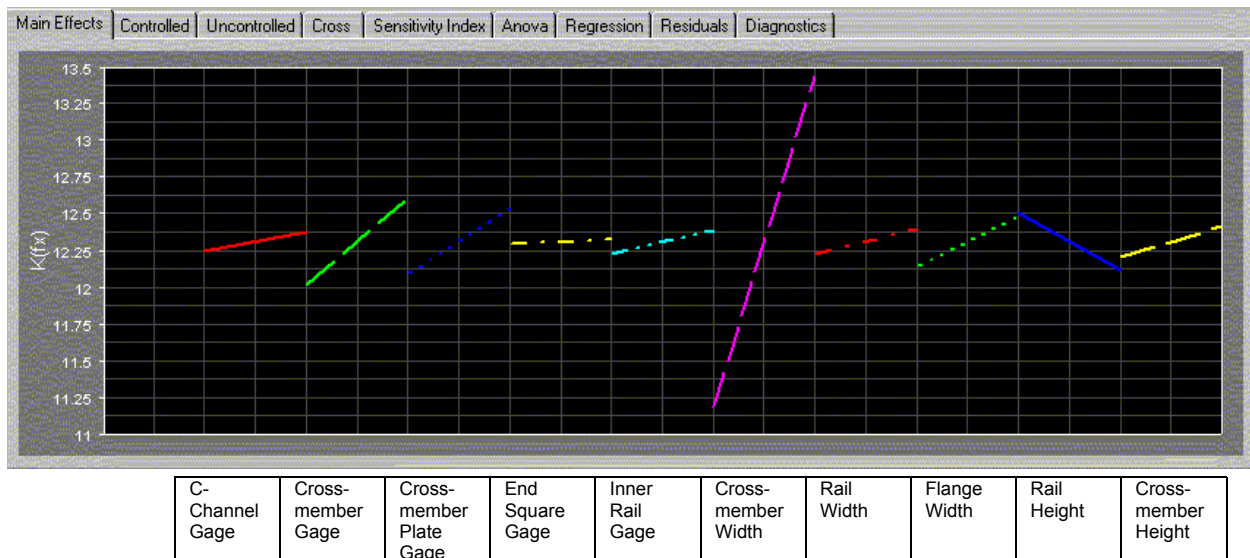
Figure 21: Main Effects Plot for Joint 2: Box to Lipped Channel Fore/Aft Bending Stiffness $K_{\theta z}$

SENSITIVITY STUDY
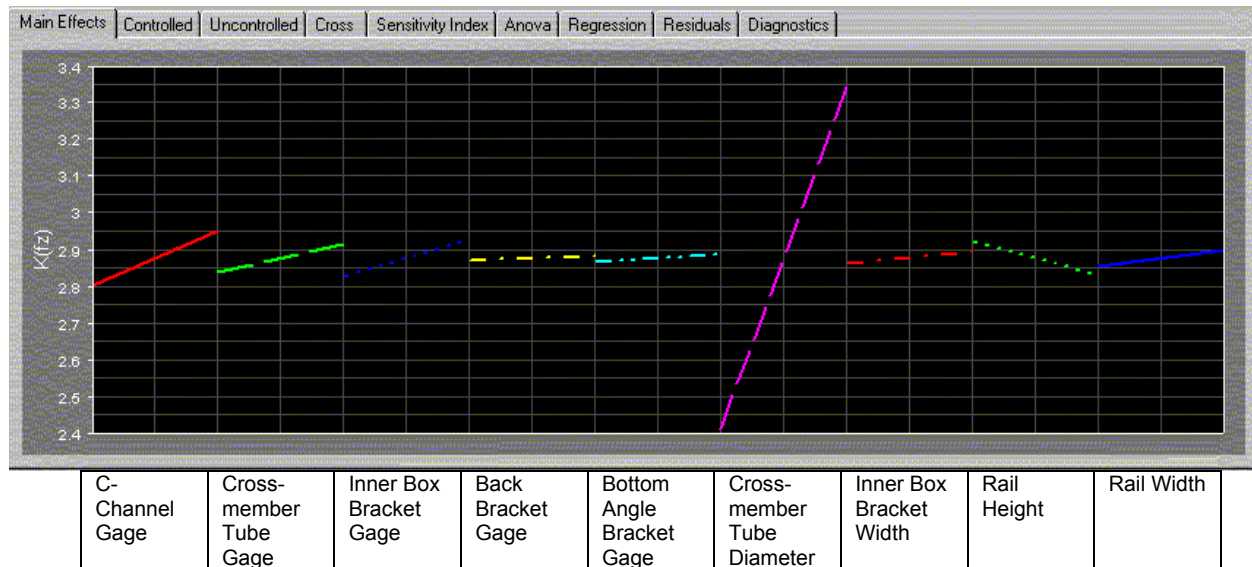
Figure 22: Main Effects Plot for Joint 3: Tube Through Tube Partially Boxed Section Vertical Bending Stiffness $K_{\theta x}$
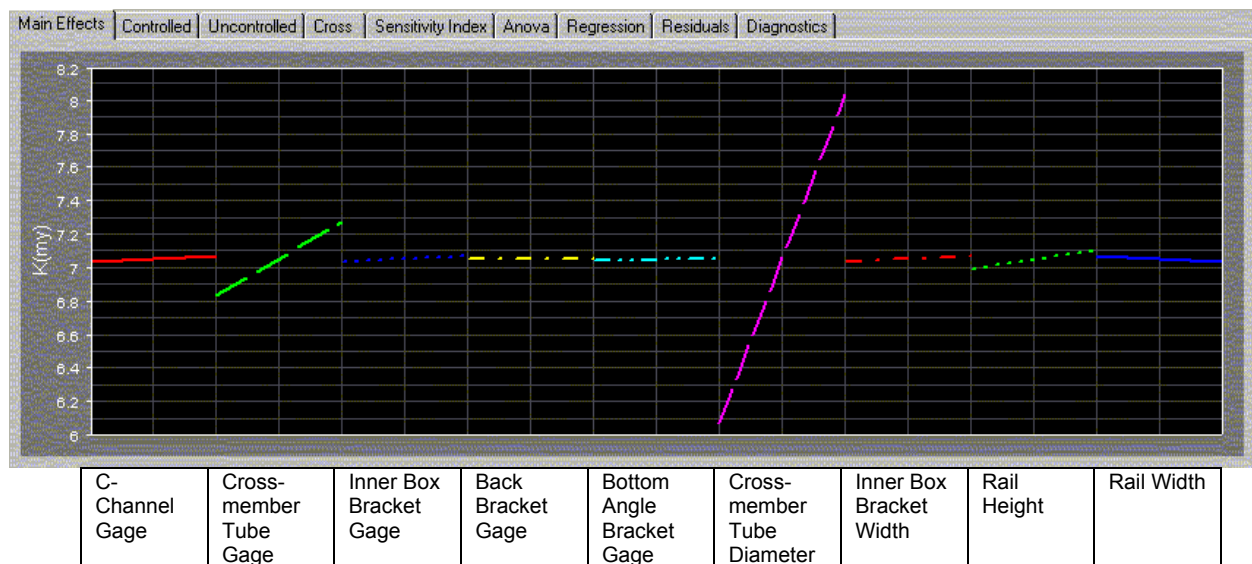
Figure 23: Main Effects Plot for Joint 3: Tube Through Tube Partially Boxed Section Bending Stiffness $K_{\theta y}$
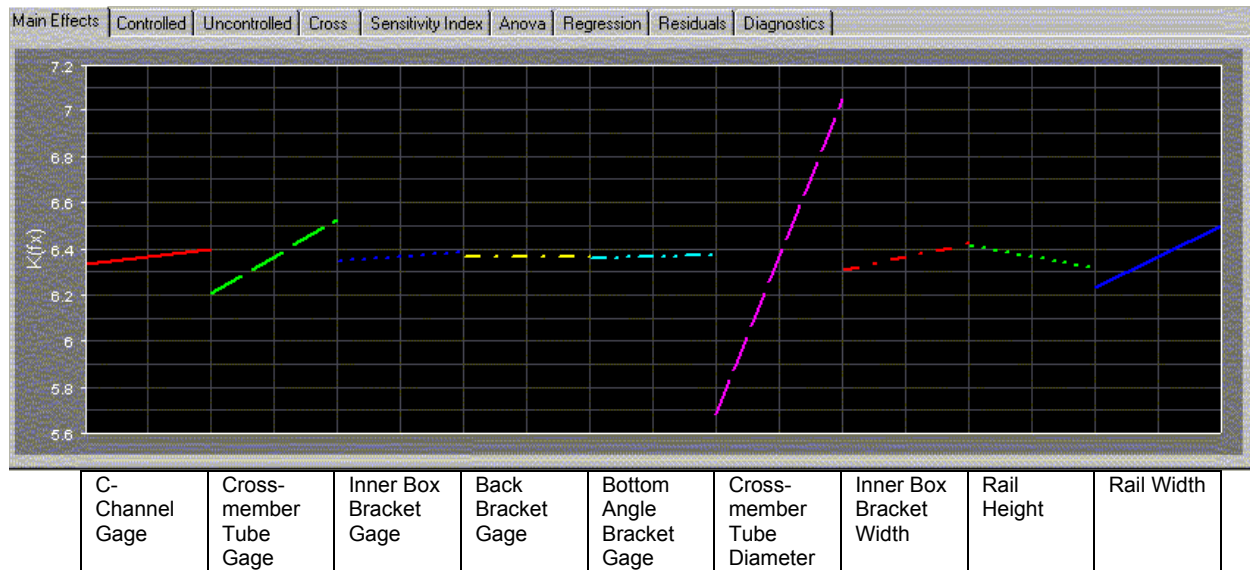
SENSITIVITY STUDY

Figure 24: Main Effects Plot for Joint 3: Tube Through Tube Partially Boxed Section Fore/Aft Bending Stiffness $K_{\theta z}$
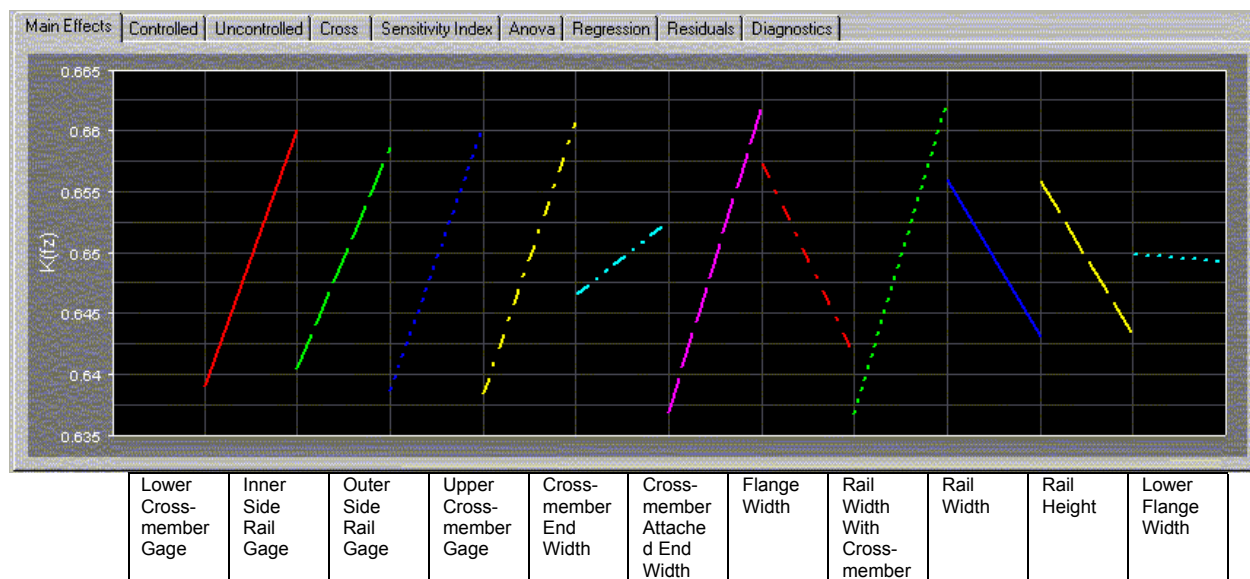
Figure 25: Main Effects Plot for Joint 4: Alligator to Box Section Vertical Bending Stiffness $K_{\theta x}$
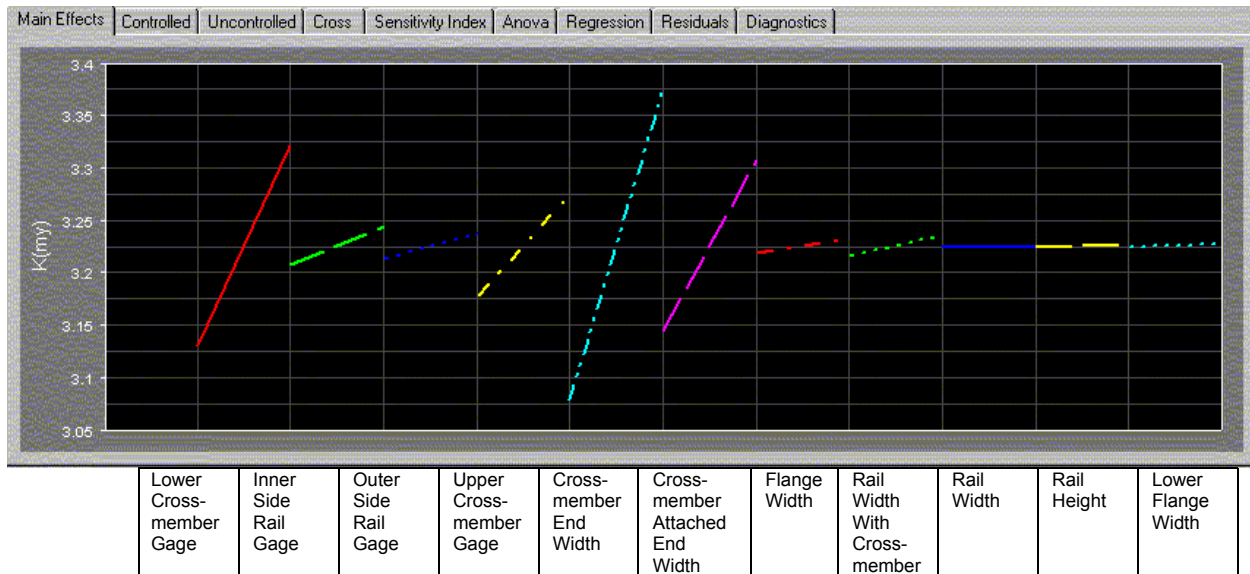
Figure 26: Main Effects Plot for Joint 4: Alligator to Box Section Bending Stiffness $K_{\theta y}$
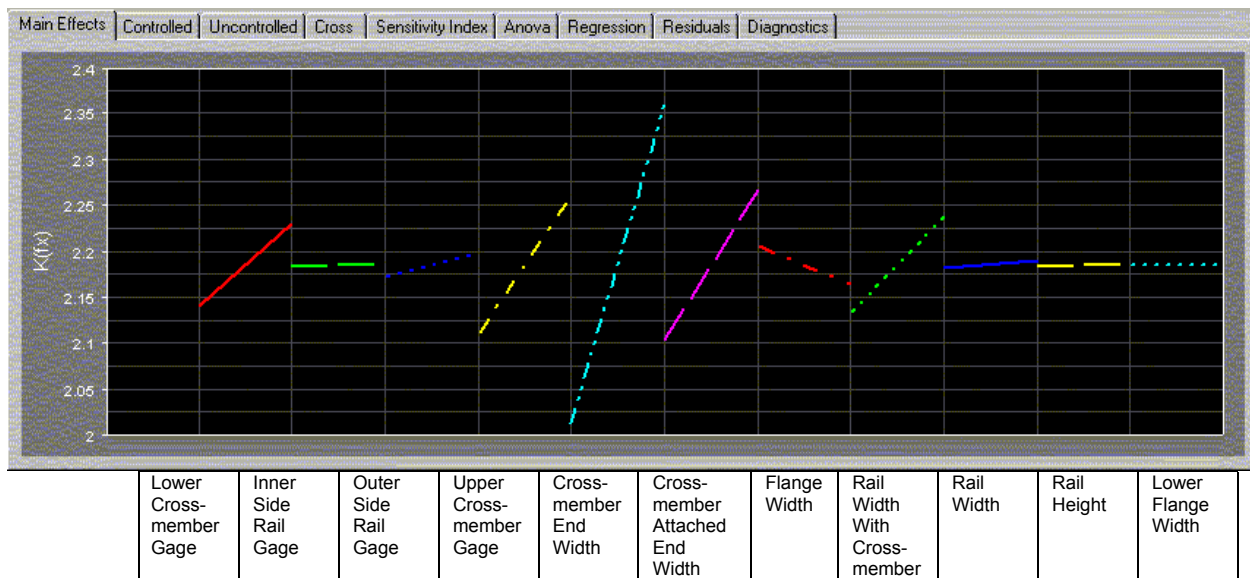
Figure 27: Main Effects Plot for Joint 4: Alligator to Box Section Fore/Aft Bending Stiffness $K_{\theta z}$

Figure 28: Main Effects Plot for Joint 5: Hat Section to Box Section Vertical Bending Stiffness K$_{\theta x}$
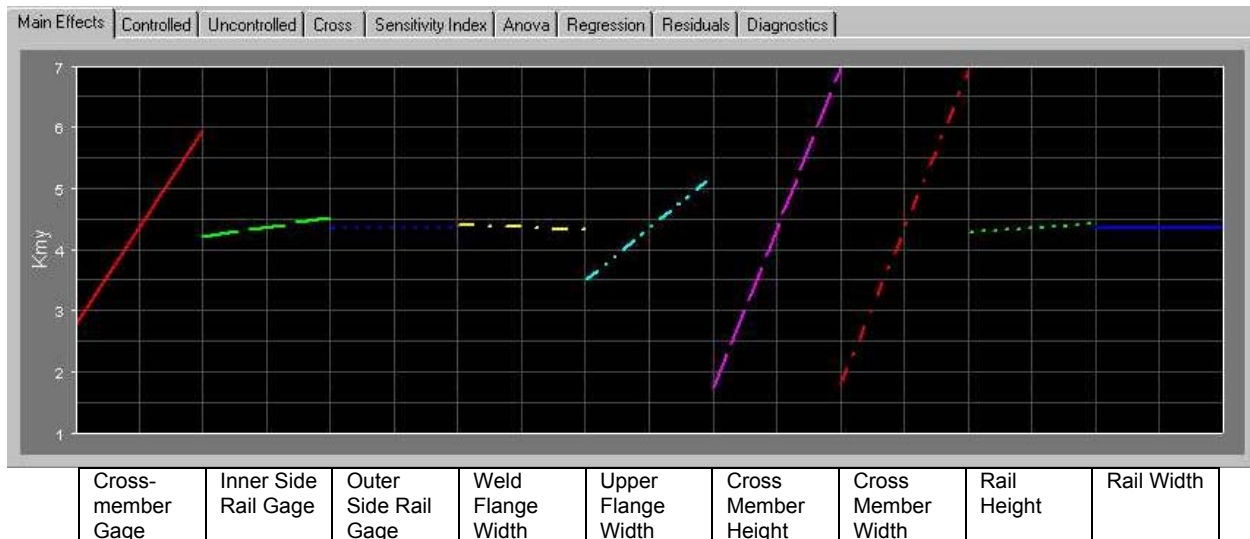
Figure 29: Main Effects Plot for Joint 5: Hat Section to Box Section Bending Stiffness K$_{\theta y}$

SENSITIVITY STUDY
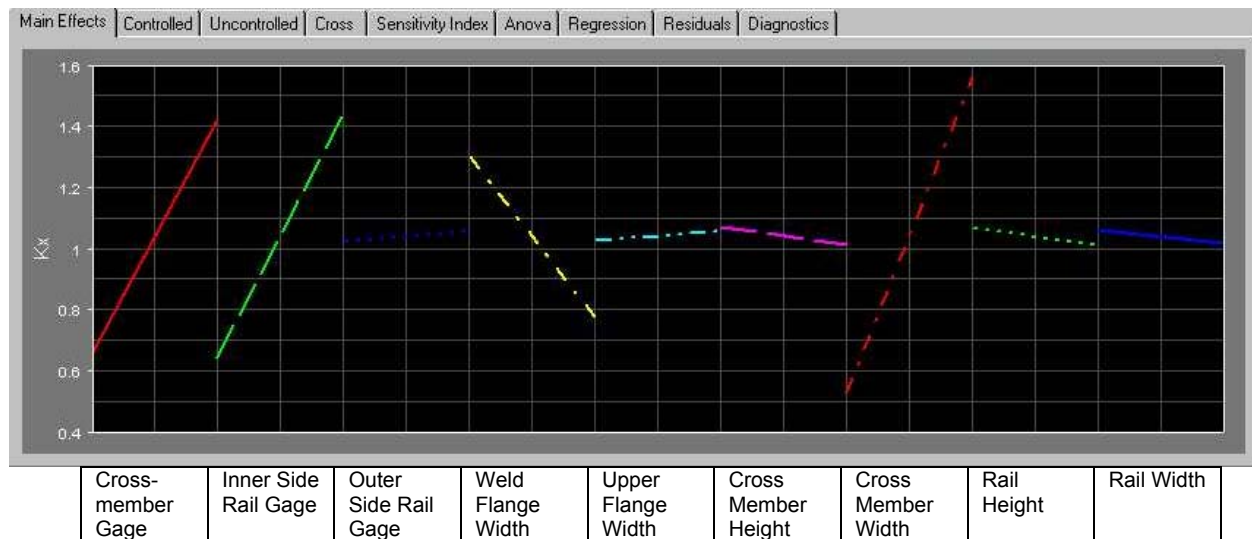
Figure 30: Main Effects Plot for Joint 5: Hat Section to Box Section Fore/Aft Bending Stiffness $K_{\theta z}$

JOINT STIFFNESS TOOLBOX

Introduction

A design experiment was run using the Altair StudyWizard. These experiments included consideration of the linearity of the joint parameters and the interactions between them on the joint stiffness. The mathematical response of each joint was programmed into an Excel spreadsheet. Designers and engineers will be able to enter joint dimensions, thickness, and any discrete variables simulated in the DOE, and obtain calculated joint stiffnesses. The Excel spreadsheet allows the user to input any joint definition that is within the DOE experiment range.

The spreadsheets also contain Design Rules and Observations to be considered when making design decisions. The Design Rules were created from finite element and sensitivity analysis data to help make stiffer joints. For example, in the case of Joints 1 and 3, where the crossmember is a round section, the design rules included two points: making the tube diameter as large as possible, and making the tube thickness as thick as large as possible. The Joint Observations contained information regarding joint deflection and welding information stemming from the analytical results.

An example overview of the spreadsheet is shown in Figure 31. The spreadsheet for each of the joints is shown in Figures 32 through 41 with two figures for each joint; the first figure shows the input and calculated results for the joint stiffness, and the second figure shows the joint observations, notes and design rules.

Figure 31: Example of the Joint Stiffness Toolbox Spreadsheet

JOINT STIFFNESS TOOLBOX

Joint #1: Tube Through Tube		Input (mm)				
Stiffness Calculations					Design Window	
	Design Variables (mm)	Case 1	Case 2	Test Joint	Min (mm)	Max (mm)
	Thickness					
	Crossmember	2.5	2.5	2.5	2	6
	Side Rail	2.8	2.8	2.8	2	6
Shape Animations	**Shape Variables (mm)**					
animations\	Crossmember Diameter	57	57	57	50	100
animations\	Side Rail Height	125	125	125	75	150
animations\	Side Rail Width	125	125	125	75	150

		Output			
Loading Animations	Stiffness Calculations	Case 1	Case 2	Test Joint	Units
animations\	Kx Bending Stiffness (Mx)	3.235	3.235	3.477	kN-m/deg
animations\	Ky Torsion Stiffness (My)	3.271	3.271	12.715	kN-m/deg
animations\	Kz Fore/Aft Stiffness (Mz)	3.507	3.507	3.662	kN-m/deg
	Mass	4.801	4.801	4.801	kg

Yellow cells are user input data.

Red cells are calculated numbers.

**Figure 32: Joint 1 Joint Stiffness Toolbox Spreadsheet
Input and Calculated Results**

JOINT STIFFNESS TOOLBOX
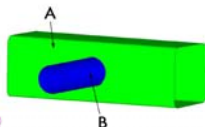
Illustration Key:
A = Side Rail
B = Crossmember

Design Rules:
* Make the crossmember diameter as large as possible.

* Make the crossmember as thick as possible.

* Thickness and diameter of the crossmember should be increased together if possible.

Joint Observations:
* The crossmember is the most important part of this joint. The thickness of the crossmember is 3X more sensitive than the thickness of the side rail.

* The maximum stress is in the crossmember at the connection to the inner side rail for all 3 Stiffness Cases.

* The outer weld (the crossmember to outer side rail) could be a partial weld because this section of the joint has low stress.

Notes:
* Modify the input values (yellow) based on your design criteria. There are two columns in which in to input and evaluate data, case 1 and case 2. The calculated stiffness will be displayed in red.

* Design variables are listed in order of influence on stiffness.

* Click on the animation to the left of the variables and loading conditions to see an animation of respective shape variable or loading condition.

* The mass calculation is based on 150 mm extension of joint members from the side rail to crossmember interface. (The crossmember is 150mm from the joint interface to the end of the crossmember). This caluclation is to serve as a reference, not the absolute value.

* The password to unprotect cells in this spreadsheet is: steel.

**Figure 33: Joint 1 Joint Stiffness Toolbox Spreadsheet
Joint Observations, Notes and Design Rules**

JOINT STIFFNESS TOOLBOX

Joint #2: Box to Lipped Channel Stiffness Calculations		Input (mm)				
Design Variables (mm)		**Case 1**	**Case 2**	**Test Joint**	**Design Window**	
					Min (mm)	**Max (mm)**
	Thickness					
	Inner Side Rail Thickness	3	3	3	2	6
	C Channel Rail Thickness	3.7	3.7	3.7	2	6
	Crossmember Thickness	3	3	3	2	6
	Crossmember Plate Thickness	3	3	3	2	6
	End Rail Square Thickness	3	3	3	2	6
Shape Animations	**Shape Variables (mm)**					
animations\	Crossmember Width	110	110	110	80	120
animations\	Side Rail Height	160	160	160	100	200
animations\	Crossmember End Height	95	95	95	75	200
animations\	Side Rail Width	65	65	65	50	100
animations\	Crossmember Plate Flange Width	40	40	40	20	60

Loading Animations	**Stiffness Calculations**	Output			
		Case 1	**Case 2**	**Test Joint**	**Units**
animations\	Kx Bending Stiffness (Mx)	40.944	40.944	40.944	kN-m/deg
animations\	Ky Torsion Stiffness (My)	79.040	79.040	79.040	kN-m/deg
animations\	Kz Fore/Aft Stiffness (Mz)	54.162	54.162	54.162	kN-m/deg
	Mass	7.007	7.007	7.007	kg

Yellow cells are user input data.

Red cells are calculated numbers.

Figure 34: Joint 2 Joint Stiffness Toolbox Spreadsheet Input and Calculated Results

JOINT STIFFNESS TOOLBOX

Illustration Key:
A = Side Rail End Square
B = Side Rail Plate
C = Crossmember
D = Side Rail C Channel

Design Rules:
* Increase crossmember thickness to increase stiffness in all three directions.

* Increase crossmember thickness to increase stiffness in all three directions.

* Increasing the side rail height increases the stiffness in the Bending (Kx) and Torsional (Ky) loading directions, but decreases the stiffness in the Fore/Aft (Kz) direction.

* All of the other design variables have a small, but significant impact on the joint stiffness.

Notes:
* Modify the input values (yellow) based on your design criteria. The calculated stiffness will be displayed in red.

* Design variables are listed in order of influence on stiffness.

* Click on the animation to the left of the variables and loading conditions to see an animation of respective shape variable or loading condition.

* The mass calculation is based on 150 mm extension of joint members from the side rail to interface. This is to serve as a reference, not the absolute value.

* The password to unprotect cells in this spreadsheet is: steel.

Joint Observations
* Fore/aft compliance is a combination of deflections in the crossmember, bottom reinforcement, and side rail after wall. The max stress occurs at the top and bottom corners of the crossmember.

* Vertical compliance is a combination of side rail, crossmember and bottom plate deflection.

* Torsion compliance is mostly in the crossmember and is probably higher because of the hole in the crossmember. High stress occurs in the bottom reinforcement plate at the weld temination and the top of the side rail.

* Thickness Importance: Crossmember thickness then outer Side Rail and plate thickness.

Figure 35: Joint 2 Joint Stiffness Toolbox Spreadsheet
Joint Observations, Notes and Design Rules

JOINT STIFFNESS TOOLBOX

Joint #3: Tube Through Partially Boxed Section Stiffness Calculations		Input (mm)			Design Window	
	Design Variables (mm)	Case 1	Case 2	Test Joint	Min (mm)	Max (mm)
	Thickness					
	Crossmember Tube Thickness	2.5	2.5	2.5	2	6
	Side Rail Thickness	3.5	3.5	3.5	2	6
	Inner Crossmember Support Bracket Thickness	3	3	3	2	6
Shape Animations	**Shape Variables (mm)**					
animations\	Crossmember Tube Diameter	72	72	72	50	120
animations\	Side Rail Height	128	128	128	60	150
animations\	Crossmember Bracket Width	104	104	104	95	200
animations\	Side Rail Width	67	67	67	50	100
		Output				
Loading Animations	**Stiffness Calculations**	Case 1	Case 2	Test Joint	Units	
animations\	Kx Bending Stiffness (Mx)	2.642	2.642	8.145	kN-m/deg	
animations\	Ky Torsion Stiffness (My)	6.499	6.499	0.708	kN-m/deg	
animations\	Kz Fore/Aft Stiffness (Mz)	5.913	5.913	6.660	kN-m/deg	
	Mass	5.666	5.666	5.692	kg	

Yellow cells are user input data.

Red cells are calculated numbers.

**Figure 36: Joint 3 Joint Stiffness Toolbox Spreadsheet
Input and Calculated Results**

JOINT STIFFNESS TOOLBOX

Illustration Key:
A = Side Rail
B = Crossmember Support Bracket
C = Crossmember

Design Rules:
* Make the crossmember diameter as large as possible.

* The crossmember and side rail thickness are the second most important design variables.

Notes:
* Modify the input values (yellow) based on your design criteria. The calculated stiffness will be displayed in red.

* Design variables are listed in order of influence on stiffness.

* Click on the animation to the left of the variables and loading conditions to see an animation of respective shape variable or loading condition.

* The mass calculation is based on 150 mm extension of joint members from the side rail to interface. This is to serve as a reference, not the absolute value.

* The password to unprotect cells in this spreadsheet is: steel.

**Figure 37: Joint 3 Joint Stiffness Toolbox Spreadsheet
Joint Observations, Notes and Design Rules**

JOINT STIFFNESS TOOLBOX

Joint #4: Alligator to Box Section

Stiffness Calculations		Input (mm)				
	Design Variables (mm)	Case 1	Case 2	Test Joint	Design Window Min (mm)	Max (mm)
	Thickness					
	Lower Crossmember Thickness	3.2	3.2	3.2	2	6
	Outer Side Rail Thickness	3.2	3.2	3.2	2	6
	Upper Crossmember Thickness	3.2	3.2	3.2	2	6
	Inner Side Rail Thickness	3.2	3.2	3.2	2	6
Shape Animations	**Shape Variables (mm)**					
animations\	Crossmember End Width	65	65	65	50	100
animations\	Crossmember Attach End Width	85	85	85	50	100
animations\	Rail Width	65	65	65	50	100
animations\	Upper Flange Width	10	10	10	5	45
animations\	Rail Height	115	115	115	100	130
animations\	Lower Flange Width	10	10	10	5	30

Loading Animations	Stiffness Calculations	Output			
		Case 1	Case 2	Test Joint	Units
animations\	Kx Bending Stiffness (Mx)	0.617	0.617	0.617	kN-m/deg
animations\	Ky Torsion Stiffness (My)	3.053	3.053	3.053	kN-m/deg
animations\	Kz Fore/Aft Stiffness (Mz)	2.175	2.175	2.175	kN-m/deg
	Mass	4.680	4.680	4.680	kg

Yellow cells are user input data.

Red cells are calculated numbers.

**Figure 38: Joint 4 Joint Stiffness Toolbox Spreadsheet
Input and Calculated Results**

JOINT STIFFNESS TOOLBOX

Illustration Key:
A = Upper Crossmember
B = Outer Side Rail
C = Lower Crossmember
D = Inner Side Rail

Design Rules:
* These are the major contributors to the joint stiffness:
   - Crossmember thickness
   - Crossmember end width
   - Crossmember attached end width

* These are the minor contributors to the joint stiffness:
   - Inner side rail thickness
   - Outer side rail thickness
   - Upper crossmember thickness
   - Flange width
   - Side rail width
   - Side rail height

Notes:
* Modify the input values (yellow) based on your design criteria. There are two columns in which in to input and evaluate data, case 1 and case 2. The calculated stiffness will be displayed in red.

* Design variables are listed in order of influence on stiffness.

* Click on the animation to the left of the variables and loading conditions to see an animation of respective shape variable or loading condition.

* The password to unprotect cells in this spreadsheet is: steel.

Joint Observations:
* The mass calculation is based on 150 mm extension of joint members from the side rail to interface. This is to serve as a reference, not the absolute value.

* Flanges on top of the side rail deflect quite a bit (local deflection).

* Lot of local deflection in the crossmember as it bends upward near the rail…Tying the crossmember together more would increase the stiffness.

Vertical Loadcase (Mx)
* There is significant deflection in the inside rail wall where the crossmember connects to the side rail.

* Slight Deflection in the top side rail.

* Stiffness would increase if the crossmember was welded together more in the area near the side rail.

Torsional Loadcase (My)
* Flanges aredeflecting in both crossmembers where they attach to the side rail.

* The stiffness would increase if the crossmembers were welded more at the joint.

Figure 39: Joint 4 Joint Stiffness Toolbox Spreadsheet
Joint Observations, Notes and Design Rules

JOINT STIFFNESS TOOLBOX

Joint #5: Hat Section to Box Section

Stiffness Calculations		Input (mm)				
				Test Joint	Design Window	
	Design Variables (mm)	Case 1	Case 2		Min (mm)	Max (mm)
	Thickness					
	Crossmember Thickness	2.5	2.5	2.5	2	6
	Inner Rail Thickness	2.5	2.5	2.5	2	6
	Outer Rail Thickness	2.5	2.5	2.5	2	6
Shape Animations	**Shape Variables (mm)**					
animations\	Crossmember Height	65	65	65	45	85
animations\	Weld Flange Width	15	15	15	10	30
animations\	Side Rail Height	210	210	210	190	230
animations\	Upper Flange Width	18	18	18	10	45
animations\	Crossmember Width	110	110	110	90	130
animations\	Side Rail Width	65	65	65	55	75

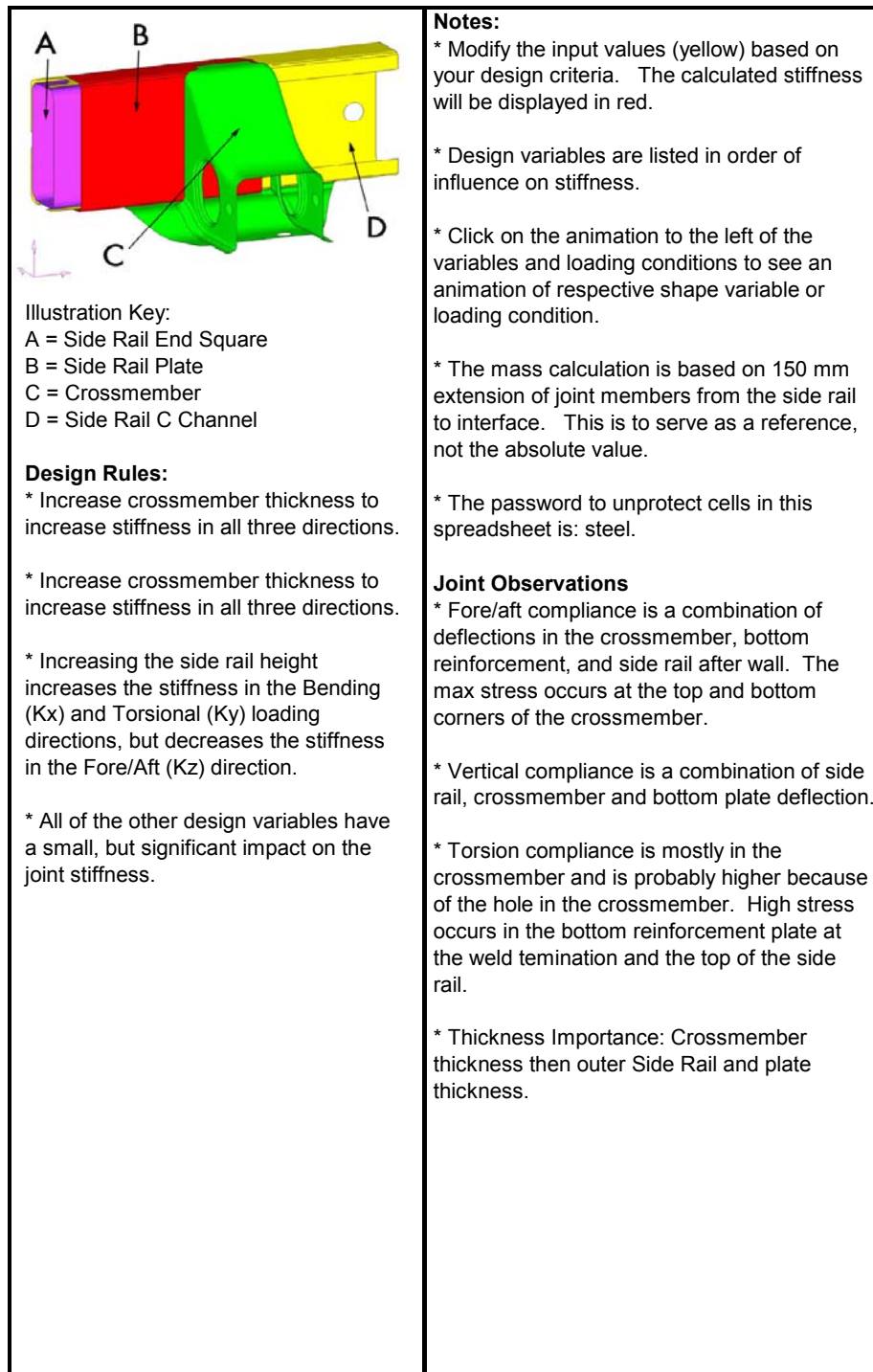| Loading Animations	Stiffness Calculations	Output			
		Case 1	Case 2	Test Joint	Units
animations\	Bending Stiffness (Mx)	0.773	0.773	0.773	kN-m/deg
animations\	Torsion Stiffness (My)	1.318	1.318	1.318	kN-m/deg
animations\	Fore/Aft Stiffness (Mz)	0.995	0.995	0.995	kN-m/deg
	Mass	6.053	6.053	6.053	kg

Yellow cells are user input data.

Red cells are calculated numbers.

**Figure 40: Joint 5 Joint Stiffness Toolbox Spreadsheet
Input and Calculated Results**

JOINT STIFFNESS TOOLBOX

Illustration Key:
A = Outer Rail
B = Inner Rail
C = Crossmember

Design Rules:
* These are the major contributors to the joint stiffness:
   - Crossmember thickness
   - Inner side rail thickness
   - Crossmember height
   - Crossmember width

* The weld flange should be as small as possible.

Notes:
* Modify the input values (yellow) based on your design criteria. There are two columns in which in to input and evaluate data, case 1 and case 2. The calculated stiffness will be displayed in red.

* Design variables are listed in order of influence on stiffness.

* Design variables are listed in order of influence on stiffness.

* Click on the animation to the left of the variables and loading conditions to see an animation of respective shape variable or loading condition.

* The mass calculation is based on 150 mm extension of joint members from the side rail to interface. This is to serve as a reference, not the absolute value.

* The password to unprotect cells in this spreadsheet is: steel.

Joint Observations:

Fore/Aft Loadcase (Mz)
* Lots of flange deflection in the crossmember and siderail.

* Side rail wall also has a lot of deflection.

Vertical Loadcase (Mx)
* Crossmember flange deflects quite a bit, especially at the top.

* Side rail wall deflects a lot.

* Side rail wall also has a lot of deflection.

Torsional Loadcase (My)
* Weak in torsion because the crossmember is an open section.

* There is a lot of flange deflection.

* The top flanges do not attach to anything-attaching to the side rail would increase the stiffness.

Figure 41: Joint 5 Joint Stiffness Toolbox Spreadsheet
Joint Observations, Notes and Design Rules

REFERENCES

1. Bernuzzi, C.; Zandonini, R.; and Zanon, P.: "Experimental Analysis and Modeling of Semi-rigid Steel Joints Under Cyclic Reversal Loading," Journal of Constructional Steel Research v38 n2 Jun 1996 Elsevier Science Ltd Oxford Engl p. 95-123 0143-974X JCSRDL

2. Chen, T.Y. and Zhang, H-Y.: "Stress Analysis of Spatial Frames with Consideration of Local Flexibility of Multiplanar Tubular Joint," Engineering Structures, June 1996

3. Chiew, S.P.; Soh, C.K.; Soh, A.K.; Fung, T.C.; and Lee, W.M.: "SCF Design Equations For Steel Maltiplanar Tubular XT-Joints," The Structural Engineer; July 1996

4. Davison, J.B.; Kirby, P.A.;and Nethercot, D.A.: "Rotational Stiffness Characteristics of Steel Beam-to-Column Connections," Construction Steel Research, 1987

5. Hull, Frederick: "Van Frame Structural Evaluation," SAE paper 790988; 1979

6. Korol R.M., Mansour M.H.: "Theoretical Analysis of Haunched-Reinforced T-Joints in Square Hollow Sections," Canadian Journal of Civil Engineering; Dec. 1979;

7. Korol, R.M.; Zanaty, M.E.; and Brady, F.J.: "Unequal Width Connections of Square Hollow Sections in Vierendeel Trusses," Canadian Journal of Civil Engineering, June 1977

8. Liew, J.Y.R.; Yu, C.H.; Ng, Y.H.; and Shanmugam, N.E.: "Testing of Semi-Rigid Unbraced Frames for Calibration of Second-Order Inelastic Analysis," Journal of Constructional Steel Research; No. 2/3

9. Lui, E. M. and. Chen, W. F: "Steel Frame Analysis with Flexible Joints," Journal of Constructional Steel Research; 1998

10. Michejda, Oskar: "Truck Frame Analysis Study," SAE paper 710594; 1971

11. Mourad, S.; Korol, R.M.; and Ghobarah, A.: "Design of Extended End-Plate connections for Hollow Section Columns," Canadian Journal of Civil Engineering, February 1996

12. Van Wingerde, A. M.: "The Fatigue Behavior of T- and X-Joint Made of Square Hollow Sections," Heron; vol 37 no. 2; 1992

13. Yeoh S-K., Soh A-K., Soh C-K.: "Behavior of Tubular T-Joints Subjected To Combined Loadings," Journal of Constructional Steel Research; 1995

14. Kim, Yoon Young; Yim, Hong Jae; Kang, Jeong Hoon; and Kim,Jin Hong: "Reconsideration of the Joint Modelling Technique: In a Box-Beam T-Joint," SAE Paper 951108

APPENDIX A: ABSTRACTS

Read Articles

1. **Experimental Studies and Design of Steel Tee Shear Connections**
   Astaneh, Abolhassan,and Nader, Marwan N.
   Journal of Structural Engineering v 116 n 10 Oct 1990 p. 2882-2902 0733-9445 JSENDH 15

   A tee-framing shear connection consists of a steel tee section connected to a beam web and to a supporting member such as a column. The main role of the tee-framing shear connections is to transfer end shear reaction of simply supported beams to the supporting members. Usually, bolt groups or weld lines are used to connect the tee element to the beam web and to the support. An experimental investigation of the actual behavior of tee-framing shear connections is conducted by testing nine full-size beam-to-column-joint assemblies. The connections are subjected to realistic combinations of shear forces and rotations. The research establishes six failure modes for these connections. The studies indicate that the tee-framing connections tested are sufficiently flexible to be considered simple connections. A summary of the experimental research is presented. The experimental data and associated analytical studies are used to adapt mechanical models of the failures and to develop and propose new design procedures.

2. **A Numerical Approach to Define the Rotational Stiffness of a Prefabricated Connection and Experimental Study.**
   Aydogan, M. and Akoz, A.Y.
   Computers & Structures, 1995

   A numerical approach is proposed to define the elastic rotational stiffness of a typical joint on the top beam of a prefabricated reinforced concrete gable frame structure. The 12 degrees of freedom triangular plane stress finite element is used to examine the connection region. Using this joint rotational stiffness value, realistic results are obtained in the frame analysis. The experimental verification is performed by means of the photoelastic method. Following the proposed method, an effective joint length with reduced moment of inertia is defined and using this concept the frame solution is simply achieved, including the existence of joint.

3. **Initial Stiffness of Semi-Rigid Steel Beam-to-Column Connections**
   Azizinamini, J.; Bradburn, H.; and Radziminski, J. B.
   Journal of Constructional Steel Research; 1987

   Semi-rigid connections of the type studied in this investigation are distinguished by moment-rotation curves which become non-linear relatively early during static loading. However, the connections exhibited linear unloading behavior, a linearity that was retained as moment was reapplied, to a maximum approaching that imposed during the initial load application. The slope of this latter curve was found to be essentially the same as the initial slope of the moment-rotation curve during first loading. Thus, the initial slope is of direct significance from a design viewpoint, in that it can be used to represent the stiffness of the connection in the analysis of the complete structural system, particularly under live load fluctuations. In this paper, an analytical procedure is developed to predict the initial stiffness of a particular type of semi-rigid connection; the predicted slopes were found to compare favorably with experimentally determined connection behavior.

4. **Experimental Analysis and Modelling of Semi-Rigid Steel Joints Under Cyclic Reversal Loading**
Bernuzzi, C.; Zandonini, R.; and Zanon, P.
Journal of Constructional Steel Research v38 n2 Jun 1996 Elsevier Science Ltd Oxford Engl p. 95-123 0143-974X JCSRDL

This paper reports on the first phase of a research project aimed at developing simple design criteria for semi-rigid steel frames in seismic zones. The experimental phase comprised of two series of tests on beam-to-column joints under cyclic reversal loading. The evaluation of the test results first allowed the influence of the loading history to be investigated and the main stiffness and strength parameters to be identified, which define the cyclic response of the connection. A simple prediction model was then developed and proposed, which enables satisfactory approximation of the joint response for use in numerical analysis.

5. **Finite Element Dynamic Analysis of an Automotive Frame**
Borowski,V. J.; Steury, R. L.; and Lubkin, J. L.
SAE Paper 730506; 1973

Using several variations of a basic finite element, the dynamic displacement response and mode shapes of an automotive frame have been predicted. Small improvements in accuracy were noted when higher-order mass representation and allowance for shear deformation were included in the analysis. Modeling accuracy was significantly increased however, by including certain effects that are normally ignored. These include an allowance for the less-than-perfect rigidity of side rail-to-crossmember joints; for the torsional behavior of short, open cross-section beams; and for the reduction of flexural inertia in welded, double-channel cross-sections. With the introduction of these factors, the predicted natural frequencies for the first eight flexural modes can be correlated with test results to within 4%. For this level of agreement, the finite element model appears to be sufficiently accurate to be used in design evaluation of frames, prior to prototype construction.

6. **Experimental and Numerical Stress Analyses of Tubular XT-Joint**
Chiew, S.P ; Soh, C.K.; and Wu, N.W. (Nanyang Tech. University, Singapore)
ASCE Journal of Structural Engineering; Nov 1999

A typical large-scale, steel, multiplanar tubular XT-joint specimen was tested, with its in-plane and out-or-plane braces subjected to a total of 11 different load cases comprising the basic axial loading as welt as axial loadings combined with in-plane-bending (IPB) and out-of-plane-bending (OPB) moments. The stress concentration factors (SCFs), strain concentration factors (SNCFs), and the SCF-to-SNCF ratio (S/N Ratio) at the potential hot spot stress locations were investigated. An average S/N Ratio of 1.16 was derived from all the test load cases. The SCFs at typical hot spot locations were also calculated using finite-element (FE) analysis. The good agreement between the numerical and the experimental SCF results confirmed the reliability of the numerical modeling of the XT-joint. In addition, the writers' SCF results were compared with Efthymiou's influence function (IF) method and the ones derived from the corresponding uniplanar T-/X-joints. A clearer understanding of the significance of the multiplanar effects for fatigue design was obtained through this comparison study.

APPENDIX A: ABSTRACTS

7. **SCF Design Equations For Steel Maltiplanar Tubular XT-Joints**
   Chiew, S.P.; Soh, C.K.; Soh, A.K.; Fung, T.C.; and Lee, W.M.
   The Structural Engineer; July 1996

   A parametric study of hotspot stresses in multiplanar tubular XT-joins has been conducted in which 180 finite element analyses were performed. The study covers a wide range of joint geometries under various combinations of axial forces. The results of the analyses are presented as a set of equations expressing the stress concentration factor as a function of the relevant geometric parameters for various combinations of axial forces. A typical full-size steel multiplanar XT-joint was selected for experimental testing to verify the numerical analyses. A comparison is also made between the results obtained for multiplanar tubular XT-joints and those of the corresponding uniplanar T-and X-joints. It was found that, when all the braces of the multiplanar effect is significant. When the out-of-plane braces are not loaded, the multiplanar effect is insignificant for small ß value when the comparison is made between the multiplanar XT-joints with uniplanar T-joints.

8. **Stress Analysis of Spatial Frames with Consideration of Local Flexibility of Multiplanar Tubular Joint**
   Chen, T.Y. and Zhang, H.Y.
   Engineering Structures, June 1996

   A polyhedral element for a multiplanar tubular joint is suggested. The stiffness matrix of the polyhedron of a flexible joint is formulated based on the local flexibility factor matrix and coordinate transformation. An offshore jacket is chosen as a numerical example. The computed results show the great effect of local flexibility of a multiplanar tubular joint on the internal forces, deformation, and stress concentration of the joint. Hence, the consideration of flexibility in the global spatial structural analysis is vital.

9. **A Study on the Beam Modeling of Box Channel Structures: for the T Type Joint Structures**
   Choi, Jong-Keun; Lee, Yong-Rae; Choi, Seok-Hwan; and Lee, Jung-Han
   SAE Paper 960554; Feb 1996

10. **Strength of Welded T-DT Joints in Rectangular and Circular Hollow Section Under Variable Axial Loads**
    Davies, G. and Crockett, P.
    Journal of Constructional Steel Research v37 n1 Mar 1996 Elsevier Science Ltd Oxford Engl p 1-31
    0143-974X JCSRDL

    Finite element methods calibrated against experimental results from tests and data bases are used to obtain interaction diagrams for the strength of hollow section T-DT joints under three-dimensional static brace loading. Suggestions are made for the use of modifying factors in conjunction with planar joint strength design recommendations. English (Author abstract) 15 Refs.

11. **Rotational Stiffness Characteristics of Steel Beam-to-Column Connections**
    Davison J.B.; Kirby, P.A.; and Nethercot, D.A.
    Construction Steel Research, 1987

    A series of tests on a variety of beam-to-column connections suitable for rectangular frames using I-section members has been conducted. The principal objective was the provision of moment-rotation data so that a comparative assessment of the performance of the different types, in terms of connection stiffness and moment capacity, could be undertaken. Thus all tests employed similar beam and column sizes, test apparatus, instrumentation and test procedures. The connections

studied were ascending order of stiffness and strength: web cleats, flange cleats, combined seating cleat and web cleats, flush end plate and extended end plate. Connections to the column flanges and the column web were included. Major sources of connection flexibility have been identified and the results prepared for subsequent use in assessments of semi-rigid joint action in steel frames.

12. **Through-Thickness Properties of Column Flanges in Welded Moment Connections**
Dexter, R. J. (Minnesota University, USA) and Melendrez, M. I. (Disney World Int., USA)
ASCE Journal of Structural Engineering; Jan 2000

Forty tee-joint specimens were tested to assure that through-thickness strength or ductility of the column flanges is not a potential failure mode for welded moment connections. The specimens were designed with 690-MPa yield-strength pull plates and a high-strength high-toughness double groove shop weld (not representative of structural welds) to attempt to induce through-thickness failures in column flanges. Despite high strain rate, high-heat input welds, and several details designed to trigger fractures, only one through-thickness failure occurred. In most cases the pull plates broke, and in all cases the stress levels exceeded 690 MPa, well above the stress level that could be delivered by structural steel beam flanges. The only specimen fabricated without continuity plates resulted in a through-thickness brittle fracture of the column flange, although the nominal pull-plate stress was quite high (698 MPa). The lack of yielding in the through-thickness direction can be explained by the existence of triaxial constraint of the column flange material.

13. **Experimental Analysis of Bolted Connections: Snug Versus Preloaded Bolts**
Faella, C., Piluso, V. and Rizzano, G. (Salerno University)
ASCE Journal of Structural Engineering, (USA) Jul 1998

The rotational stiffness of bolted connections can be properly predicted by means of the so-called 'component method.' In this method, the T-stub plays a fundamental role, because it is used to compute the stiffness contribution of the most important joint components. For this reason, an experimental analysis on bolted T-stub assemblies has been performed. On the basis of this analysis, the possibility of predicting the axial stiffness of the T-stub assembly is investigated. In addition, as the joint behavior is strongly influenced by the bolt preloading, the experimental analysis has been performed applying three different levels of bolt preloading and, starting from the obtained experimental results, simple rules to take it into account are suggested. Finally, the reliability of the relationships derived from the T-stub analysis has been verified through the application of the component method to the prediction of the rotational stiffness of a wide number of tested specimens concerning extended end plate connections, both with snug-tightened and pretensioned bolts, collected in the technical literature.

14. **Practical-Theoretical Analysis of Chassis Torsion by Finite Element Analysis**
Fragoso, Helio R.
SAE Brasil 93; Paper 931705

The structural calculation of a complete light truck frame using the Finite Element Method requires the knowledge of the torsional stiffness of the cargo box, cab and front end of the vehicle. This paper presents a practical way to obtain the necessary data, avoiding the mathematical modeling of the whole vehicle, to reduce time and machine requirements. Lab measurements of the torsional stiffness are performed, in the frame alone and with each of the body components, allowing the definition of a mathematical model for the whole vehicle.

15. **Deformations Car Body Joints Under Operating Conditions**
Garro, Lorenzo and Vullo, Vincenzo
SAE Paper 861397 1986

In this paper an analysis of the dynamic behavior of typical bodywork joints subjected to two typical actual load conditions is presented. This analysis is carried out by finite element method and experimental verified by holographic interferometry measurements. The obtained results show unequivocally that along the weld spots the plate edges tend to detach one from the other and that under operational conditions the weld spots of a car bodywork essentially by unbuttoning.

16. **Moment-Rotation Relationship of Blind Bolted Connections for HSS Columns**
Ghobarah, A.; Mourad, S.; and Korol, R.M.
Source: Journal of Constructional Steel Research v 40 n 1 Oct 1996 Elsevier Science Ltd Oxford Engl p 63-91 0143-974X JCSRDL

An analytical model representing connection response capable of simulating its behavior of blind bolted connections for Hollow Structural Section columns in terms of its moment-rotation relationship was developed for the determination of the overall frame response. The model evaluates the main connection parameters such as its initial stiffness and plastic moment capacity on the basis of few secondary parameters obtained from test results. The accuracy of the analytical model was examined by comparing the model results with experimental measurements. The model predicted the connection rotation with reasonable accuracy at different levels of loading. A numerical example is provided to illustrate how the connection model can be applied in the design.

17. **Van Frame Structural Evaluation**
Hull, Frederick H.
SAE paper 790988; 1979

This paper describes the structural evaluation of a van production chassis frame, a light weight frame design and four other modified production frames. Static structural properties were determined by a combination of laboratory joint stiffness measurements and a finite element model incorporating empirical stiffness values. The finite element analysis results are compared to laboratory frame bending and torsion measurements.

18. **Columns with Semirigid Joints**
Jones , Stephen W.; Kirby, Patrick A.; and Nethercot, David A.
ASCE Journal of Structural Engineering; Feb 1982

The influence of a semi-rigid end restraint on the strength and behavior of steel concrete columns is examined. A method of analysis has been developed which incorporates the effects of initial out-of-straightness, initial residual stresses and spread of yield. Results have been compared with available experimental data and this data correlates well. Possible column design economies due to the actual end restraint are outlined.

19. **Reconsideration of the Joint Modelling Technique: In a Box-Beam T-Joint**
Kim, Yoon Young; Yim, Hong Jae; Kang, Jeong Hoon; and Kim, Jin Hong
SAE Paper 951108

In this paper, joint modeling techniques are investigated in a box beam T-joint, which may be viewed as a simplified model of typical vehicle body joints. For low-frequency vibration analysis, joints are

typically modeled by torsional spring elements and the importance of reasonable spring rates has been noted in many investigations. The effects of the joint branch lengths on the spring rates are investigated and it is shown that converging results are obtained only with proper branch lengths. We also discuss some facts to consider for estimating consistently the spring rates when the branches of the T-joints meet oblique angles. Finally, a possibility of using short beam elements instead of conventional spring elements to account for the joint flexibility is examined. The consequence of short beam modeling is that the sensitivity analysis on the natural frequencies with respect to the joint flexibility can be easily performed.

20. **An Experimental Investigation of Double Chord HSS Trusses**
Korol, R.M.; Mirza, F.A.; and Chiu, E.T.C.
Canadian Journal of Civil Engineering, June 1983

The results of a series of five large scale experiments on Warren trusses comprised of square HSS and utilizing the concept of a double chord are presented. The trusses were simply supported and loaded at their top chord panel points, thus simulating gravity loading. It was found that the bolted type, the back-to-back with overlap configuration, caused a member failure. The joints showed little or no duress. On the other hand, the two standard type trusses suffered joint failures principally by chord shearing at the ends of the top chord. This amounted to a reduction in strength of about 20% of the values of the other trusses. In this paper some design details are presented to help alleviate the problem of inadequate end joint strength.

21. **Finite Element Analysis of RHS T-Joints**
Korol R.M. and Mirza, F.A.
Journal Structural Division, Sept. 1982

The finite element method is used to model the structural behavior of T-joints in rectangular hollow sections beyond the elastic limit. Their ultimate load and working strengths are determined. Also calculated are the punching shear and rotational stiffnesses under branch axial force and bending moment.

22. **Plate Reinforced Square Hollow Section T-Joints of Unequal Width**
Korol, R.M.; Mitri H.; and Mirza, F.A.
Canadian Journal of Civil Engineering, June 1982

The carrying capacity of square hollow structural section T-joints stiffened by a rectangular flange plate is investigated for both branch bending moment and punching shear. The ultimate moment or load is determined from the simple yield line method of which one of three failure modes is applicable depending on the plate length. A large number of combinations of branch, chord, and plate sizes are analyzed to provide a statistical basis for making recommendations of optimum plate lengths and thicknesses for stiffened joints in Vierendeel truss applications.

23. **Predicting the Behaviour of HSS Double Chord Trusses—A Comparison With Test Results**
Korol, R.M., Miraza, R.A., and Chiu E.T.C.
Canadian Journal of Civil Engineering, June 1983

Predictions from a previously developed analytical model that takes into account plastic hinging action and includes the effects of axial load and moment interaction are compared with the results of tests on double chord RHS trusses. The model incorporates a shear spring mechanism that is applicable to gap joints of HSS trusses. Load displacement curves generated by the program are in

reasonable agreement with the majority of truss tests. Calculated moment-axial force interaction curves tend to predict trends of behavior rather than to be accurate.

24. **Theoretical Analysis of Haunched-Reinforced T-Joints in Square Hollow Sections**
Korol, R.M. and Mansour, M.H.
Canadian Journal of Civil Engineering; Dec. 1979

A theoretical analysis has been undertaken for unequal width T-joints, haunch-reinforced, in square hollow structural sections (HSS). The unreinforced joint is merely a special case. The theory was based on a finite difference solution to the elastic chord flange plate equation and predicts the branch-to-chord joint stiffnesses under both bending and axial force. The effects of varying the width ratio overall haunch length-to-width ratio, and chord width-to-thickness ratio b c were studied for different plate edge boundary conditions. The latter parameter has the greatest effect on stiffness, but the other two, including haunch size, are also significant. There is reasonable agreement between the joint rotational stiffness factor.

25. **Unequal Width Connections of Square Hollow Sections in Vierendeel Trusses**
Korol, R.M.; Zanaty, M.E.; and Brady, F.J.
Canadian Journal of Civil Engineering, June 1977

With the advent of hollow structural steel sections, the potential for Vierendeel trusses has greatly increased. The absence of simplified design methods has led to an extensive research program, the results of which are reported here. A total of 29 specimen comprising five distinct connection types were tested and their strength and stiffness properties were recorded. Most of the joints tested behaved in a semi-rigid fashion, so that a stiffness method for analyzing Vierendeel trusses has been developed. Design curves for prediction of joint strength are proposed and design examples of trusses under panel point loading are analyzed. Two types of joint are recommended: the haunch type of connection and the cord flange stiffener, both of which have adequate strength and stiffness characteristics.

26. **On the Definition of Beam-Wall Joint Rotations in the Analysis of Coupled Wall-Frame Structures**
Kwan, A.K.H.
Engineering Structures, 1993

In the analysis of coupled wall-frame structures, several different definitions for the beam-wall joint rotations have been adopted. However, the various definitions used are not equivalent. By formulating the coupling beam element as a Timoshenko beam element with both horizontal and vertical fiber rotations at each end, it is shown that the proper definition for nodal rotation at a beam-wall joint should be the rotation of the vertical fiber at the beam-wall interface; the use of other definitions may lead to errors in the effective stiffness of the coupling beams. A quantitative assessment of the errors so caused is made and it is found that in cases where coupling beams are short and stiff, the errors could be quite significant. It is therefore proposed that existing methods which use definitions other than the vertical fiber rotations at the joints should be reviewed and, if necessary, reformulated to have the definition of the beam - wall joint rotations amended.

APPENDIX A: ABSTRACTS

27. **A Study on the Improvement of the Structural Joint Stiffness for Aluminum BIW**
Lee, Young Woong; Kwon, Yong Woo; Kwon, Soon Yong; and Cho ,Won Suk
SAE Paper 970583; Feb 1997

The application of aluminum Body-In-White has several technical barriers in press forming, joining, and chemical conversion treatment processes. Among them, the optimization of joining processes with which structural stiffness and durability will be assured might have the key role for the success of aluminum applications to BIW. In this study, stiffness, strength and fatigue strength of BIW joints with aluminum sheets were evaluated as a function of joining methods, such as resistance spot welding and weld bonding, via both experimental and analytical routes (FEM). For the evaluation, single-lap joint and T-shaped joints were made, with each joining method, as variation of pitch, sheet thickness and even materials – steel sheets. Based on the experimental and FEM analysis results, the optimum joining method for the aluminum BIW which is suitable for weight saving and has equivalent stiffness and strength to steel is suggested. In addition, for obtaining optimum processes with improved stiffness, and strength of the joining method, design parameter, such as the influence of the spot pitch on the structural joint stiffness and the minimum wall thickness of aluminum which is able to maintain the equivalent stiffness and strength to steel are discussed.

28. **Testing of Semi-Rigid Unbraced Frames for Calibration of Second-Order Inelastic Analysis**
Liew, J.Y.R.; Yu, C.H.; Ng, Y.H.; and Shanmugam, N.E.
Journal of Constructional Steel Research; No. 2/3;   1

This paper examines the behavior of semi-rigid unbraced frames through a series of tests on a variety of rectangular frames as well as their joints so that the analysis and design methodology can be developed and verified against the test results. The frame and joint tests employed similar beam and column sizes and had the same connection details. The two types of connections studied were top-seat-double-web angle and extended end-plate. Column-base connections were also included in the studies. Load-displacement plots are presented for all the test frames subjected to gravity loads applied to the beam and columns, and a horizontal load applied at the beam level. The principal objective of the joint tests is to provide a comprehensive set of moment-rotation data, in terms of stiffness and moment capacity, so that a comparative assessment of the frame performance due to the different connection types could be undertaken. Detailed descriptions of test arrangement, load sequences, test methods and data acquisition techniques are given. The general observed behavior is discussed. Results from the frame tests are compared with the corresponding theoretical results obtained from a second-order inelastic analysis.

29. **The Flexibility of a Tubular Welded Joint in a Vehicle Frame**
Lubkin, James L.
SAE Paper 740340, 1974

Automotive frames frequently consist of thin tube members thick enough for much of the structure to be modeled adequately by bar elements. However, previous results show that a typical welded joint cannot be handled by the classical "rigid joint" assumption of frame analysis. Those results include tests of a joint type common in passenger car frames, and establish errors of over 60% in analytical predictions for some of the lower natural frequencies. The present paper attempts to see how much improvement we can achieve by simply accounting for the actual tubular shape in the vicinity of the joint, without allowing for the flexibility of the weld line itself. The study uses the NASTRAN computer program. The joint region is treated as a small substructure in a model otherwise composed of bar elements. This procedure is economical because only those portions which really have to be analyzed using plate elements are so treated. Parameters investigated include joint length, and two ways of attaching a shell to adjacent bar elements. The present results reduce the worst two

frequency errors, 38% and 60%, to less than 7% and 11%, respectively. This is good enough for many purposes. Residual discrepancies are believed to be due, in part, to actual weld line flexibility. In vibration modes involving a particular kind of bending deformation, the slightly larger discrepancies are also tentatively attributed to a nonlinear-effect; i.e., changes of cross-section shape in the relatively thin rectangular tubing used.

30. **Steel Frame Analysis with Flexible Joints**
Lui, E. M. and Chen, W. F.
Journal of Constructional Steel Research; 1998;

The first part of the paper discusses various mathematical models that have been proposed to represent the nonlinear moment-rotation behavior of the semi-rigid steel beam-to-column connections. This is followed by a brief description of two simplified and a rigorous analysis capable of dealing with these models in flexibly-connected steel frames. Numerical studies of frames made using these simplified and rigorous analysis methods are presented. Observations regarding the effects of flexible connections on the strength, deflection and internal force distribution of steel-framed structures are discussed.

31. **Truck Frame Analysis Study**
Michejda, Oskar
SAE paper 710594; 1971

A method of truck frame analysis is proposed to include the effects of forces acting in three dimensions as well as the effects of variable cross sections, off shear-center loading, and joint flexibility. The interaction between the frame and other components of the vehicle is discussed and a method is proposed to include these effects in the static and dynamic stress analysis of the frame components. The dynamic effects on stresses are proposed to be included in experimentally determined dynamic stress factors defined in terms of dimensionless probability density functions for various frame components and on and off highway conditions. An experimental program is outlined for the evaluation of stiffness characteristics of the flexible joints; the upper bound of the horizontal force acting at the front axle, and the dynamic stress factors. General analysis of forces and deformations in the chassis due to drive-shaft impact and twisting of the vehicle is included in the Appendices.

32. **Elasto-Plastic Finite Element Analysis of Double Chord Rectangular Hollow Section T-Joints**
Mirza, F.A.; Shehata, A.A.; and Korol, R.M.
Computers & Structures, 1984

Elasto-plastic response of T-joints consisting of double chord, rectangular hollow sections (RHS) has been modeled by treating the chord's mated flanges as thin plates supported by coupled springs that simulate the action of the side walls and bottom flanges. The finite element formulation includes rectangular plate and edge boundary springs in which both in-plane and out-of-plane actions are considered. Material nonlinearities are incorporated through the Von-Mises yield criterion and its associated flow rule and the Newton-Raphson method is used for the nonlinear analysis. The model is used to determine the ultimate strength and the load-deformation curves for both double and single chord T-joints.

33. **Development of an Automotive Joint Model Using an Analytically-Based Formulation**
Moon, Y.M. (Michigan University); Jee, T.H. (Korean Passenger Car R&D Center); and Park, Y.P. (Yonsei University)
Journal of Sound & Vibration, (UK) 4 Mar 1999

A FE model of an automotive structure consists of beam and shell elements. Generally, the pillars and rockers are modeled as beam elements and other parts as shell elements. Beam elements are used since they are more efficient than shell elements. A joint is defined as an intersection region of beam elements, and is generally modeled as coupled rotational springs. In this study, a joint modeling methodology is presented. First, the definition and assumptions of the joint are discussed. Second, the joint stiffness analytical model is proposed using static load test results. The proposed method is more efficient and accurate than existing evaluation methods. Third, the sensitivity analysis method (Nelson's method) and a joint stiffness updating algorithm are presented. To verify these methods, the FE analysis results of a half size structural model of an automobile with rigid joints and rotational spring joints are compared with experimental modal analysis results.

34. **Stress Concentration Factors in Tubular K-Joints Under In-Plane Moment Loading**
Morgan, M. R. and Lee, M. M. K.
Journal of Structural Engineering; April 1998; v 124

An extensive parametric study is presented of the distributions of stress concentration factors in tubular K-joints commonly found in offshore platforms. The study covers a comprehensive range of geometric joint parameters for balanced in-plane moment loading. The results of the study were first used to assess two sets of widely used parametric equations, which predict the maximum stress concentration factors on the outer surfaces of the chord and the brace. The new database of finite-element results was then used to develop parametric equations for predicting stress concentration factors at key locations around the intersection on the outer as well as the inner surfaces of the chord. The reliability of the proposed and existing parametric equations was then assessed using an acrylic test joint database and some published test data measured from a steel model. Fracture mechanics fatigue calculations were also performed to demonstrate that the information provided from the proposed equations could be utilized to obtain accurate, and safe, fatigue life estimates.

35. **Design of Extended End-Plate Connections for Hollow Section Columns**
Mourad, S.; Korol, R.M.; and Ghobarah, A.
Canadian Journal of Civil Engineering, February 1996

Extended end-plate connections have been widely used in moment-resisting steel frames with W-shape columns, due to their sufficient stiffness and moment capacity. In addition, such connections are easy to install and permit good quality control. Extended end-plate connections can also be employed in moment-resisting frames with hollow structural section columns by using high strength blind bolts. These bolts have been developed for installation from one side only where the rear side of the connection is inaccessible. In this study, a quantitative procedure for detailing and designing beam extended end-plate connections for rectangular hollow structural section columns using high strength blind bolts is proposed. The design procedure is consistent with the design philosophy given in limit-state codes. The proposed design is based on the results obtained from an experimental program and an analytical study.

APPENDIX A: ABSTRACTS

36. **Dynamic Response of Hollow Section Frames with Bolted Moment Connections**
Mourad, S.; Ghobarah, A;. and Korol, R.M.
Engineering Structures, 1995

The behavior of moment-resisting steel frames under various types of loads is dependent on the type of beam-to-column connections and their flexibilities. The extended end-plate connection is a practical field bolted moment connection that can be adopted in moment-resisting steel frames with hollow structural steel (HSS) columns, by using high strength blind bolts. The objective of this work was to study the behavior of blind bolted extended end-plate connections for HSS columns under cyclic loading. With proper detailing and modeling of such connections, it has been possible to investigate the effect of joint flexibility on the response of the frame when subjected to dynamic loading and then to compare its response to that of a rigid frame. It is concluded that the proposed bolted joint behaves in a predictable manner that can be modeled and analyzed using standard frame analysis programs. The study also showed that the inclusion of the connection flexibility in frame analysis is essential to obtain a more realistic frame behavior.

37. **Towards an Exact Value for the Flexural Stiffness of Tall Rigid Frames**
Olowokere, D.; Aktan H.; and Akanni, A.N.
Computers & Structures, 1991

The contribution of the flexural stiffness of tall rigid frames to the overall lateral stiffness of the building is evaluated. The parametric study is conducted for nine different rigid frame geometries representing shear wall-frame buildings commonly employed. Each frame of appropriate grid geometry and pre-sized cross-sections is subjected to prescribed lateral loading. The lateral deflection of the various column joints is computed using the stiffness method. Subsequently, retaining the same moment of inertia, the cross-sectional areas of all columns are increased to simulate an axially infinitely stiff column and each frame is re-analyzed using the same lateral loading. The difference in the computed horizontal joint deflection from each of the analyses represents the lateral displacement of the frame due to axial strains in the columns and, hence, a measure of the 'flexural' deformation of the frame.

38. **Stress Concentration Factors for Non-90° X-Connections Made of Square Hollow Sections**
Packer, J.A. and Wardenier, J.
Canadian Journal of Civil Engineering v 25 n 2 Apr 1998

A number of fatigue experiments and stress concentration factor measurements on non-90°, square hollow section X-connections have been carried out. Comparison of the measured stress concentration factors with those derived from existing parametric formulae for 90° T- and X-connections showed a strong influence of the brace angle. A tentative extension of the range of validity of the parametric formulae for 90° T- and X-connections for other brace angles has been derived. English (Author abstract) 15 Refs.

39. **Automotive Body Joint Analysis for Improved Vehicle Response**
Rao, Zebrowski, and Crabb

A comprehensive analysis system for defining the flexible characteristics of body structural joints is described. A static test methodology of obtaining joint stiffness characteristics is presented. A joint databank, consisting of linear joint stiffness characteristics, is developed. A mini-computer based dynamic joint stiffness testing methodology for obtaining dynamic joint stiffness characteristics, which can be integrated into finite element body models, is explained. Finite element joint modeling procedures for obtaining joint stiffness characteristics, before hardware availability, are outlined. A

joint modification technique integrating finite element analysis, laboratory testing and vehicle evaluation, which significantly improved vehicle NVH response, is described.

40. **Welded Interior Box-Column to I-Beam Connections**
Shanmugam, N.E. and Ting, L.C.
ASCE Journal of Structural Engineering; May. 1995; 3

This paper deals with experimental investigations to study the ultimate load behavior of I-beam to box-column connections stiffened externally. Specimens representative of interior columns in a steel building frame were fabricated with connections stiffened by T-sections butt-welded at the junction of the beam and column flange. They were tested to failure under static and fluctuating loads applied separately. Ultimate load-carrying capacity and typical load-deflection and moment-rotation responses obtained experimentally are presented; the results for those specimens tested under static loading are compared with the corresponding results using the elasto-plastic finite-element method. Close agreement is observed between the experimental and theoretical moment-rotation curves. Results show clearly that these connections satisfy the basic criteria; sufficient strength, sufficient rotation capacity, and adequate stiffness for a moment connection. The proposed connections are capable of developing load-carrying capacity in excess of the plastic capacity of the beam framing into the joint.

41. **Transferred Load and Its Course in Passenger Car Bodies**
Shinobu, Manabu;, Okamoto, Daichi;, Ito, Shuta; Kawakami, Hirofumi; and Takahashi, Kunihiro
SAE of Japan Review 16; 1995

A method to express the concept of load transfer and the course of the transferred load in the structure is introduced. Transferred load in an actual passenger car body is investigated experimentally. The degree of joint stiffness between the members of the vehicle body can also be discussed based on this concept. Difference can be shown between the course from the front suspension and that from the rear suspension under the condition of the torsional loading.

42. **The Fatigue Behavior of T- and X-Joint Made of Square Hollow Sections**
Van Wingerde, A.M.
Heron; vol 37 no. 2; 1992

This work presents the results of experimental and numerical research on the fatigue behavior of T- and X-joints between square hollow sections of which the brace is welded to the face of the chord, without any additional stiffeners. The work has been carried out in the framework of the CIDECT program 7K "Fatigue behavior of uniplanar joints", and an earlier ECSC program "Fatigue strength of welded unstiffened RHS joints in latticed structures and Vierendeel girders" (CECA Convention nr. 7210-SA/111). Furthermore, experimental results of the CIDECT program 7H "The low cycle fatigue behavior of axially loaded T-joints between rectangular hollow sections" have been used in this work. The aim of the research programs is to establish a better design method for the fatigue strength of joints in square hollow sections, based on the hot spot stress method. The results are to be proposed for inclusion in Eurocode 3. In the experimental investigation, the strain concentration factors are measured at various locations of the joint for comparison with results of the numerical investigations and Sr(h.s.)-Nf curves are determined. The numerical work provides SCF values at weld toes for a range of parametric variations in the joint dimensions. These results form the basis for a set of parametric formulae. These formulae allow the determination of the SCF values at the weld toes of the brace and chord, depending on the non-dimensional parameters (β, 2γ and &tau). The results of tests and formulae are used to check the final validity of the formulae in combination with the Sr(h.s.)-Nf lines. English (Author abstract) 123 Refs.

APPENDIX A: ABSTRACTS

43. **Behavior of Tubular T-Joints Subjected to Combined Loadings**
Yeoh S.K..; Soh, A.K.; and Soh, C.K.
Journal of Constructional Steel Research; 1995

A large-scale test rig was specially designed and built to study the behavior of tubular joints subject to combined loadings. A round-to-round tubular T-joint was subjected to axial load, in-plane bending, out-of-plane bending and combinations of the three load cases. The study reveals that the peak hot spot position on the T-joint under combined loads shifts in location from that of the basic load cases. The study also shows that the peak hot spot stress under combined loads was underpredicted by superposition of basis load cases in some instances. Comparison with existing combined hot spot procedures reveals that some existing procedures are inadequate for predicting the peak hot spot stress of tubular T-joints.

Articles Read, Not Pursued

1. **3D Simulations of Bolted Connections to Unstiffened Columns-II. Extended Endplate Connections**
Bahaari, M.R. and Sherbourne, A.N.
Journal of Constructional Steel Research; Dec. 1996

Traditionally, column web stiffeners are used to increase the load carrying capacity and rigidity of extended endplate, bolted, moment connections in structural steelwork. However, elimination of these stiffeners in such connections is favored because of significant fabrication economy and simplification of connection details. Besides, the optimum analysis and design of the frame may demand joint moments other than the full plastic capacity of connecting members making column stiffening unnecessary. In this context, the principal bending planes of the column flange and endplate are orthogonal and, thus, only a three-dimensional (3D) model can address connection behavior. For this reason, there are only a limited number of experimental analytical reports concerning this phenomenon. A description and application of such a model, using inelastic finite elements, has already been provided in Part I, a companion paper (Journal of Constructional Steel Research, 1996, Vol. 40, 169-187), in which deformation and prying action are studied for T-stub connections. This paper presents the structural properties, both stiffness and strength, of an extended endplate connected to an unstiffened column flange using high strength prestressed bolts.

2. **An Approximate Method for Estimation of Bending Moments in Continuous and Semirigid Frame**
Chikho, A.H. and Kirby, P.A.
Canadian Journal of Civil Engineering, December 1995

A simple hand method of estimating member bending moments in flexibly connected multistorey frames is presented in this paper. The method allows for semigrid joint action and can be used in conjunction with any of the current rigid methods of frame design. The load factor at elastic instability of flexibly connected frames can be obtained by the proposed method. Also, a procedure for calculating a linearized approximation of the joint stiffnesses in a multistory frame subjected to vertical and horizontal loads accounting for the nonlinearity of the joint's moment-rotation characteristic is included. Comparison of the prediction of the proposed method with an accurate analysis shows that the proposed method leads to an accuracy that is satisfactory for design purposes.

3. **Rigid Latticed Steel Frames: Tow Large-Scale Tests and Failure Predictions**
Ellis, J.S
Canadian Journal of Civil Engineering, Oct 1987

This work is concerned with the predictions of failure under static load for two identical free-standing latticed cantilever frames. Each structure was 3m high and consisted of three stories with panel points 1m apart; in plan it was lm2; its diagonals were at 45 degrees in the form of St. Andrew's cross; all joints were welded and were considered rigid. The four bases were bolted to the laboratory floor and the static load was applied at the top as two compressive horizontal forces parallel to the sides of the structure. The individual members were all solid mild steel round rods; the verticals were of uniform cross section of 25.4mm in diameter with a slenderness of 157; the horizontal cross-arms were of uniform cross section of 19mm in diameter; and the diagonals were of uniform cross section of 15.9mm in diameter. The diagonals were cut at their mid-lengths and welded to give a flush joint. The total horizontal loads that caused failure of the two structures were 79.6 and 79.2kN. In both cases failure occurred by the sudden buckling of one of the bottom-story vertical legs, inwards towards the center of the structure. Also upon failure, the diagonals in the bottom story of the compression face buckled inwards and the compression diagonal of the side contiguous to the buckled leg also buckled.

4. **Behaviour of Tubular Steel Trusses With Cropped Webs**
Ghosh, A. and Morris, G.
Canadian Journal of Civil Engineering; Mar. 1981

The consecutive testing of failure of four test joints in each of two identical 7.3m span x 1.8m deep tubular steel trusses with cropped webs is described. The behavior of each of the test joints is discussed and compared to that of similar joints previously tested as isolated specimens. Following large chord-face deformations and bending of the webs in the truss plane, failure occurs by out-of-plane buckling of the compression web at those test joints with slender webs, or by yielding and tearing of the tension web at those with stocky webs. Stiffness are in close agreement for corresponding truss and isolated joints. Strengths of the truss joints are from 0)23% lower than those of the isolated joint specimens. Joint deformation contributes less than 5% to truss deflection.

5. **Nonlinear Analysis of Lattice Structures**
Kitipornchai, S and, Al-Bermani, F.G.A.
Journal of Constructional Steel Research; 1992

The paper describes a nonlinear analytical technique developed by the authors in recent years for predicting the structural response of large-scale lattice structures. This type of structure is generally more sensitive to imperfections; hence, the analysis method needs to consider the various nonlinear effects. Sources of nonlinearity affecting the ultimate behavior of lattice structures include geometric nonlinearity, material nonlinearity, joint flexibility and slippage. Geometric nonlinearity can be accounted for by incorporating the effect of initial stress as well as geometrical variations in the structure during the loading process. For large-scale lattice structures, the material nonlinearity can be incorporated by using the lumped plasticity model, while the effect of joint flexibility can be incorporated by modifying the tangent stiffness of the element using an appropriate moment-rotation relation for the joint. The nonlinear formulation has been applied to a number of example problems selected to demonstrate the applicability and versatility of the method.

APPENDIX A: ABSTRACTS

6. **Connection Element Method for the Analysis of Semi-Rigid Frames**
   Li, T.Q.; Choo, B.S.; and Nethercot, D.A.
   Journal of Constructional Steel Research; 1995

   A general procedure for incorporating the effects of joint flexibility into standard methods for the analysis of frames is presented. The method can allow for joint flexibility associated with all six degrees of freedom normally considered when analyzing three-dimensional frames, including coupling between deformations. It can also allow for the finite size and exact location of connections. Simple examples using the moment distribution technique, slope deflection equations and matrix stiffness method illustrate the application of the proposal. Additional examples to illustrate the effects of connection length on the frame moment distribution, lateral drift and column load capacities are also present.

7. **Determination of Rotation Capacity Requirements for Steel and Composite Beams**
   Li, T.Q.; Choo, B.S.; and Nethercot, D.A.
   Journal of Constructional Steel Research; 1995

   A method is presented for the calculation of the necessary joint rotations to permit the use of moment redistribution as the basis for the design of semi-continuous steel and composite frames. The method is based on the use of moment-curvature relationships obtained from consideration of the basis steel and concrete stress-strain curves. It simplifies the determination of the support rotations required for specific percentage redistributions of support moments to the mid-span cross-section as used in EC4 by considering these to be composed of an elastic and a plastic part. Several different load cases are considered, together with a wide range of beam properties. The resulting calculation method, which uses only formulae and graphs, is illustrated by an example.

8. **A Practical Method for Incorporation Flexible Connections in Plane Frame Analysis**
   Lo, D.S.K and Stiemer, S.F.
   Canadian Journal of Civil Engineering

   A practical method for incorporating realistic flexible connections in plane frame analysis, including the effect of connection sizes and shear deflection, is presented. The general algorithm can be easily implemented in a standard plane frame analysis program and, one implemented, it can be an ideal tool for production work in the steel industry. Connection stiffness is programmed directly into the analysis using the moment-rotation equations developed by Frye and Morris or may be entered separately as data. Practical application of this method of analysis is demonstrated by modifying a standard plane frame analysis program to include the effect of flexible connections. Solutions obtained using this modified program, Plane, were verified against the findings of Moncarz and Gerstel. A simple plane frame structure was analyzed under various lateral load intensities for different connection assumptions. It was found that the inclusion of connection behavior significantly altered the internal force distribution and design of the structure.

9. **Behavior of Axially Loaded Tubular V-Joints**
   Scola, S.; Redwood, R.G.; and Mitri, H.S.
   Journal of Constructional Steel Research; 1990

   The results of an experimental test program comprising seven tubular V-joints and five tubular T-joints consisting of circular hollow sections and subject to branch axial loading are reported. The tested specimens has branch-to-chord diameter ratios varying from 0.22 to 0.65, and chord radius-to-thickness ratios of 13 to 23. The angle between branches of the V-joints was 60, 90 or 120 degrees. The behavior of the joints is examined through a comparison of ultimate strengths, stiffness

characteristics and hotspot stresses of comparable T and V specimens. Addition of a loaded out-of-plane branch member of a T-joint increases the strength of the T-joint when the angle between the branches is low, and decreases it when the angle is large.

10. **3D Simulations of Bolted Connections to Unstiffened Columns-I T-Stub Connections**
    Sherbourne, A.N. and Bahaari, M.R.
    Journal of Constructional Steel Research, Dec. 1996

    The paper presents a finite element methodology in a three-dimensional (3D) framework to study numerically the stiffness and strength of the T-stub to unstiffened column flange bolted connection as part of a comprehensive research program to investigate the behavior of endplate bolted connections. In such connections, the axes of rotation of the T-stem and column flange are at right angles; the planes containing the tensile forces are also perpendicular to each other. Therefore, they are highly interactive spatially. The main objective here is to study the applicability of the model to such a connection, so that most of the important features that are not accessible to routine experiments, like prying action and gradual plasticity of components, can be monitored. ANSYS, version 4.4, a large-scale general purpose finite element code is selected for this analysis. Initially, the simplest connection with the bolt groups in tension, which is a symmetric T-stub hanger with a single line of bolts paralleled on each side of the web, is considered. Then the T-stub connection to an unstiffened column flange is discussed.

11. **Criteria for the Fatigue Assessment of Hollow Structural Section Connections**
    Van Wingerde, A.M.; Packer, J.A.; and Wardenier, J.
    Journal of Constructional Steel Research, 1995

    Discussion of fatigue design criteria is presented for connections between hollow structural sections, based on knowledge gained from an extensive study on the fatigue behavior of 90-T- and X-connections made of square hollow sections. After a general discussion of the various fatigue assessment method available the paper focuses on considerations behind the definition of the hot spot stress. On this basis, the current fatigue design guidelines are discussed. Based on knowledged gained from experiments and having identified the important fatigue design criteria, a hot spot definition is established, together with the outline of a proposal for future fatigue design guidelines of hollow section connections.

12. **Study on Residual Stress Relief of Welded Structural Steel Joints**
    Weng, C.C. and Chen, J.J.
    Journal of Materials in Civil Engineering; May 1993

    This paper presents the results obtained from the residual stress relief tests on 21 welded structural steel joints: 17 butt-welded, two tee, and two corner joint specimens. The A572 grade 50 structural steel plates of two different thicknesses, 15 and 32mm, were used. All specimens were welded by the submerged arc welding (SAW) process and were designed according to the prequalified welded joints specified by the American Welding Society. In this study, a controlled low-temperature stress-relief method was used for residual stress relief. The experimental result show that by using an appropriate combination of the heating temperature, heating distance, and cooling method, the original high-tensile residual stresses near the weld of the joint can be reduced effectively. The residual stresses before and after the heat treatment were measured by using the blind hold-drilling method. A reduction of more than 50% of the original tensile residual stresses adjacent to the weld was observed.

Altair Engineering

APPENDIX B: MATERIAL TESTING REPORT

Samples of each material (coupons) were removed from each frame member and sent to a local material testing laboratory. The samples were tested to failure in a standard ASTM material testing rig. Plots of stress v strain for each sample are plotted for the full range of the material. An additional plot of the linear range of the material is also included for each sample. A list of coupons and their origin is below.

Coupon #1	Joint 5 Inner Side rail
Coupon #2	Joint 5 Outer Side rail
Coupon #3	Joint 5 Crossmember
Coupon #4	Joint 4 Side rail
Coupon #5	Joint 4 Crossmember
Coupon #6	Joint 3 Side rail
Coupon #7	Joint 3 Crossmember
Coupon #8	Joint 2 Side rail
Coupon #9	Joint 1 Side rail
Coupon #10	Joint 1 Crossmember

Joint 5- Material Test Coupons

Coupon 1-Side Rail Inner
Coupon 2-Side Rail Outer
Coupon 3-Crossmember
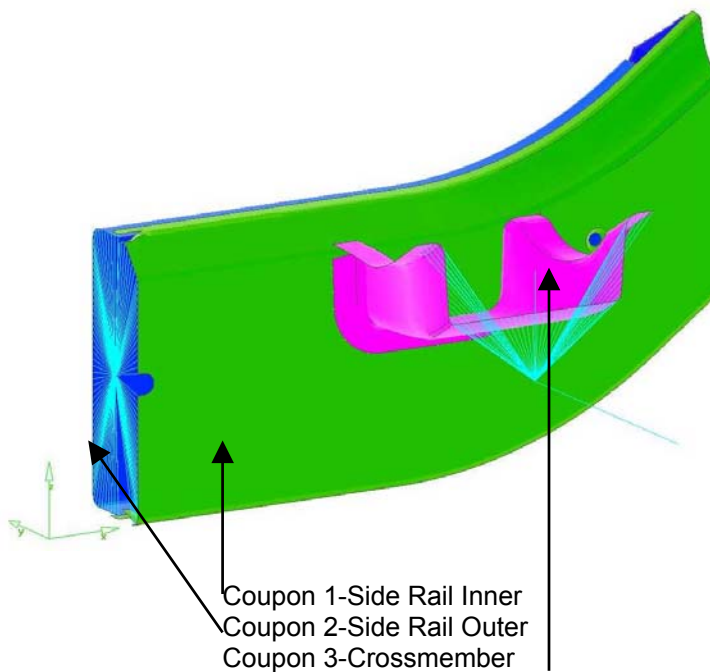
APPENDIX B: MATERIAL TESTING REPORT

Plot 1-Full Strain Range

Coupon #1-Joint 5 Inner Side Rail

Stress vs Strain

```
00007019
04-24-2001
00:56:44 AM

JOB NUMBER:      14078B
CLIENT:          Altair
SPECIMEN ID:         #1
REQ. TENSILE STRENGTH
REQ. YIELD STRENGTH
REQ. ELONGATION
WIDTH , INCHES   0.496
THICKNESS, INCHES 0.0981
COMMENT: n-VALUE CALCULATED
FROM 10% TO 20% STRAIN.
T.E.U:B008
```
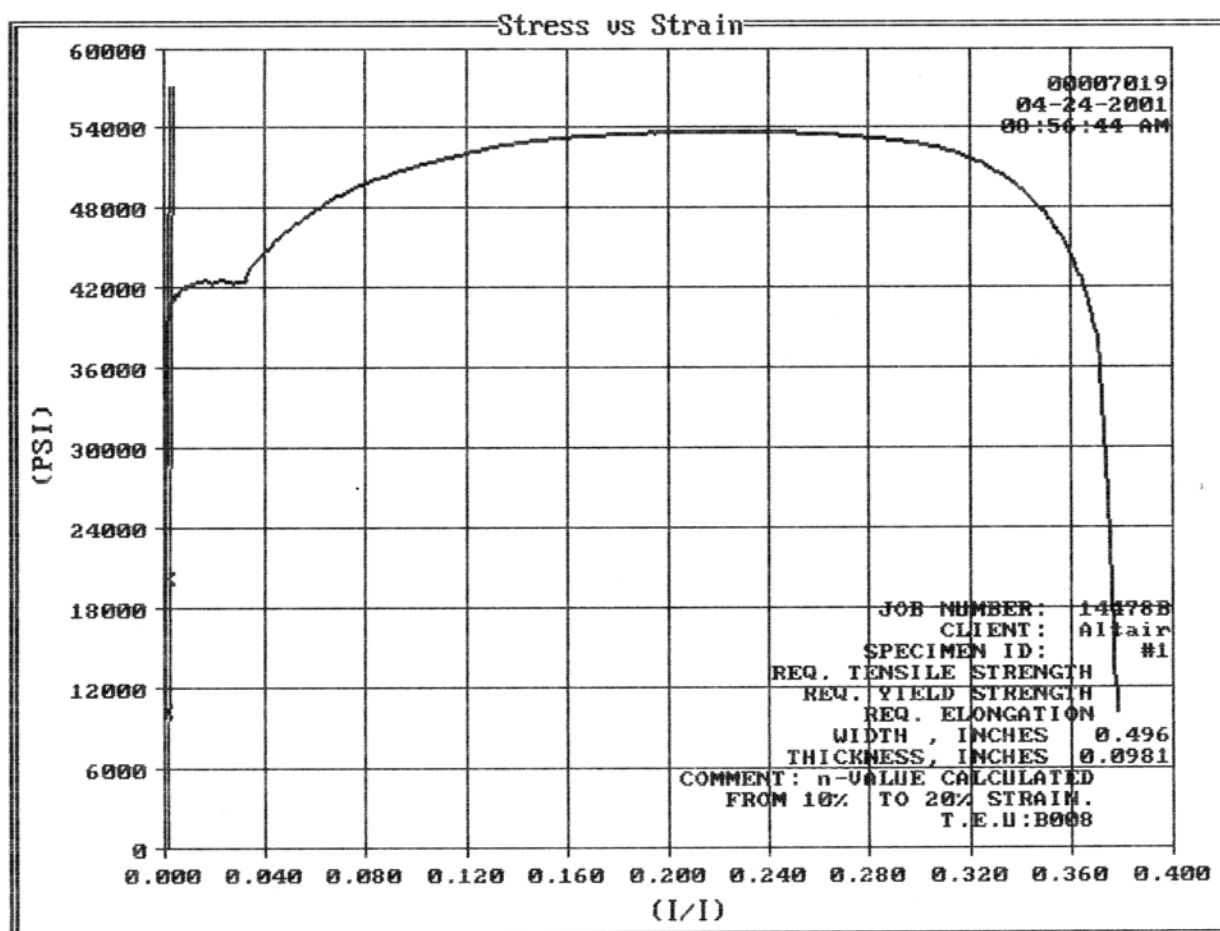
APPENDIX B: MATERIAL TESTING REPORT

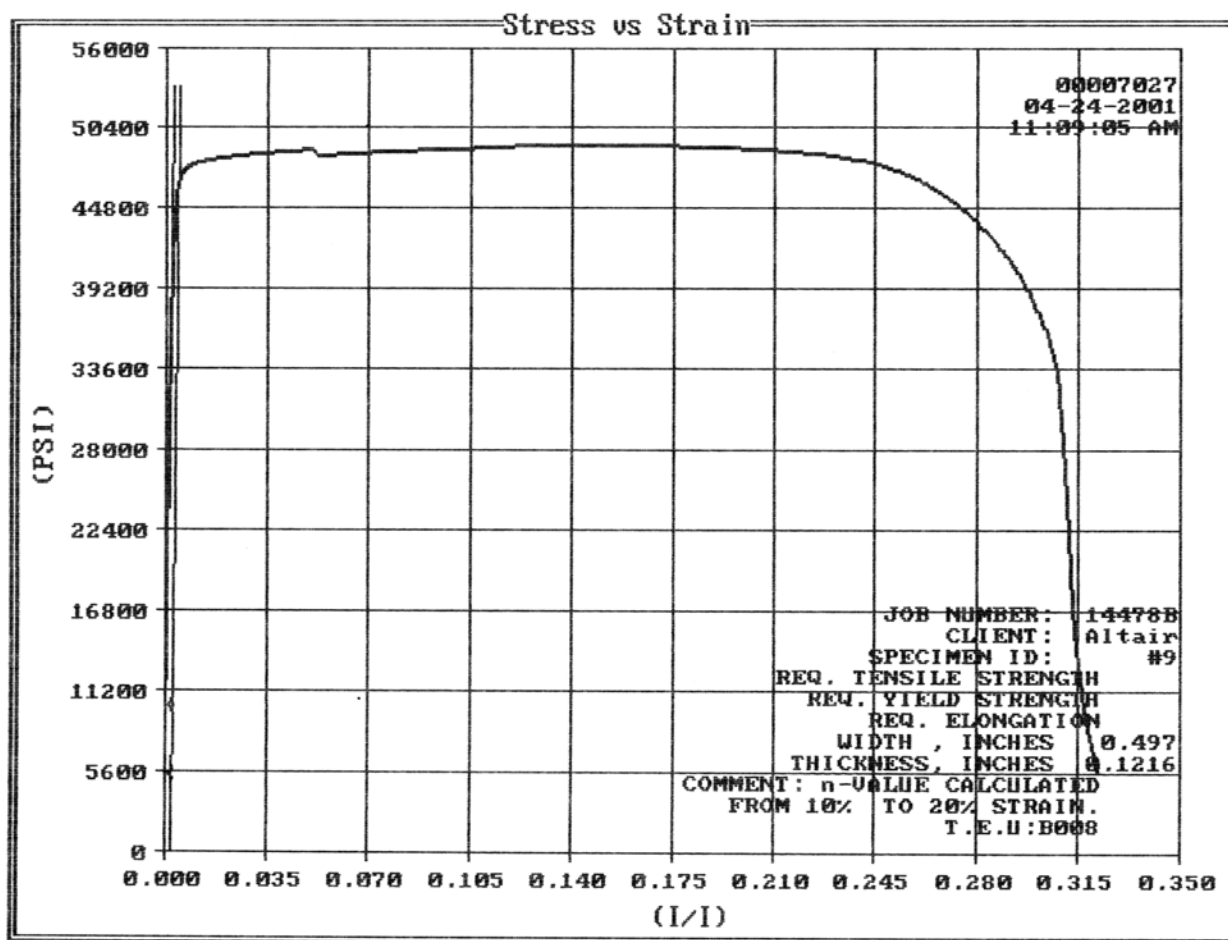## Plot 2-Linear Strain Range

Coupon #1-Joint 5 Inner Side Rail
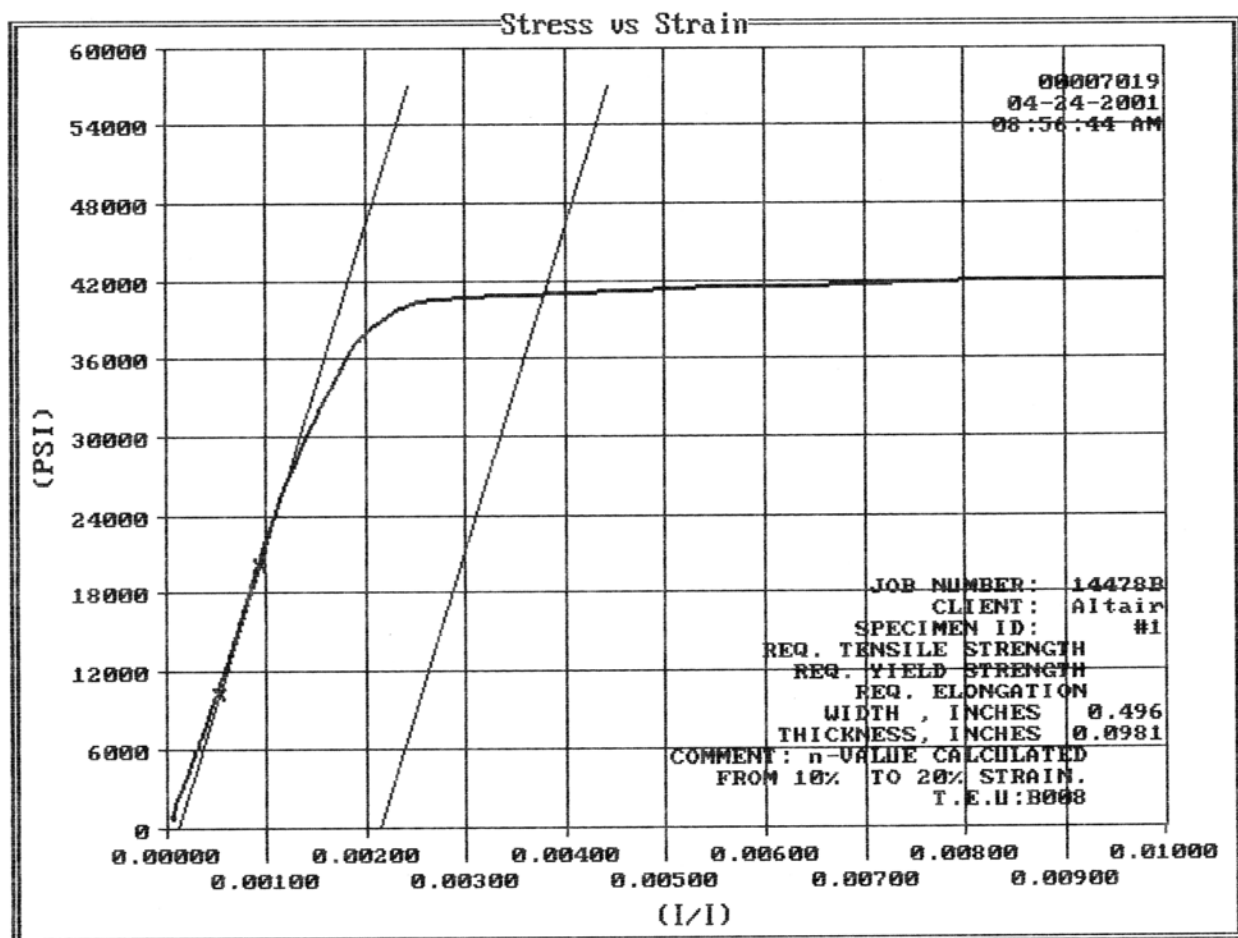
APPENDIX B: MATERIAL TESTING REPORT

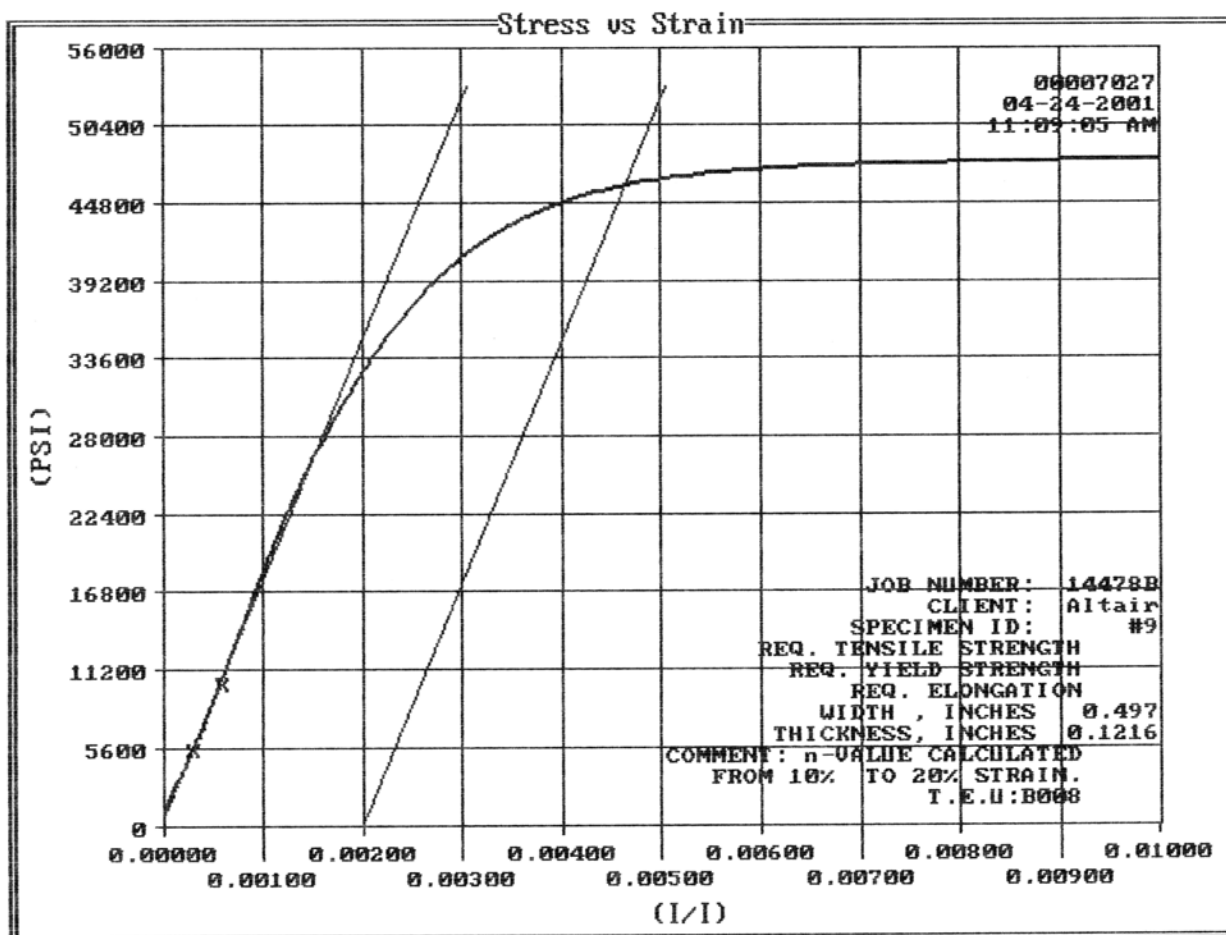## Plot 3-Full Strain Range

Coupon #2-Joint 5 Outer Side Rail
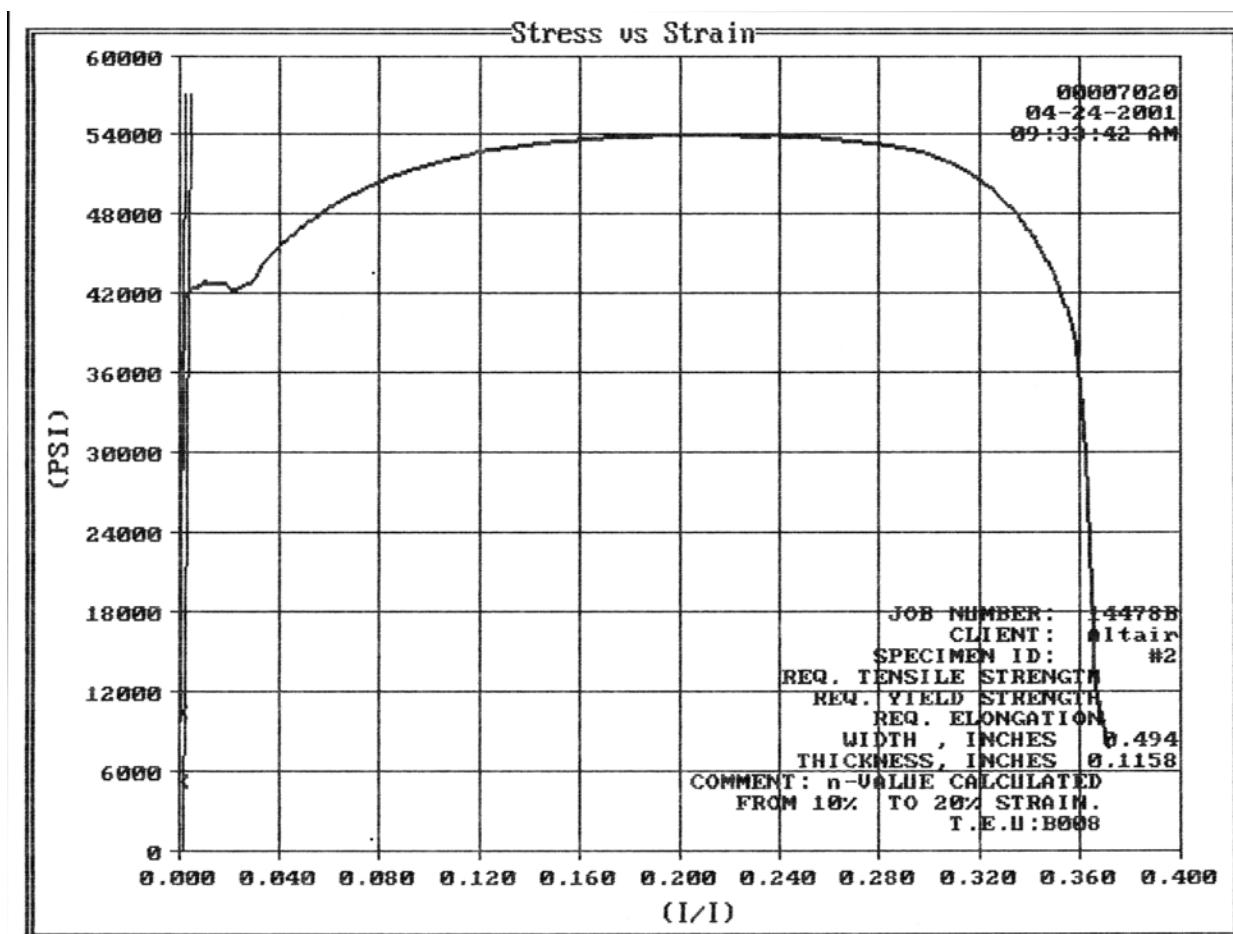
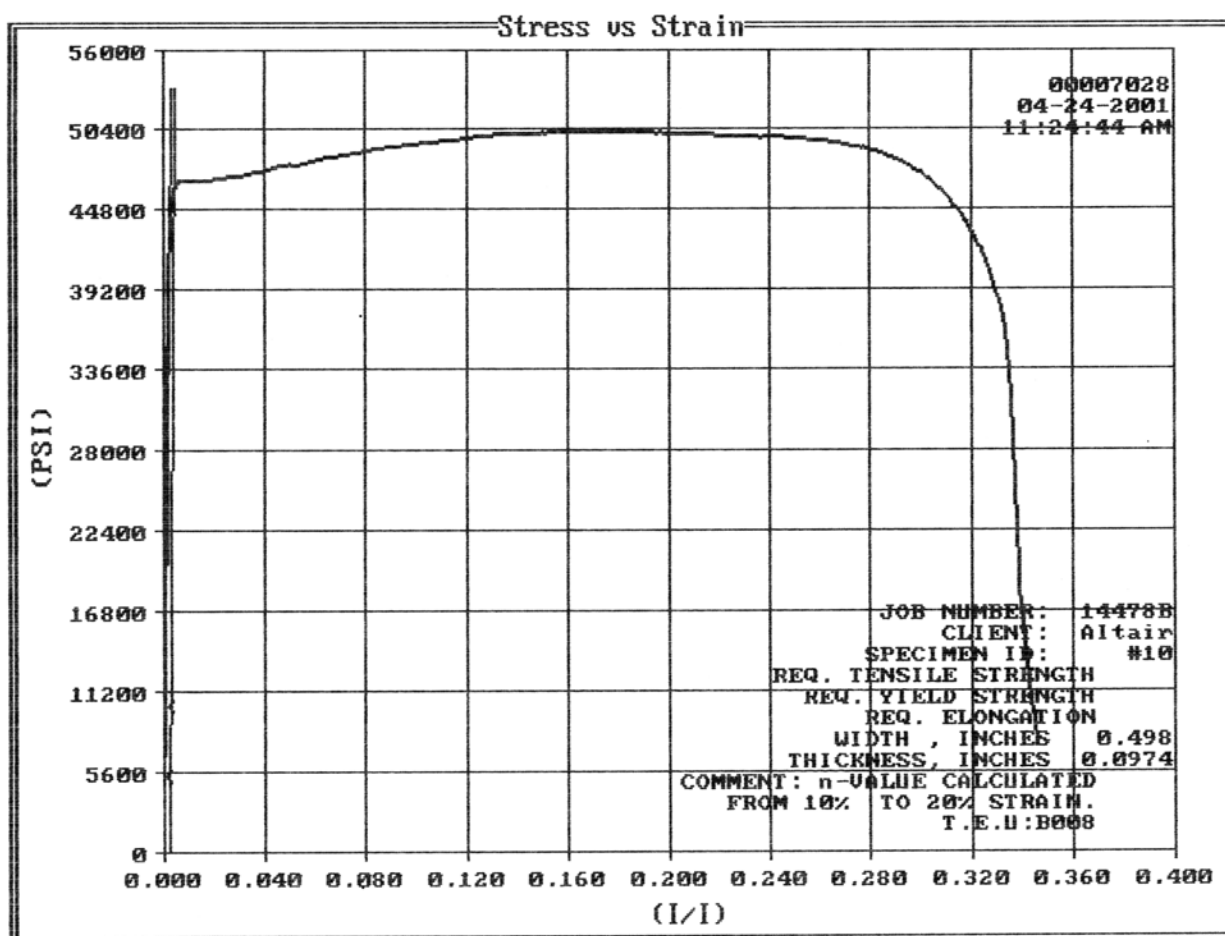# APPENDIX B: MATERIAL TESTING REPORT

Plot 4-Linear Strain Range

Coupon #2-Joint 5 Outer Side Rail
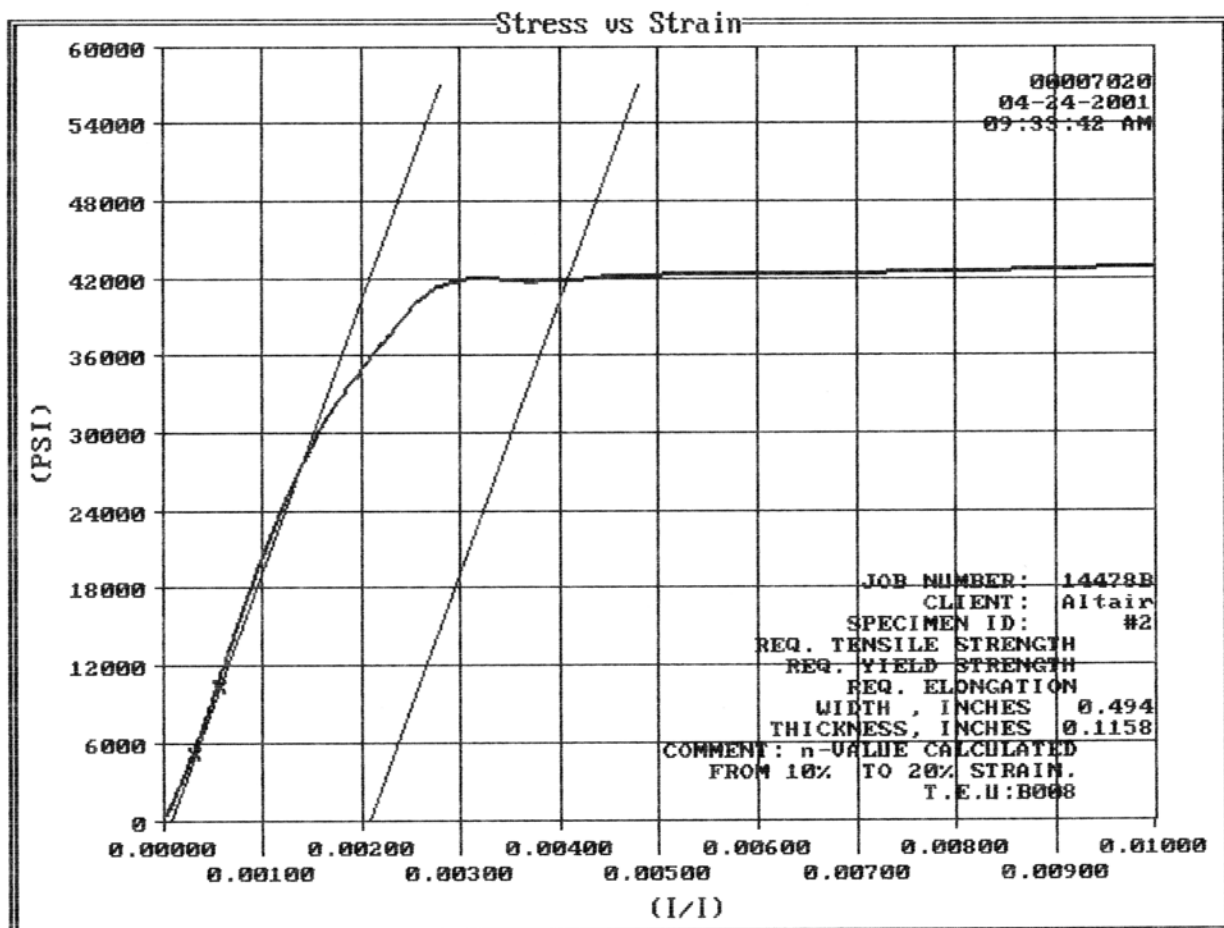
# APPENDIX B: MATERIAL TESTING REPORT

Plot 5-Full Strain Range

Coupon 3-Joint 5 Crossmember
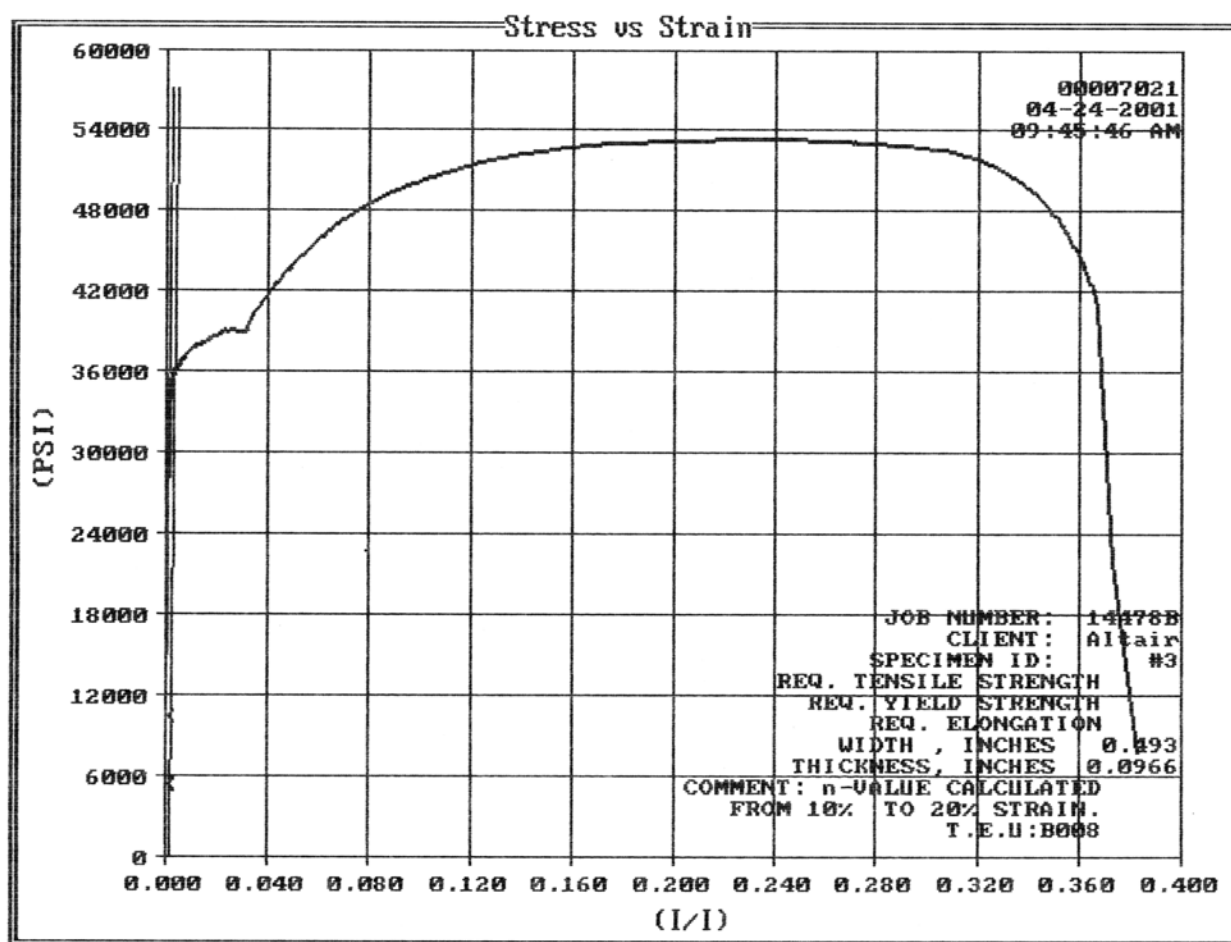
APPENDIX B: MATERIAL TESTING REPORT

Plot 6-Linear Strain Range

Coupon 3-Joint 5 Crossmember

APPENDIX B: MATERIAL TESTING REPORT
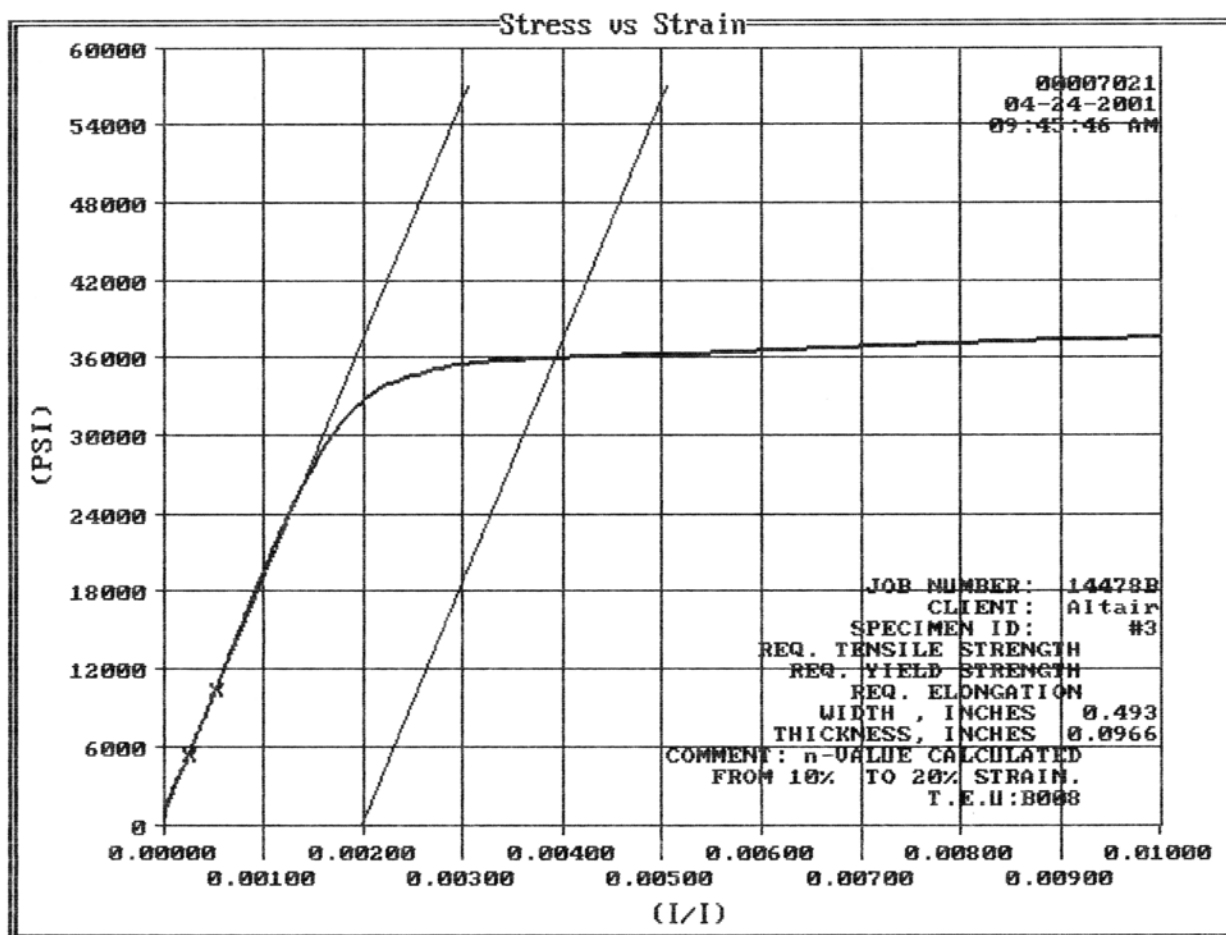
Coupon #4-Joint 4 Side Rail
Coupon #5-Joint 4 Crossmember
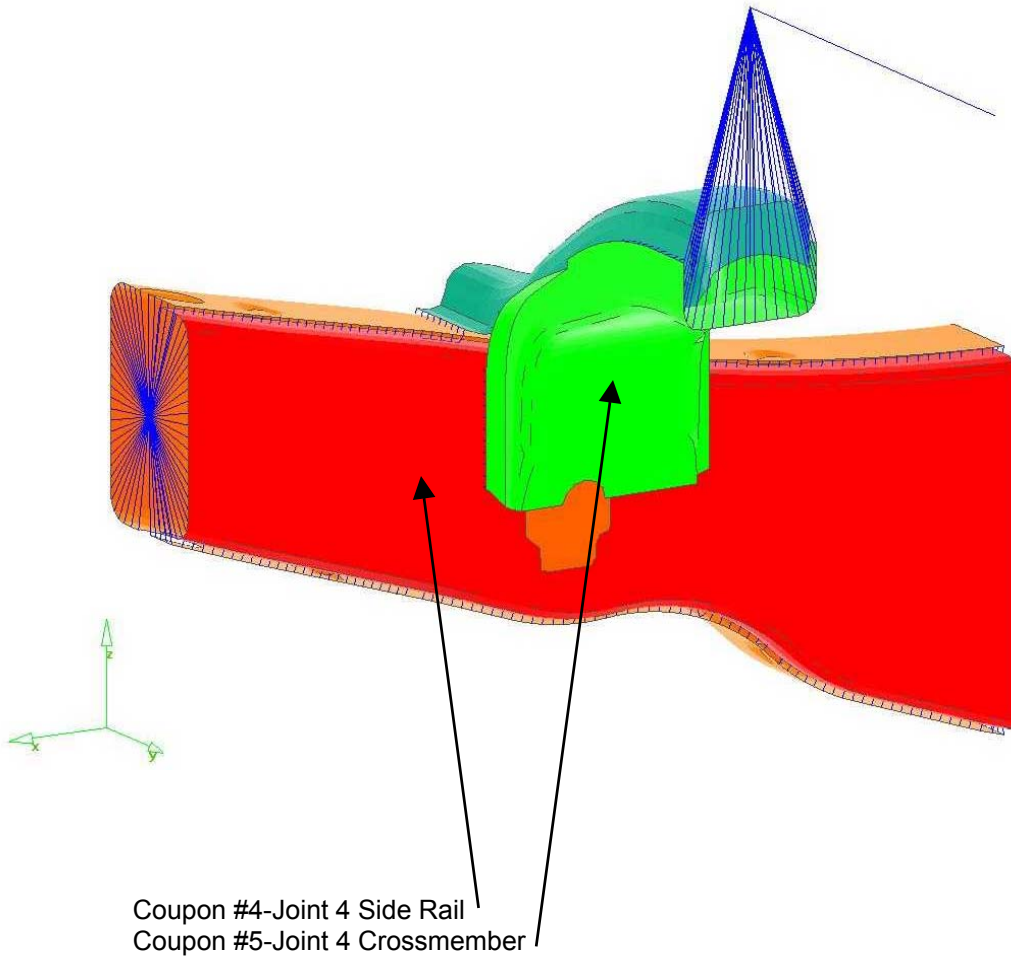
APPENDIX B: MATERIAL TESTING REPORT

Plot 7-Full Strain Range

Coupon #4-Joint 4 Side Rail
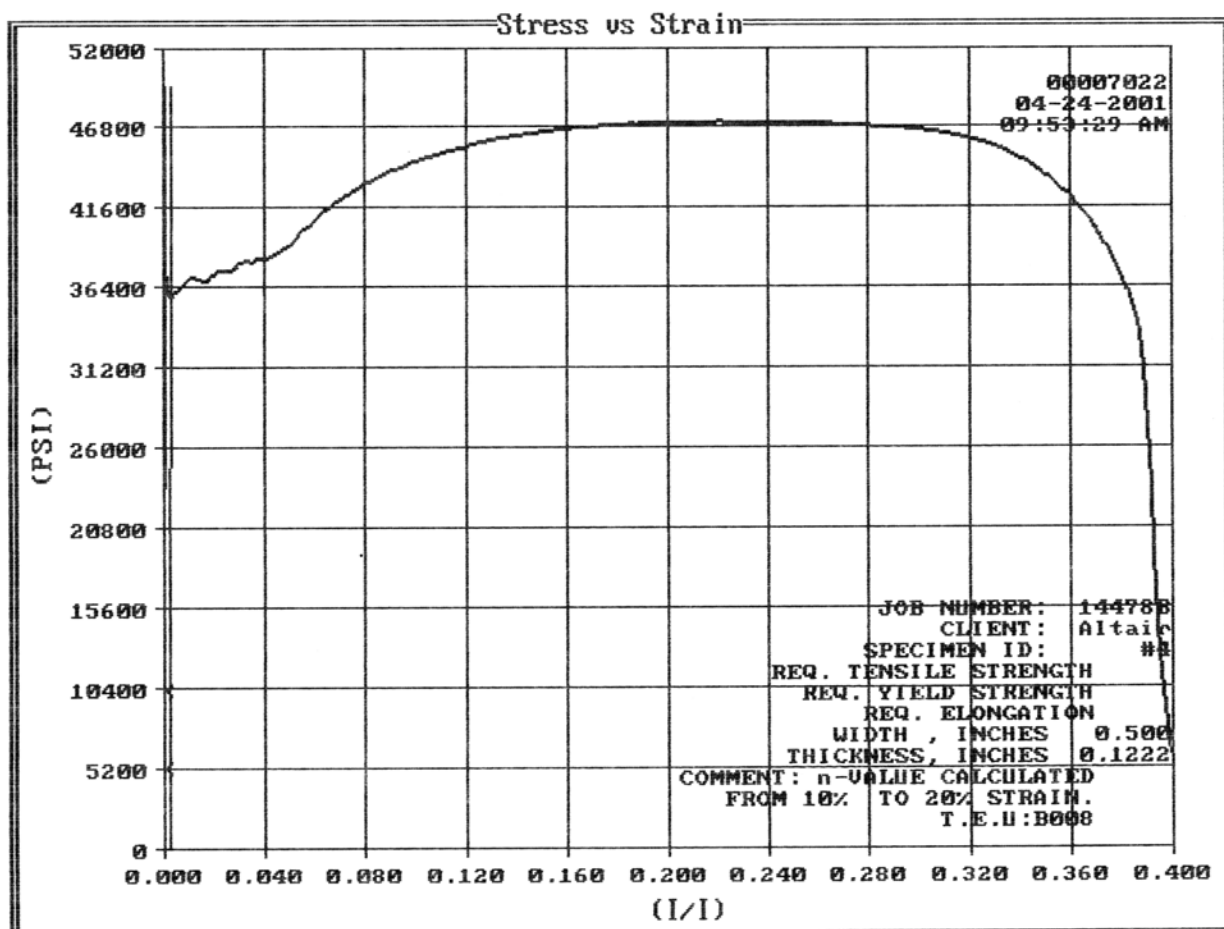
APPENDIX B: MATERIAL TESTING REPORT

Plot 8-Linear Strain Range

Coupon #4-Joint 4 Side Rail
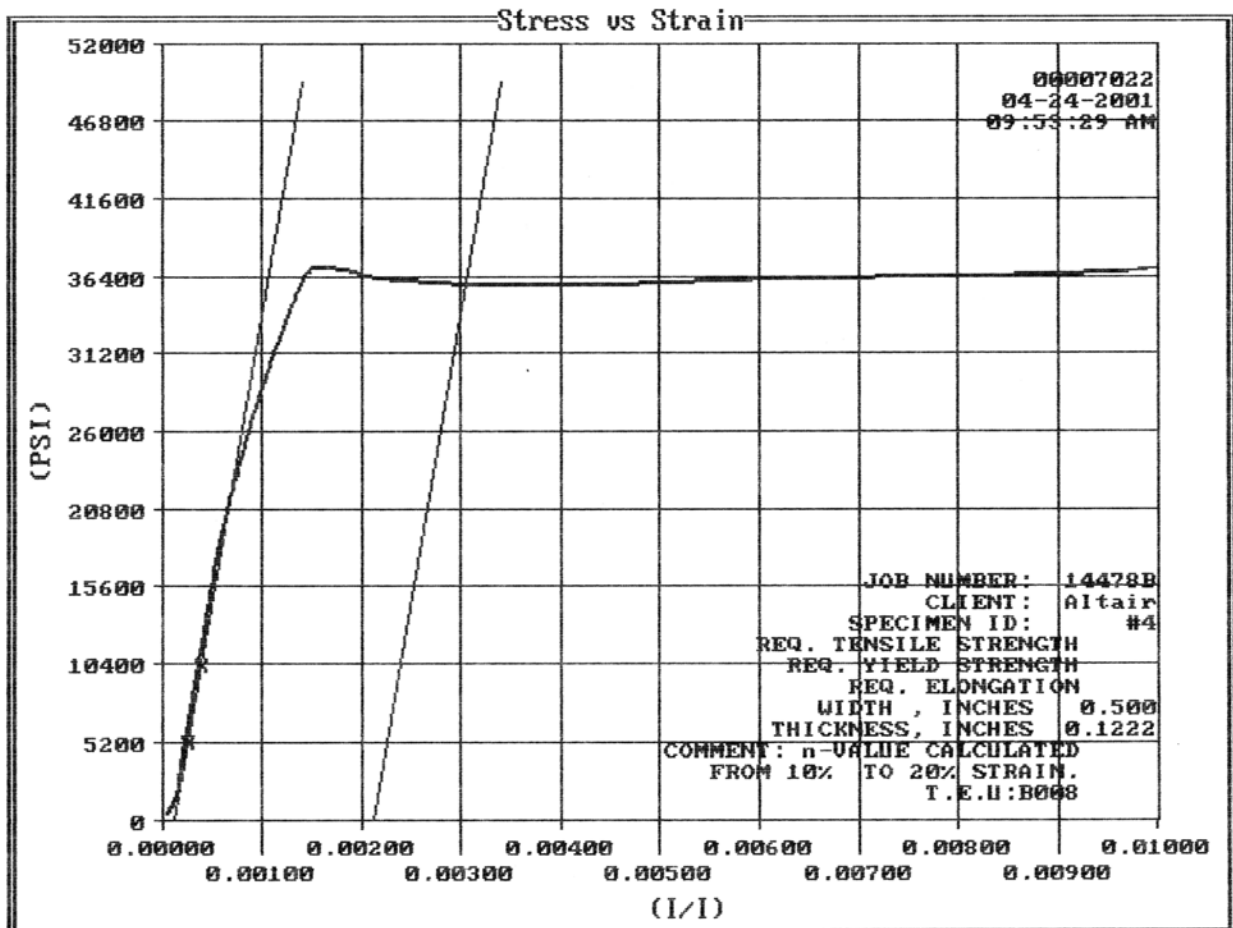
APPENDIX B: MATERIAL TESTING REPORT

Plot 9-Full Strain Range

Coupon #5-Joint 4 Crossmember
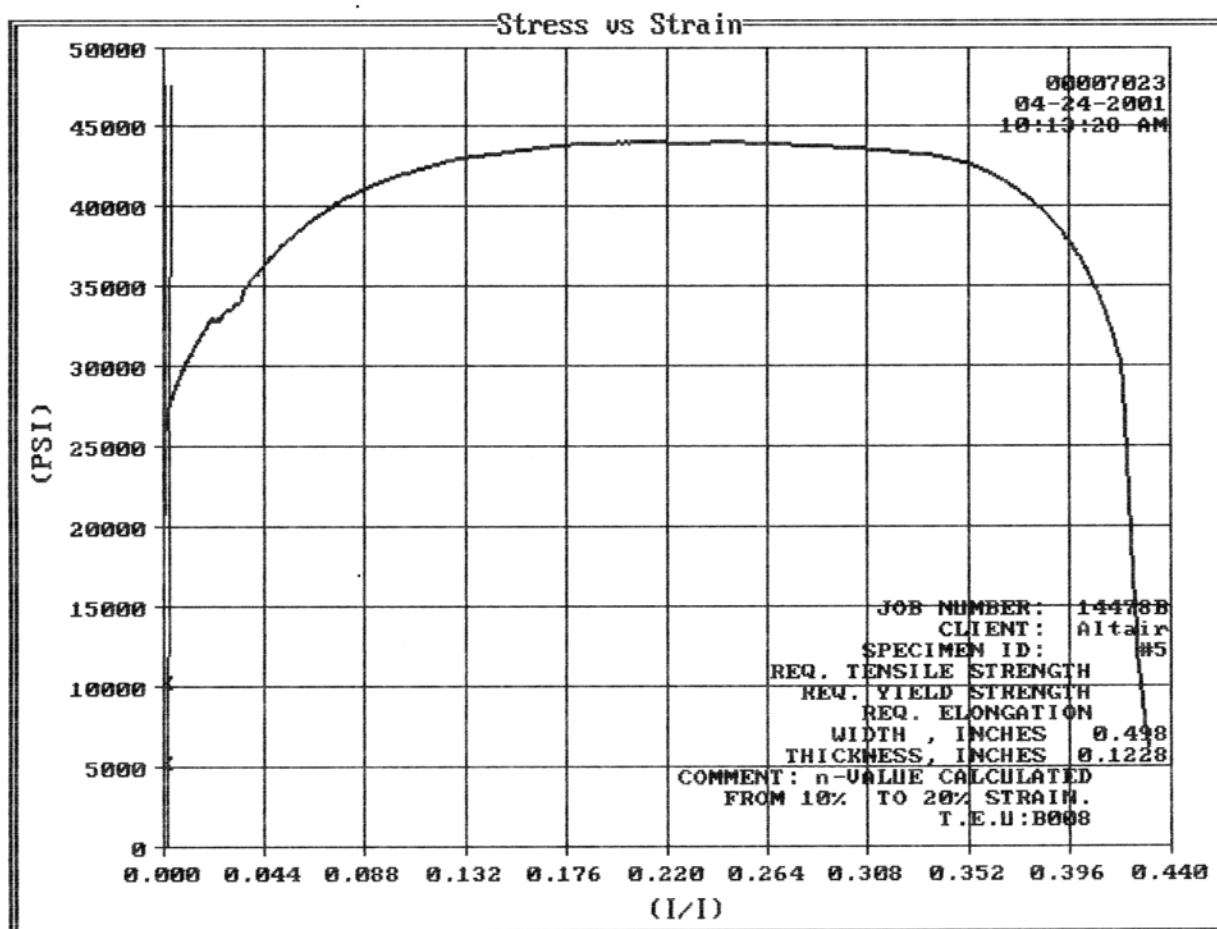
# APPENDIX B: MATERIAL TESTING REPORT

Plot 10-Linear Strain Range

Coupon #5-Joint 4 Crossmember

APPENDIX B: MATERIAL TESTING REPORT
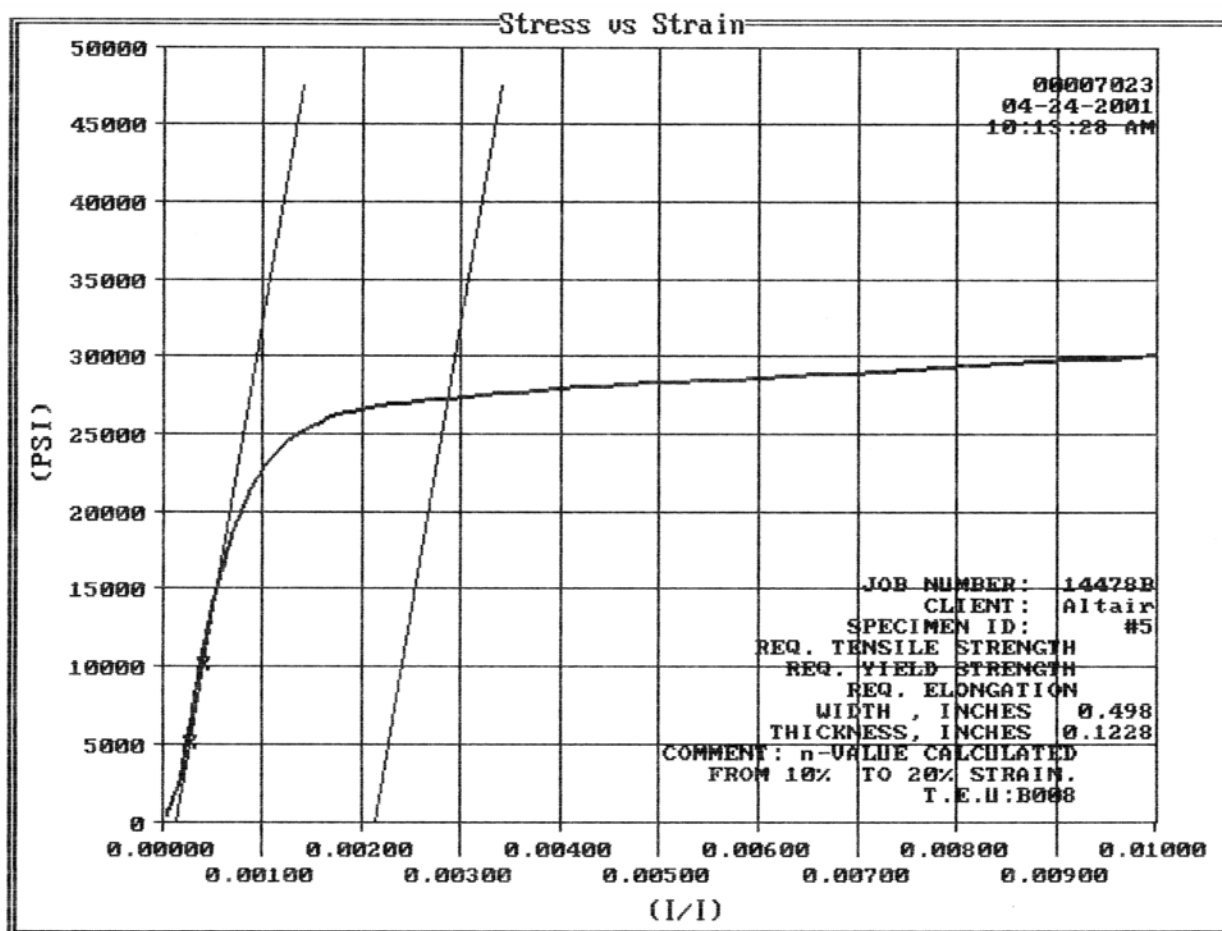
Coupon #6-Joint 3 Side Rail
Coupon #7-Joint 3 Crossmember
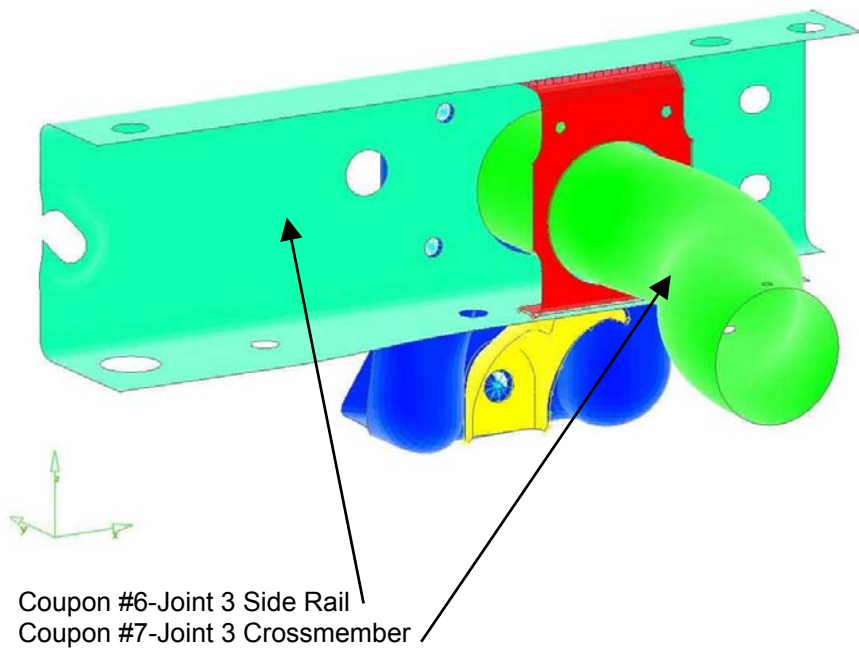
APPENDIX B: MATERIAL TESTING REPORT

Plot 11-Full Strain Range

Coupon #6-Joint 3 Side Rail

Altair Engineering
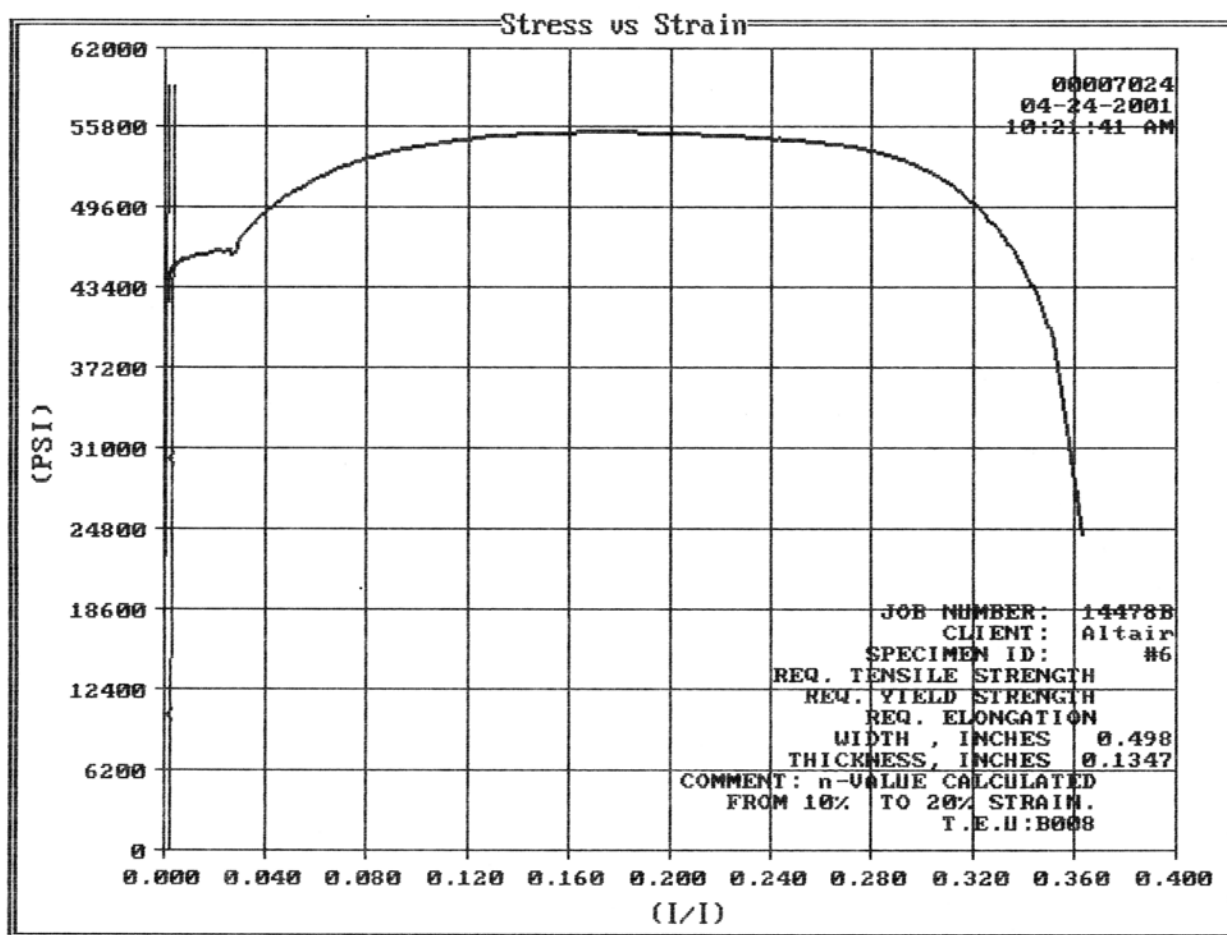
APPENDIX B: MATERIAL TESTING REPORT

Plot 12-Linear Strain Range

Coupon #6-Joint 3 Side Rail
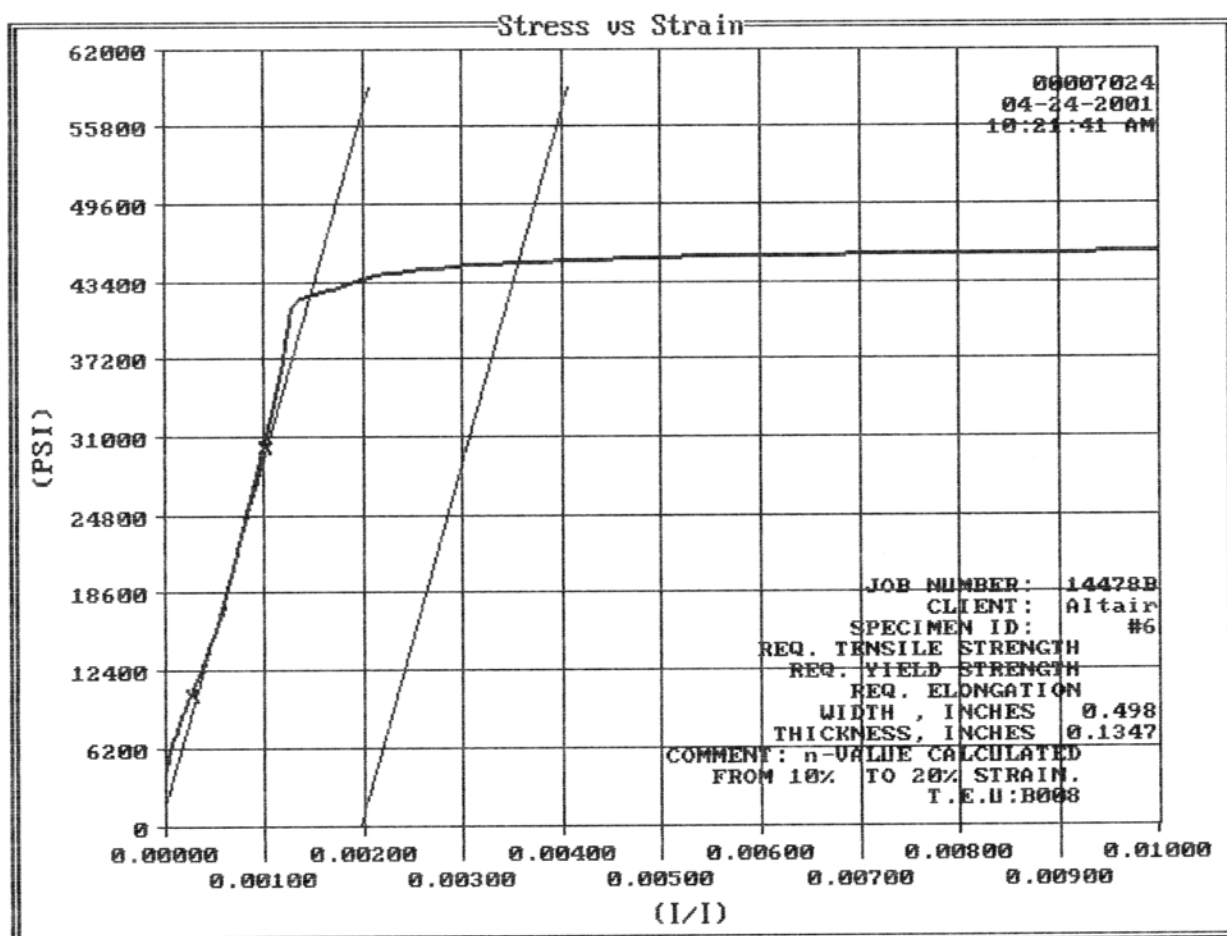
APPENDIX B: MATERIAL TESTING REPORT

Plot 13-Full Strain Range

Coupon #7-Joint 3 Crossmember
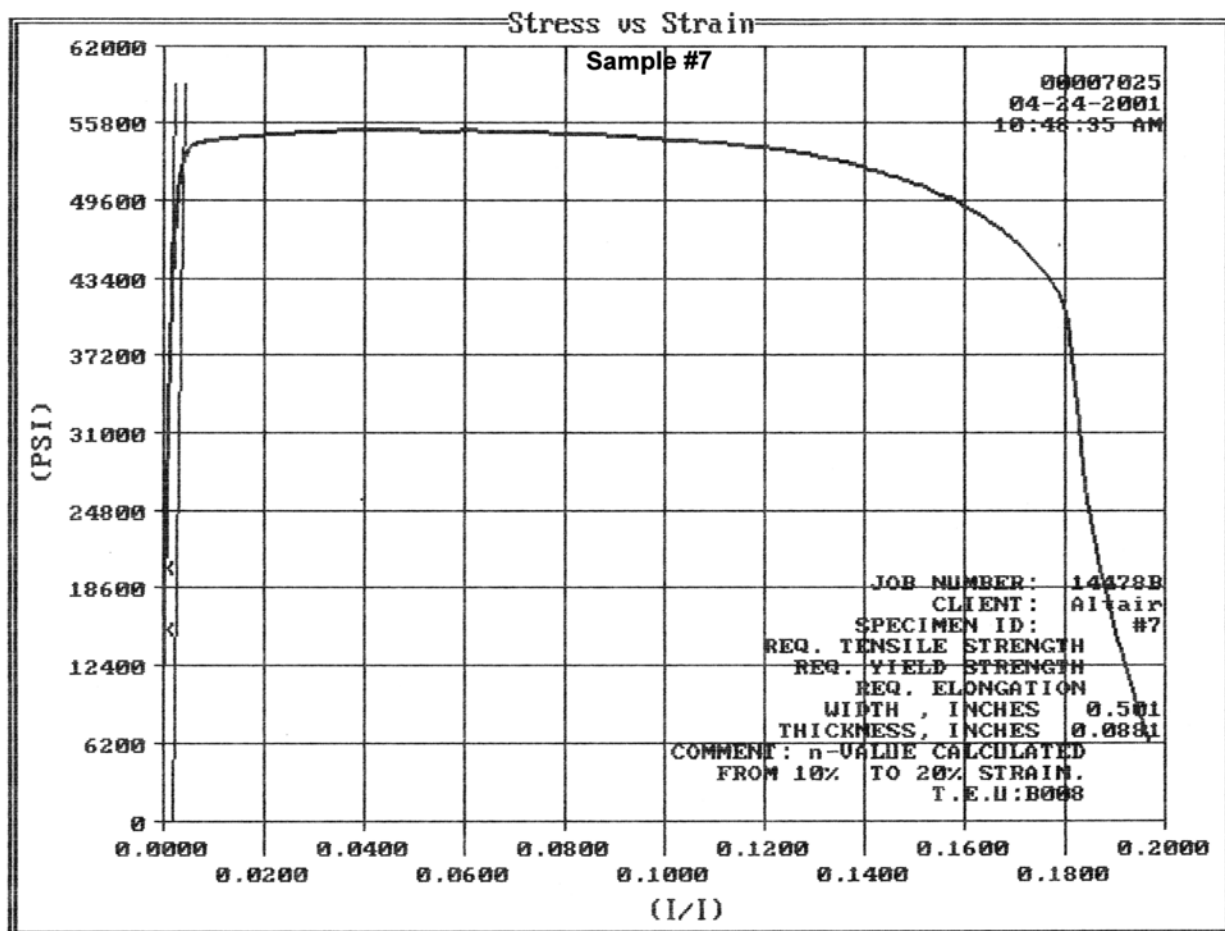
APPENDIX B: MATERIAL TESTING REPORT

Plot 14-Linear Strain Range

Coupon #7-Joint 3 Crossmember
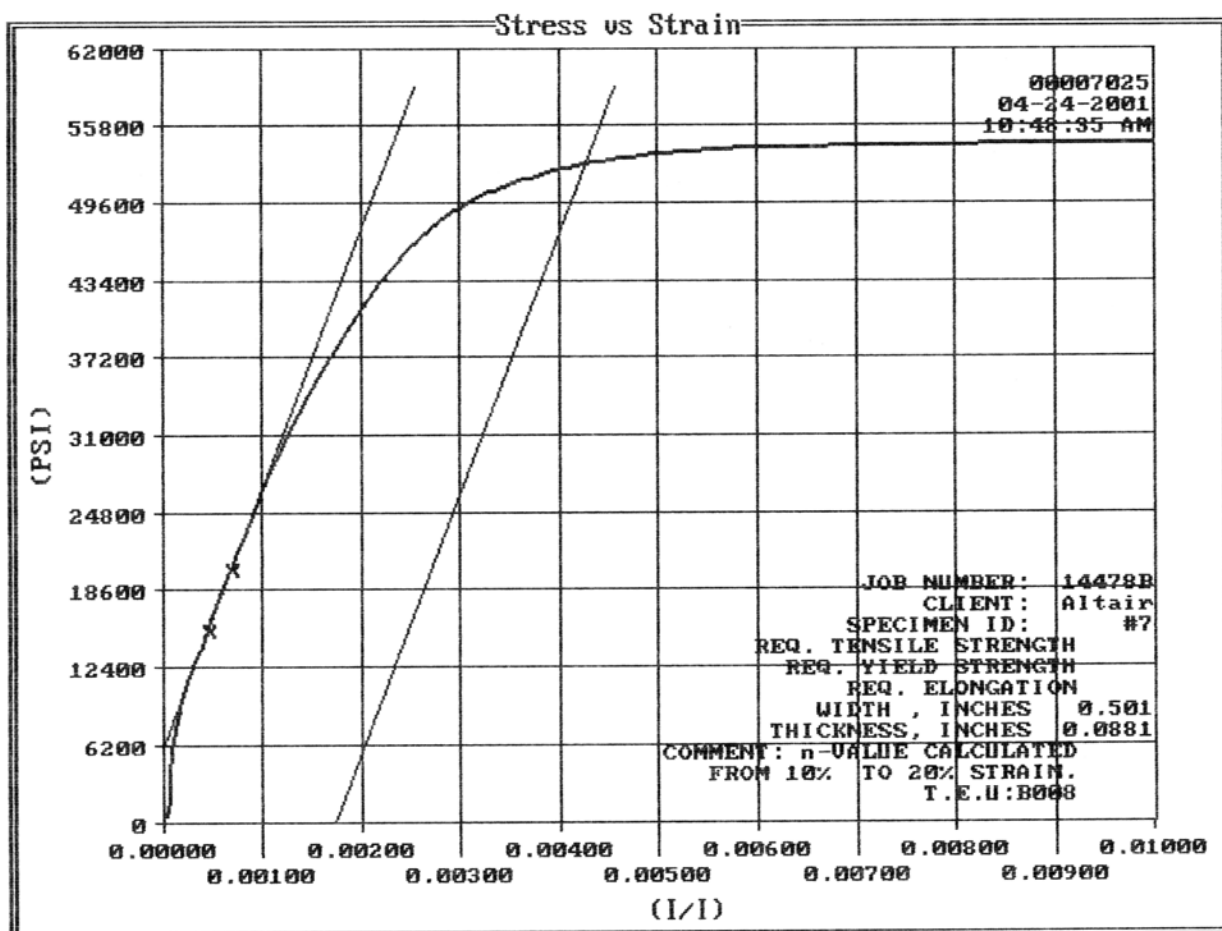
APPENDIX B: MATERIAL TESTING REPORT

Plot 15-Full Strain Range

Coupon #8-Joint 2 Side Rail
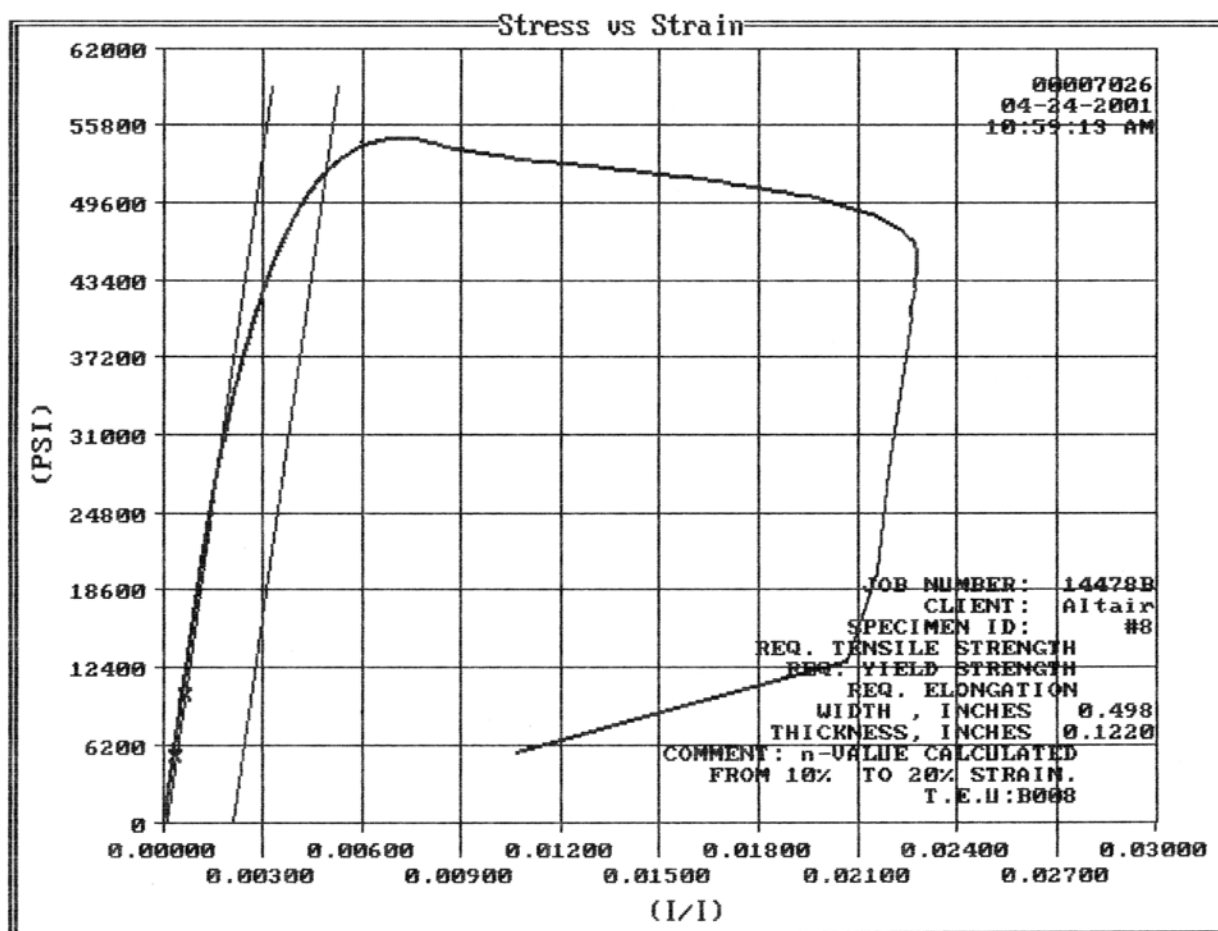
APPENDIX B: MATERIAL TESTING REPORT

Plot 16-Linear Strain Range

Coupon #8-Joint 2 Side Rail

Stress vs Strain
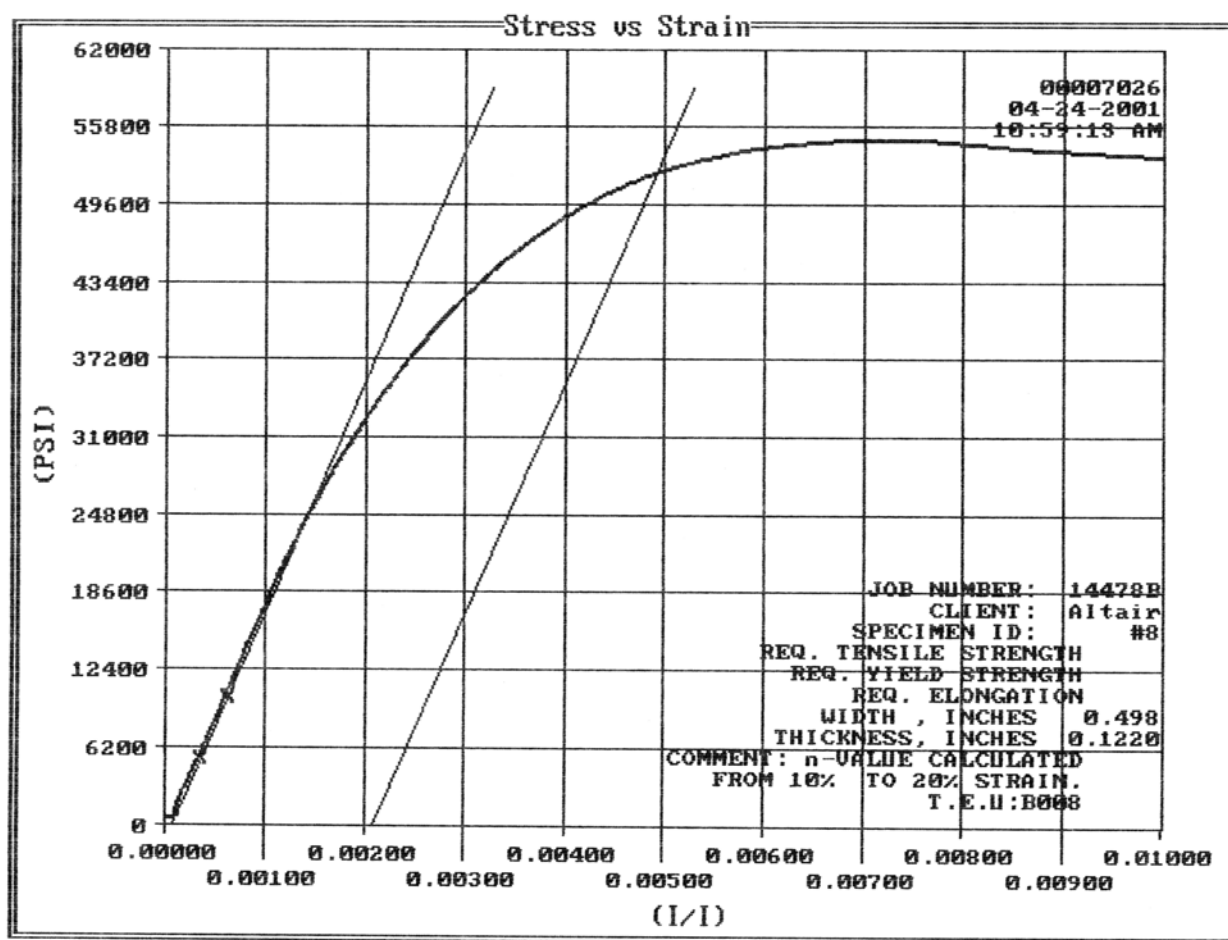
APPENDIX B: MATERIAL TESTING REPORT

Plot 17-Full Strain Range

Coupon #2-Joint 5 Outer Side Rail

APPENDIX B: MATERIAL TESTING REPORT

Plot 18-Linear Strain Range

Coupon #2-Joint 5 Outer Side Rail

APPENDIX B: MATERIAL TESTING REPORT

Plot 19-Full Strain Range

Coupon #10-Joint 1 Crossmember

# APPENDIX B: MATERIAL TESTING REPORT

Plot 20-Linear Strain Range

Coupon #10-Joint 1 Crossmember
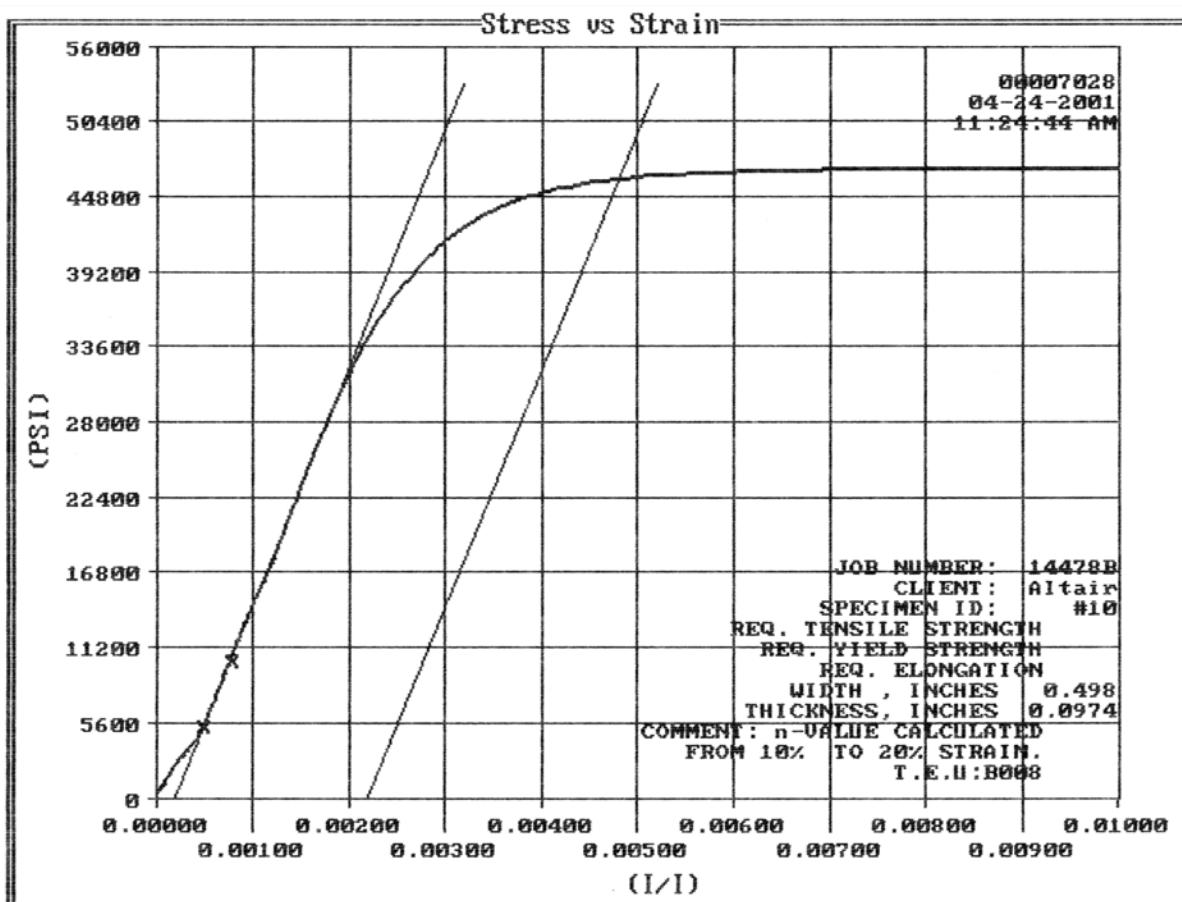
APPENDIX C: TEST RESULTS
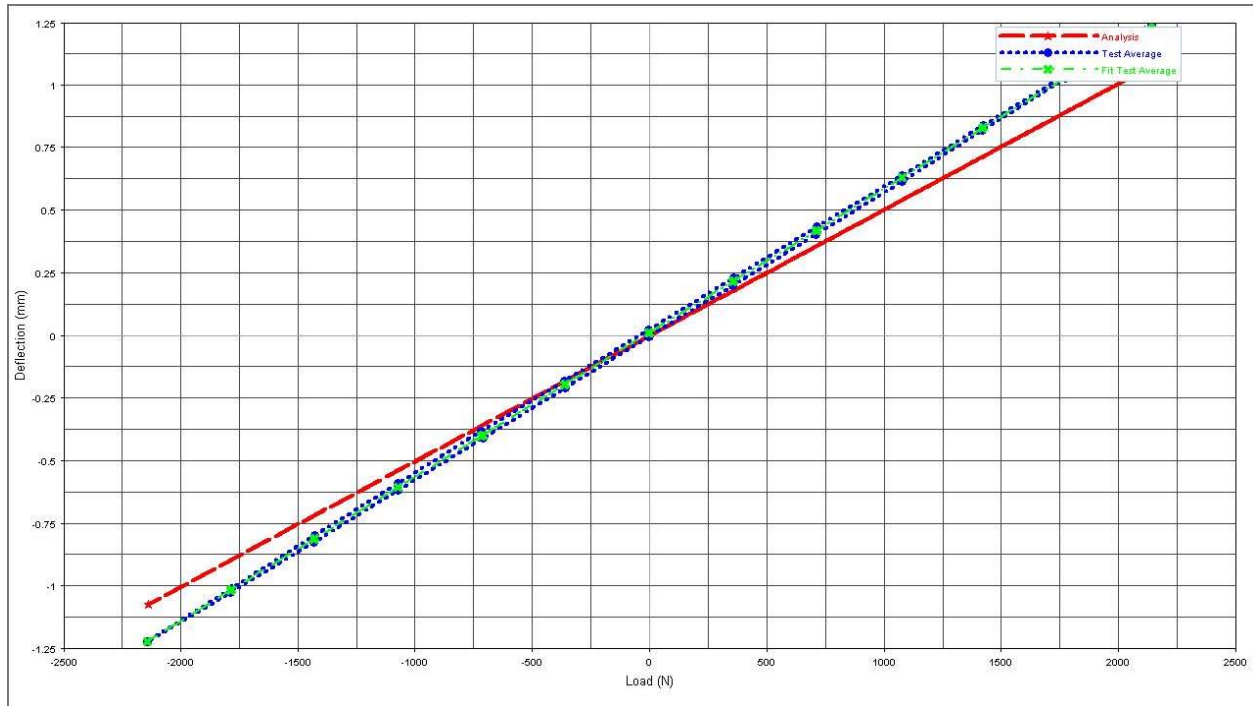
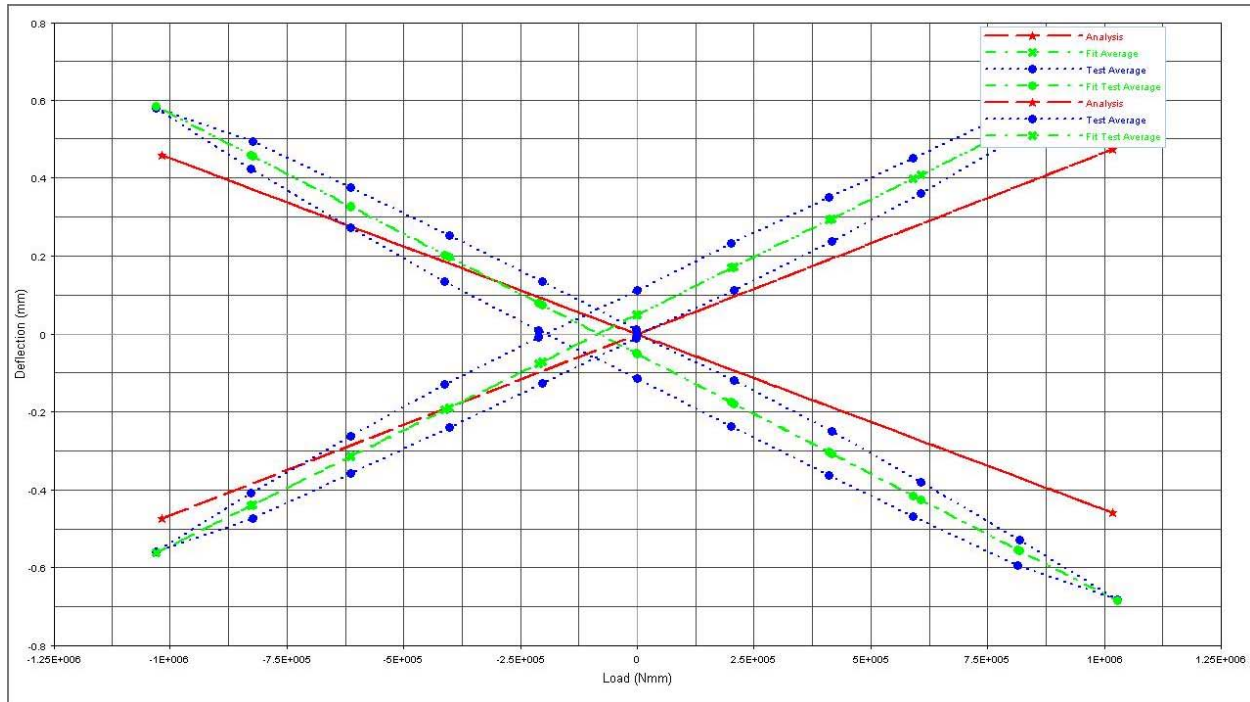
Joint 1 Fore/Aft Load Test vs. Analysis
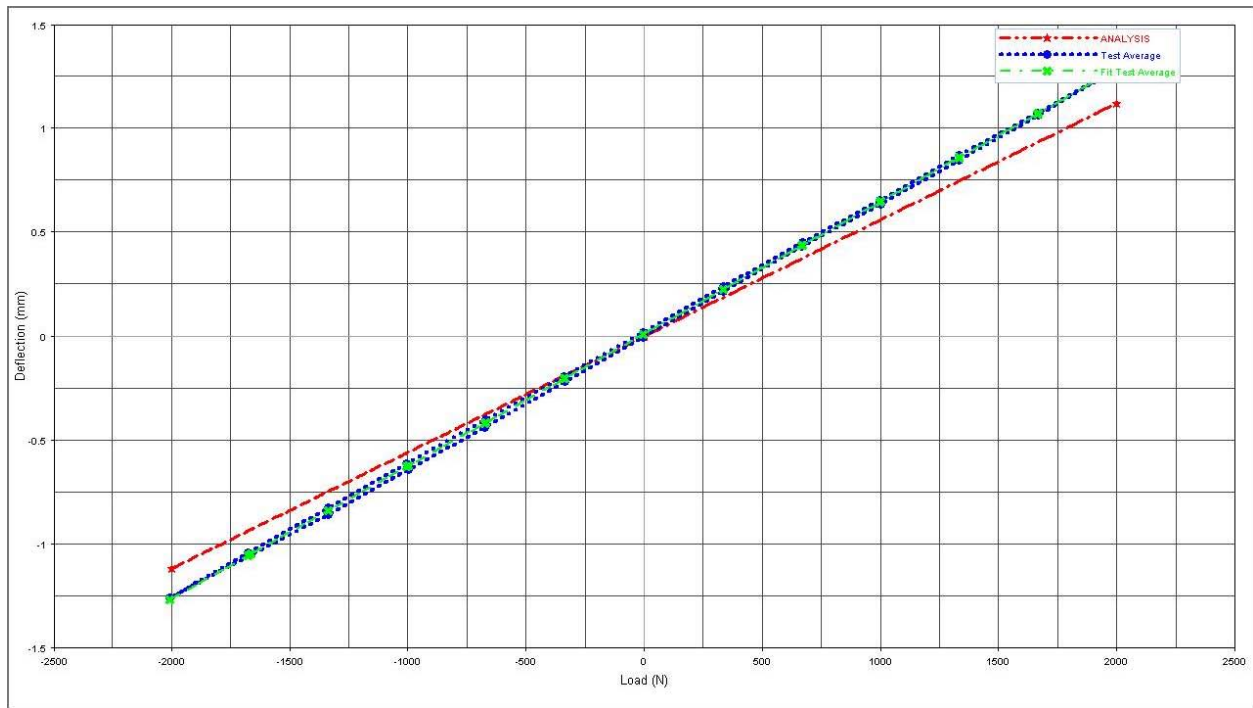
Joint 1 Vertical Load Test vs. Analysis

APPENDIX C: TEST RESULTS
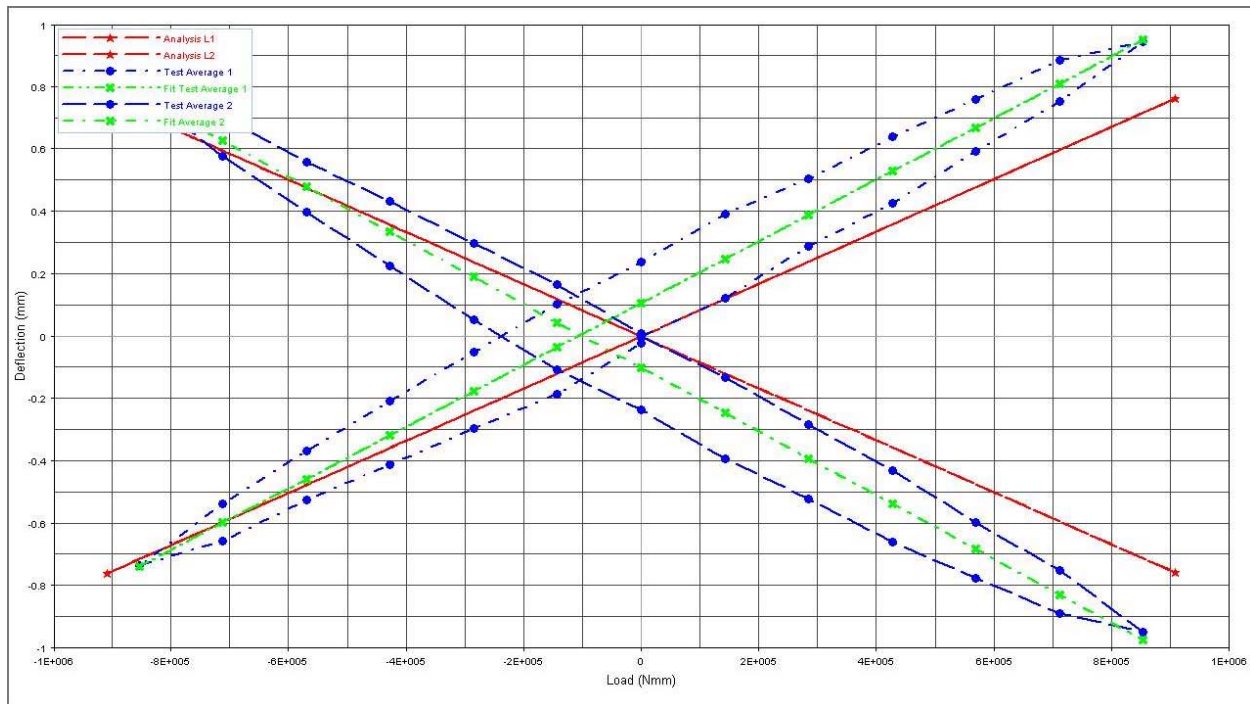
Joint 1 Torsion Load Test vs. Analysis
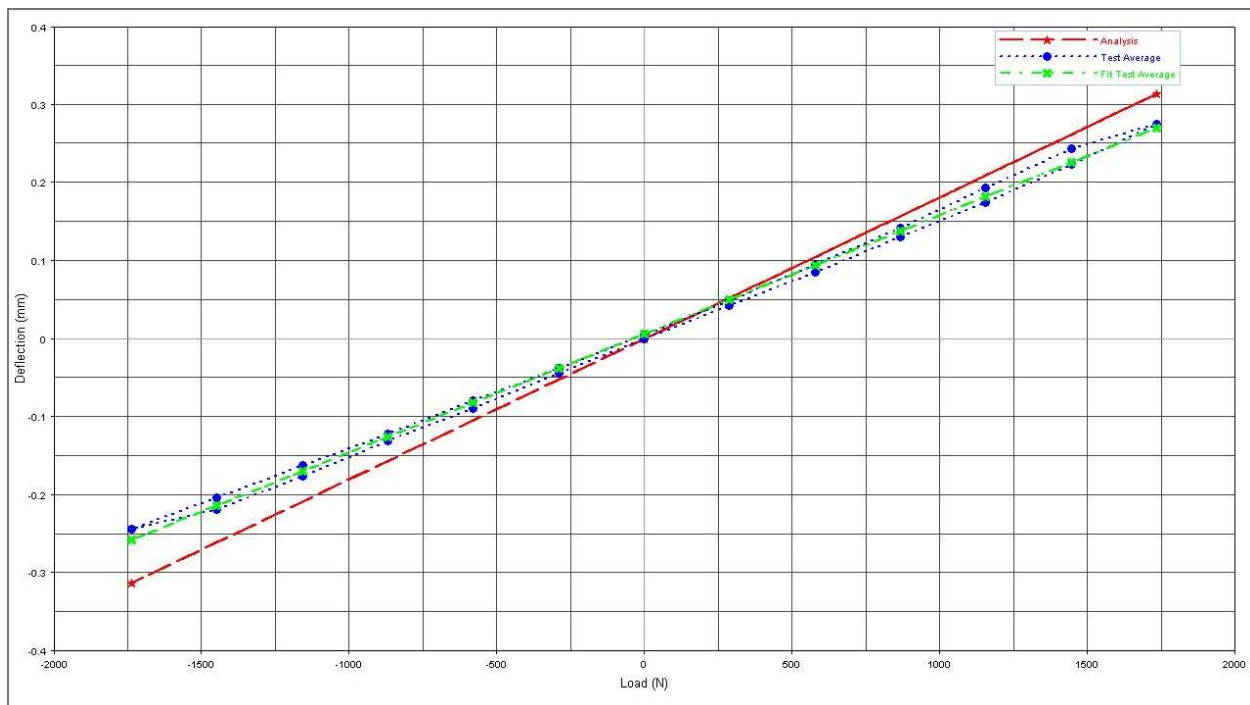
Joint 2 Fore/Aft Load Test vs. Analysis

APPENDIX C: TEST RESULTS
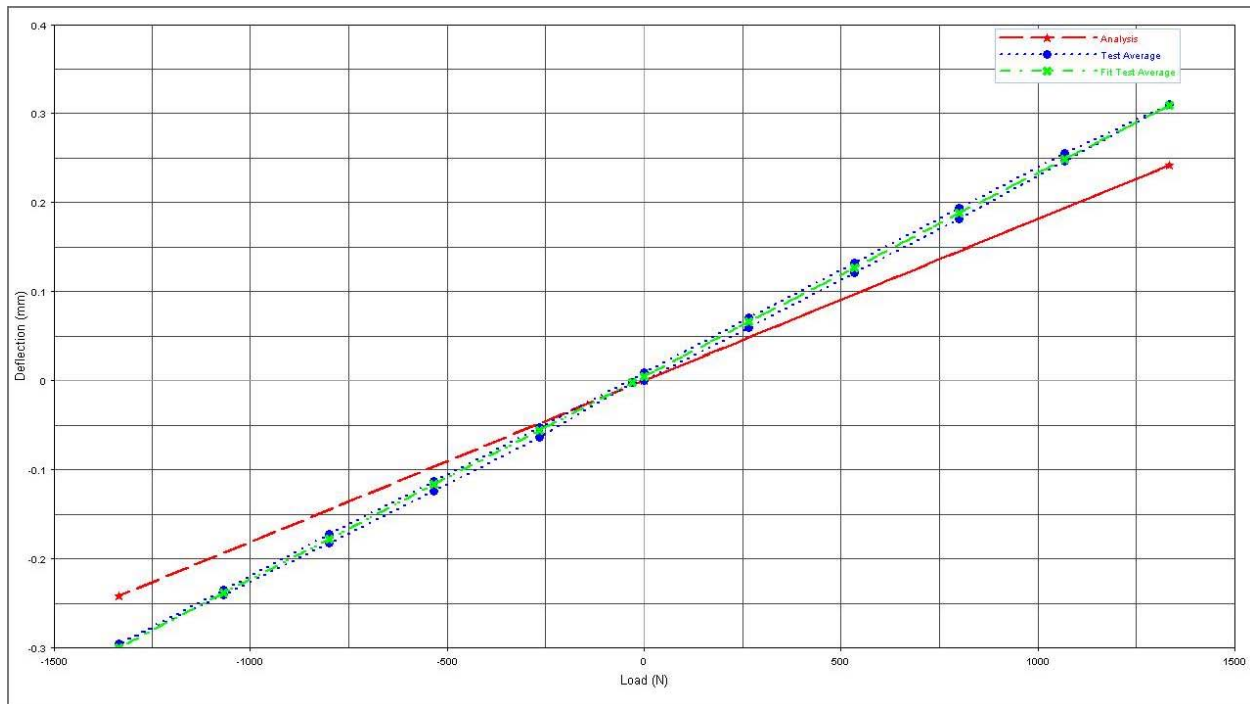
Joint 2 Vertical Load Test vs. Analysis
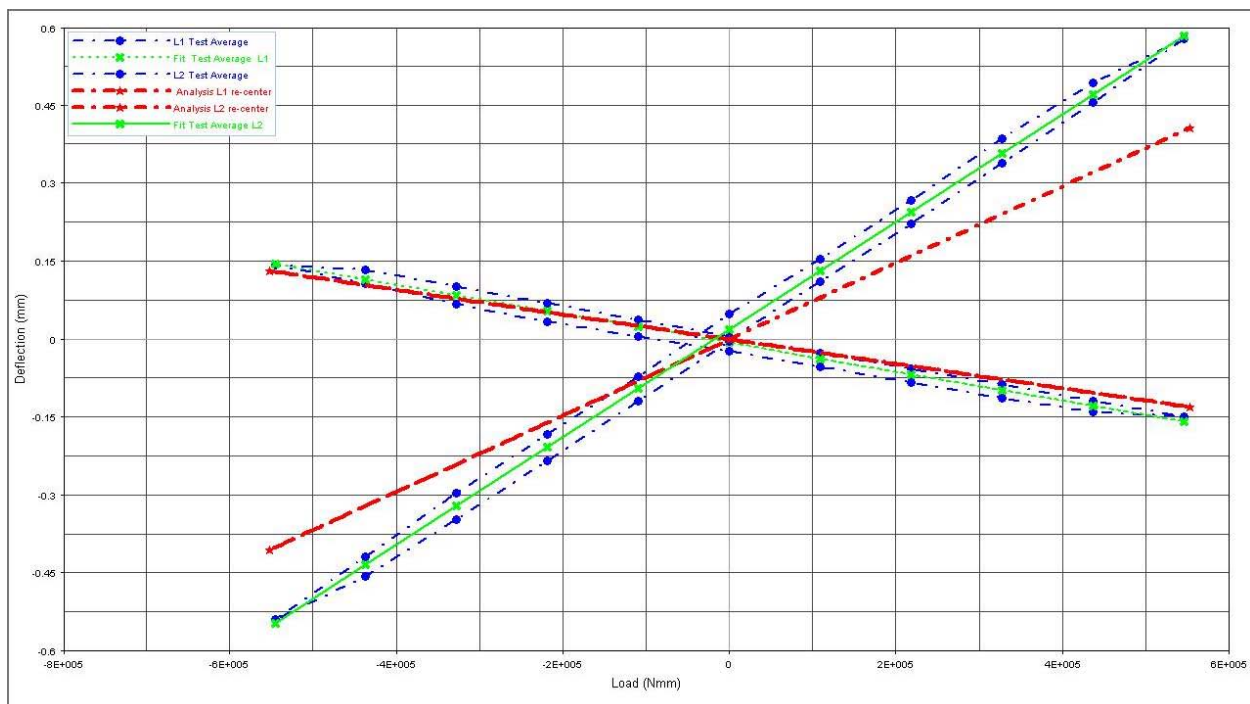
Joint 2 Torsion Load Test vs. Analysis

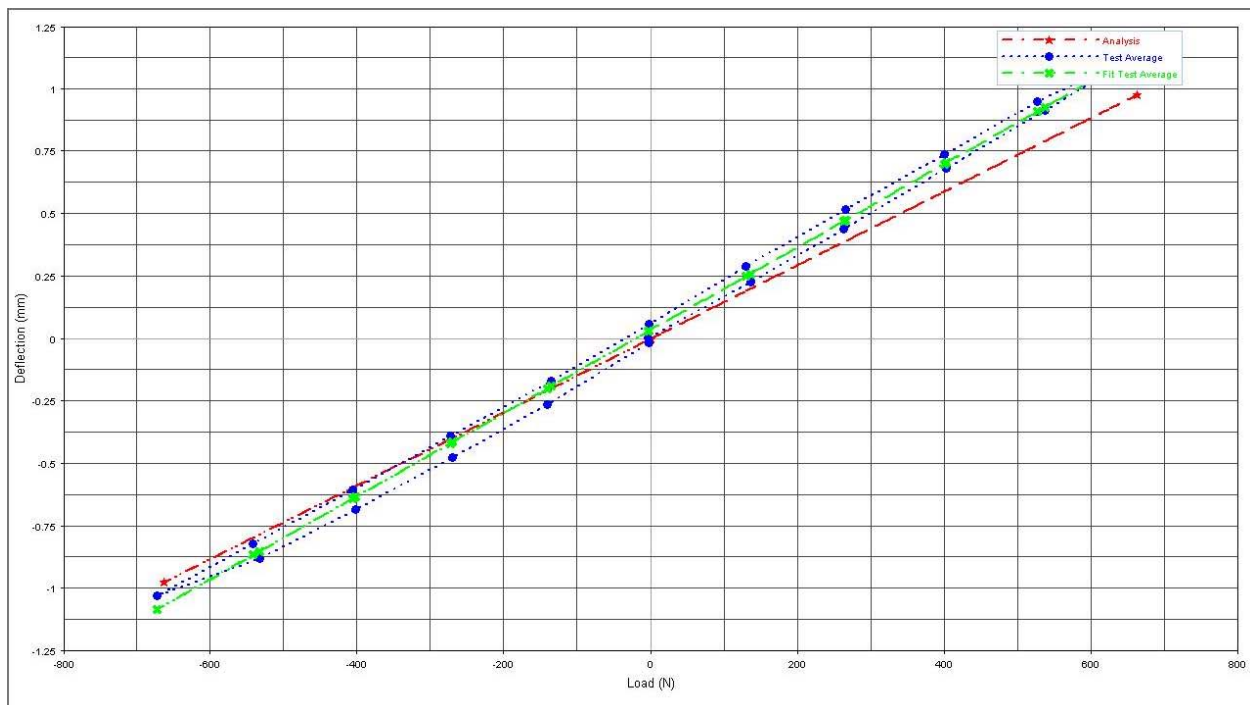# APPENDIX C: TEST RESULTS
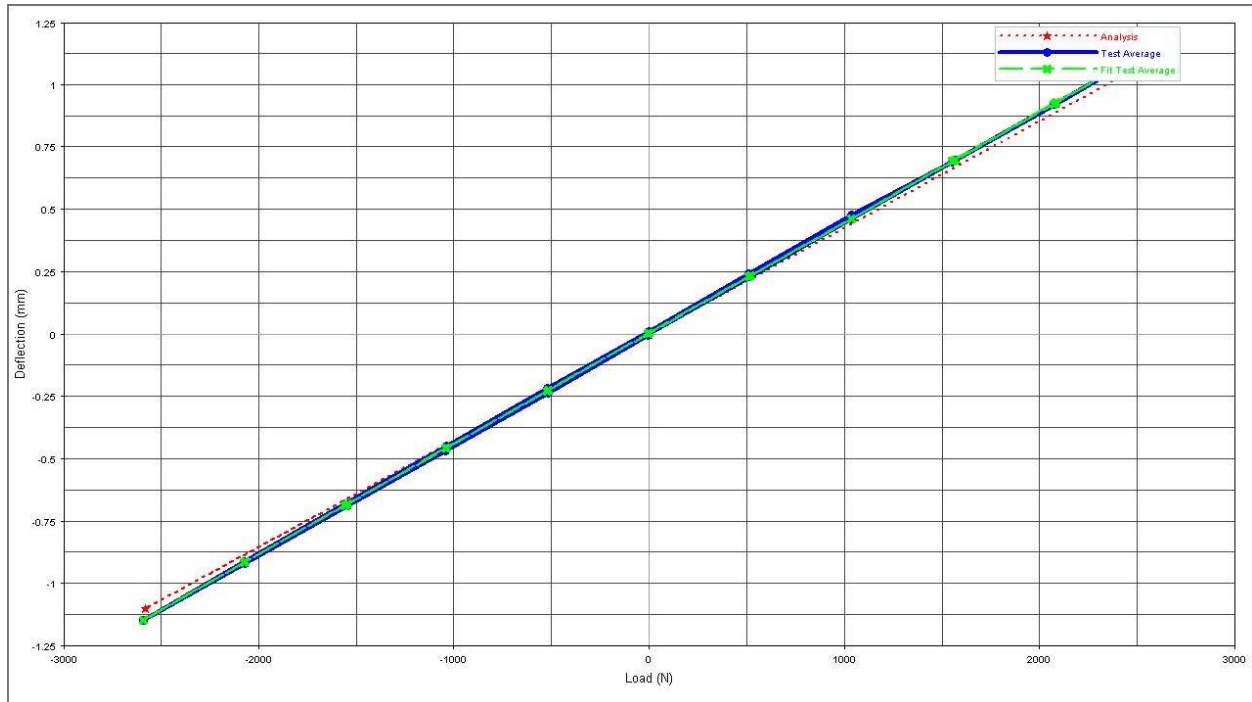
Joint 3 Fore/Aft Load Test vs. Analysis
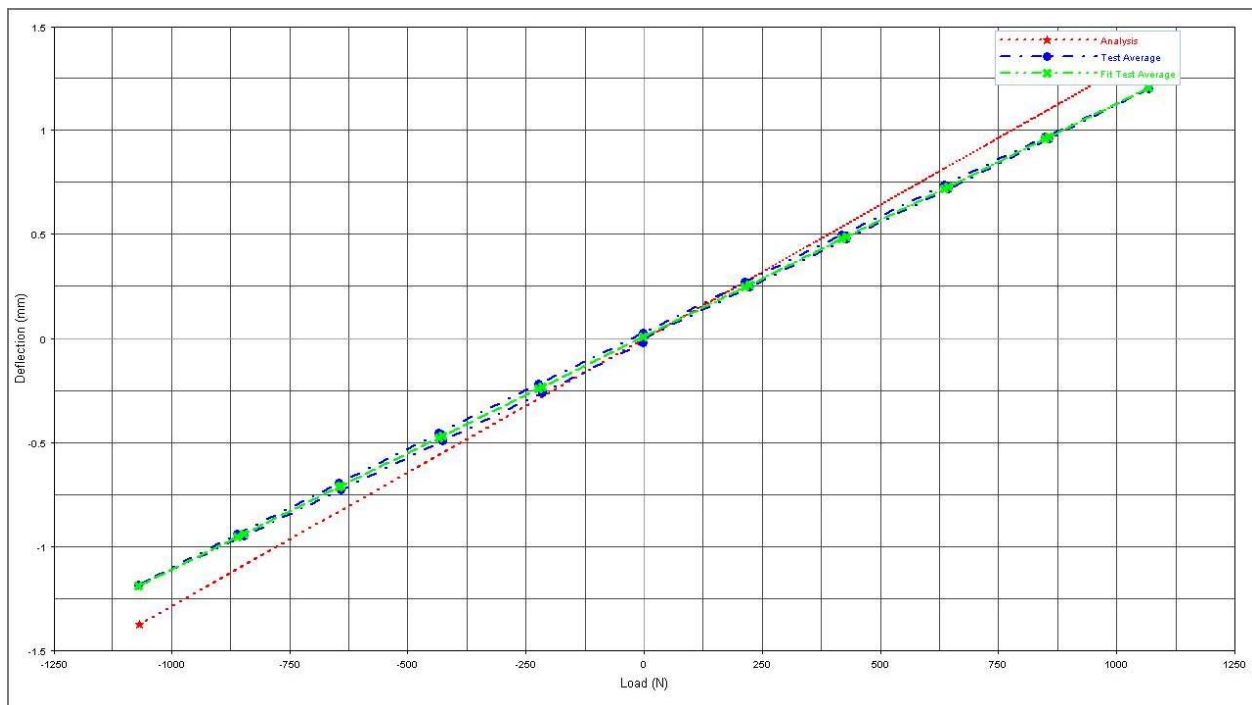
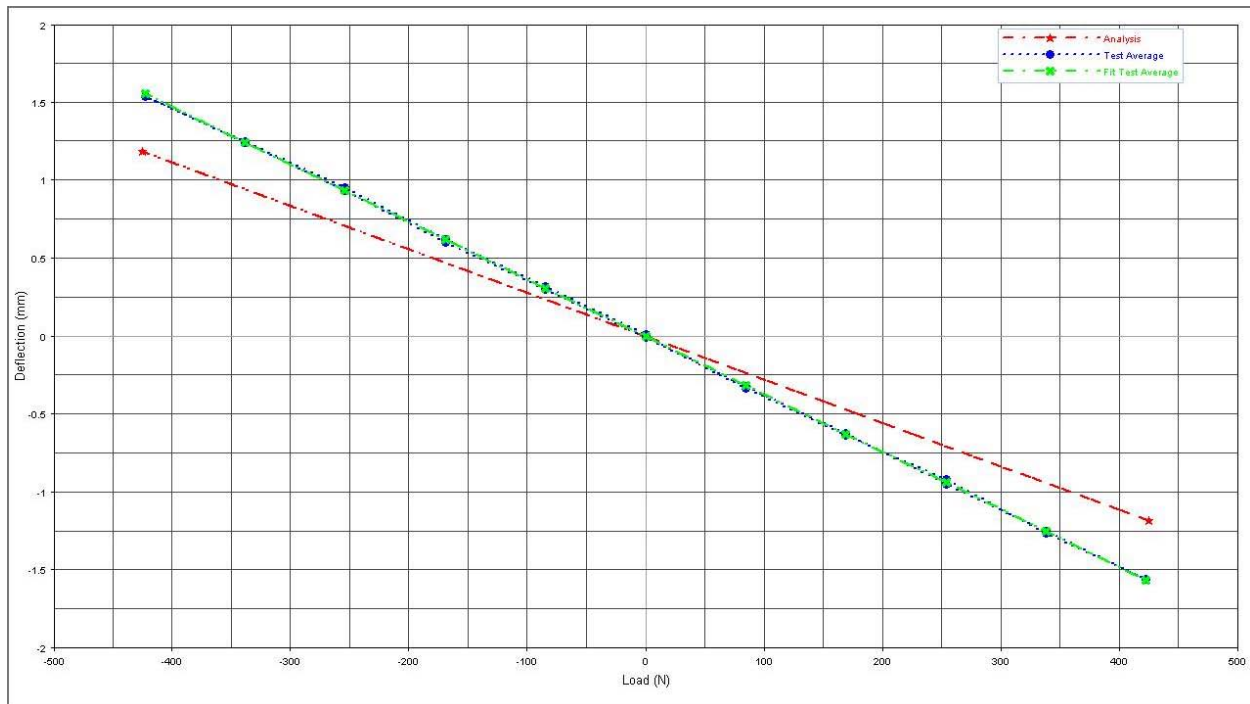Joint 3 Vertical Load Test vs. Analysis

APPENDIX C: TEST RESULTS

Joint 3 Torsion Load Test vs. Analysis
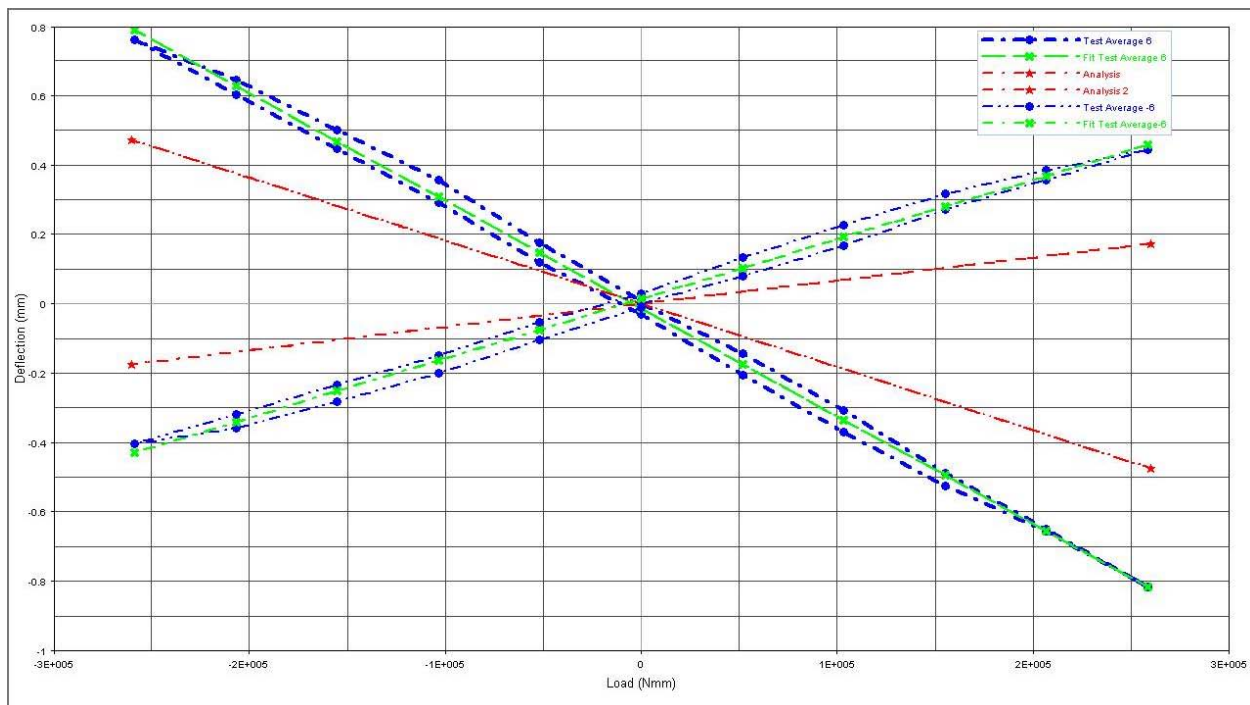

Joint 4 Fore/Aft Load Test vs. Analysis

APPENDIX C: TEST RESULTS

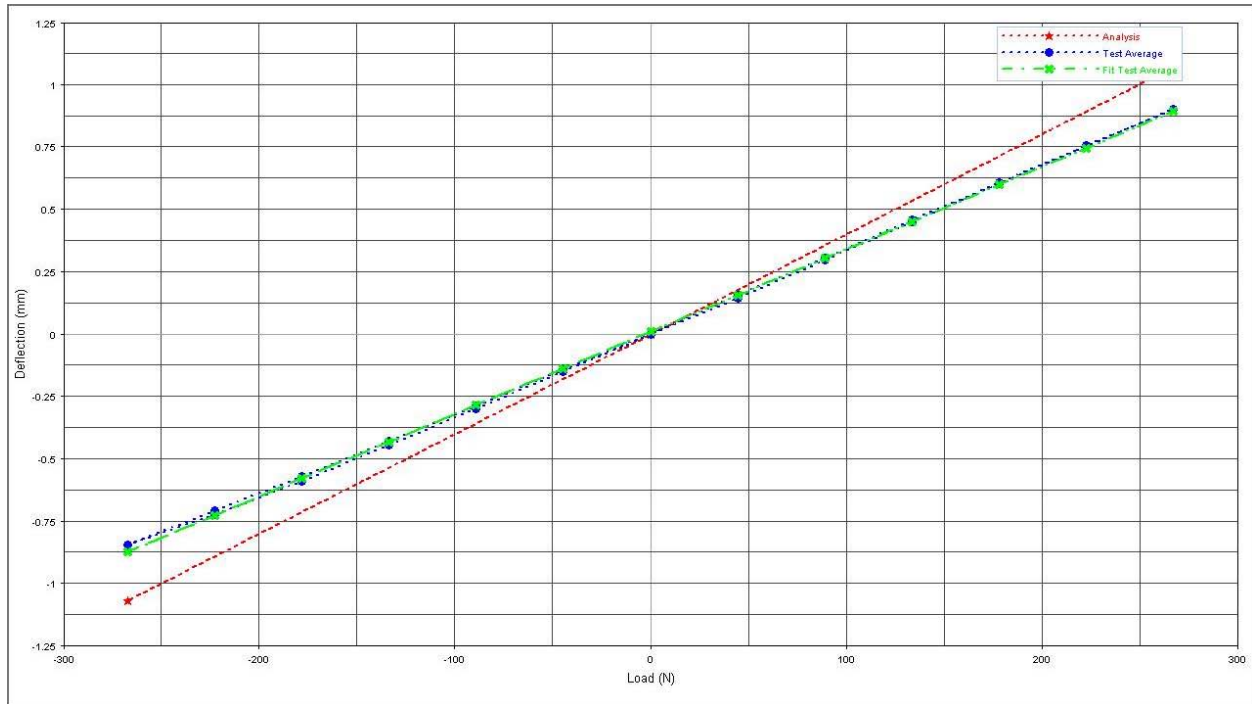

Joint 4 Vertical Load Test vs. Analysis

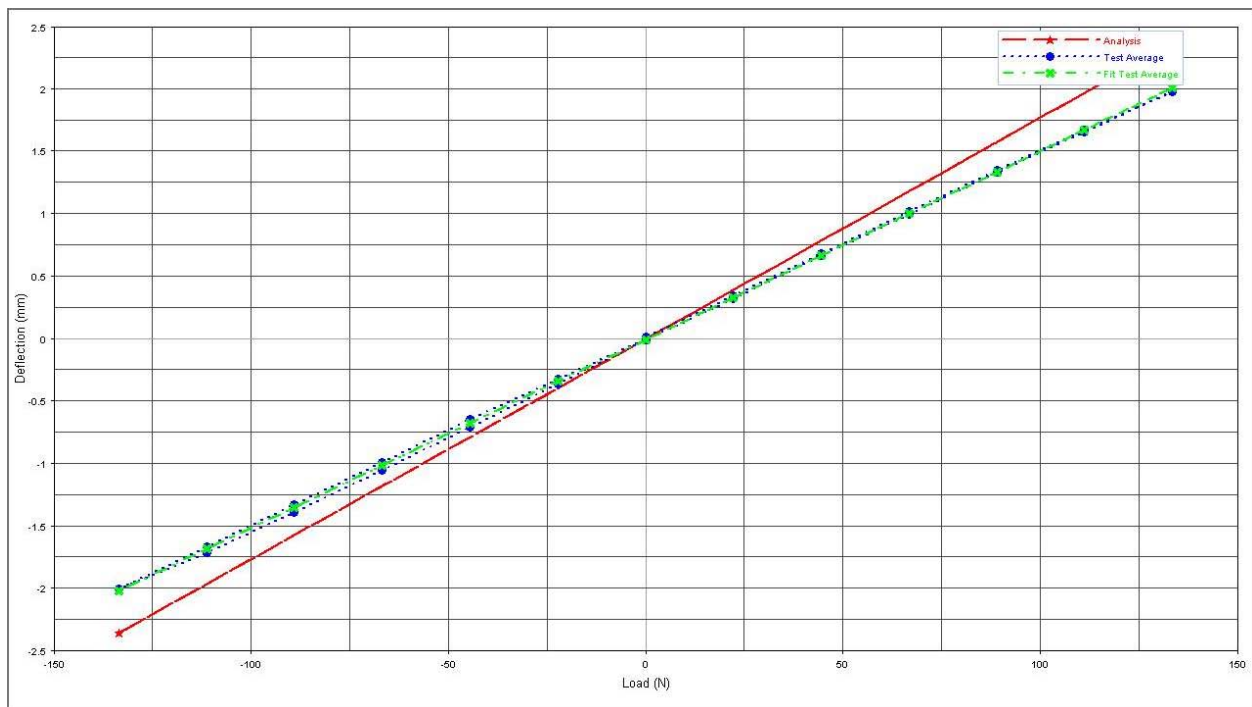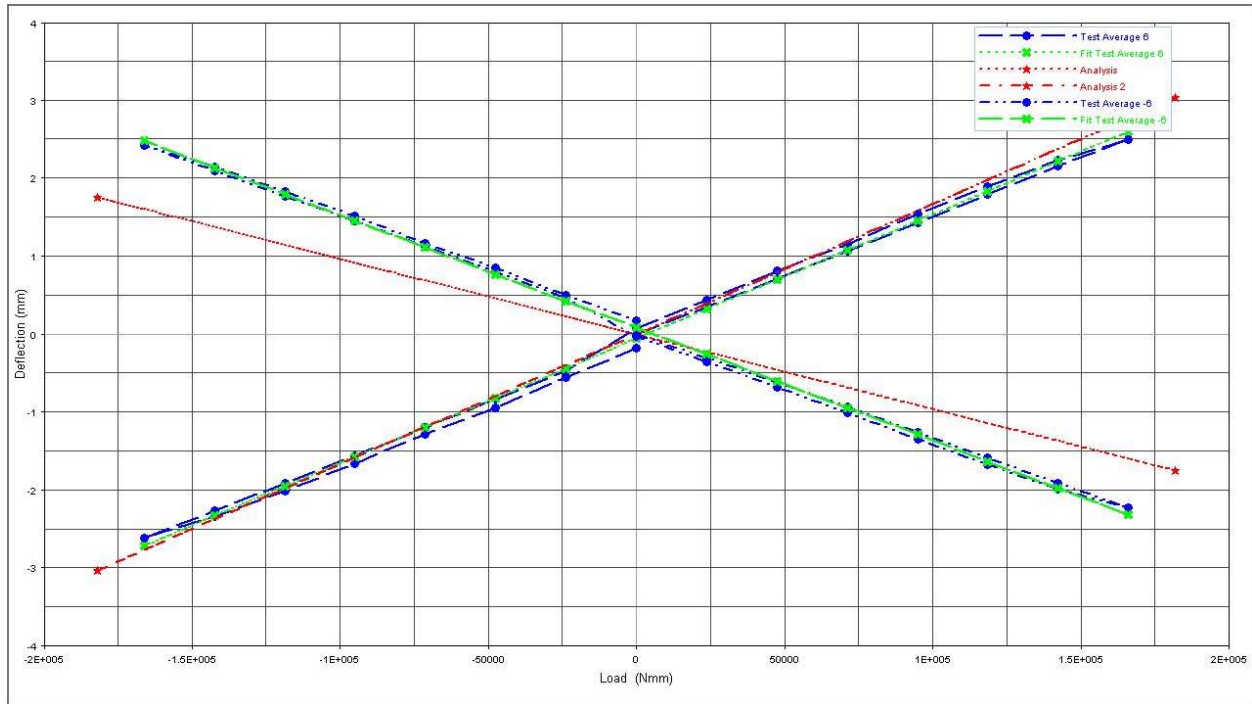Joint 4 Torsion Load Test vs. Analysis

APPENDIX C: TEST RESULTS
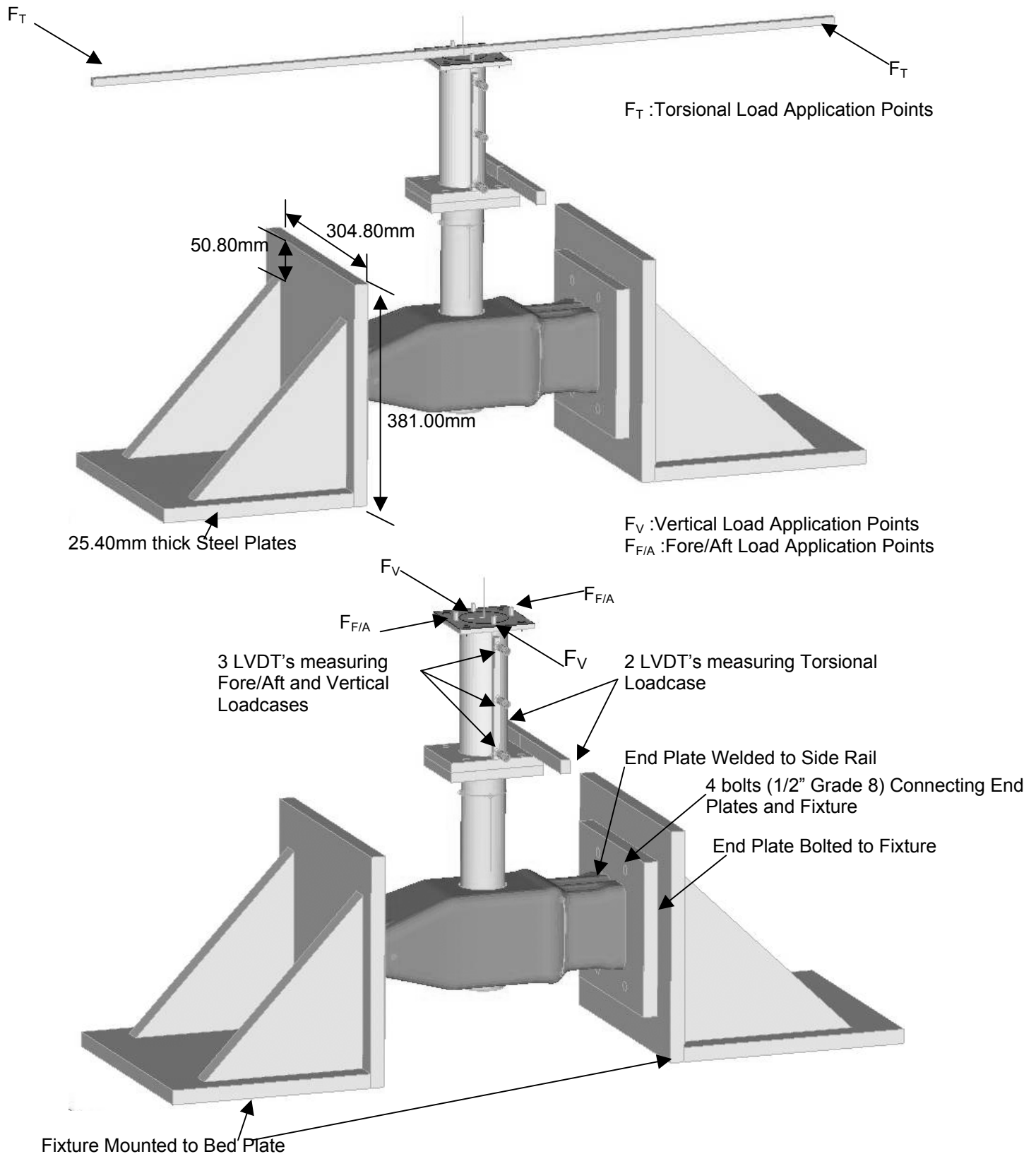

Joint 5 Fore/Aft Load Test vs. Analysis

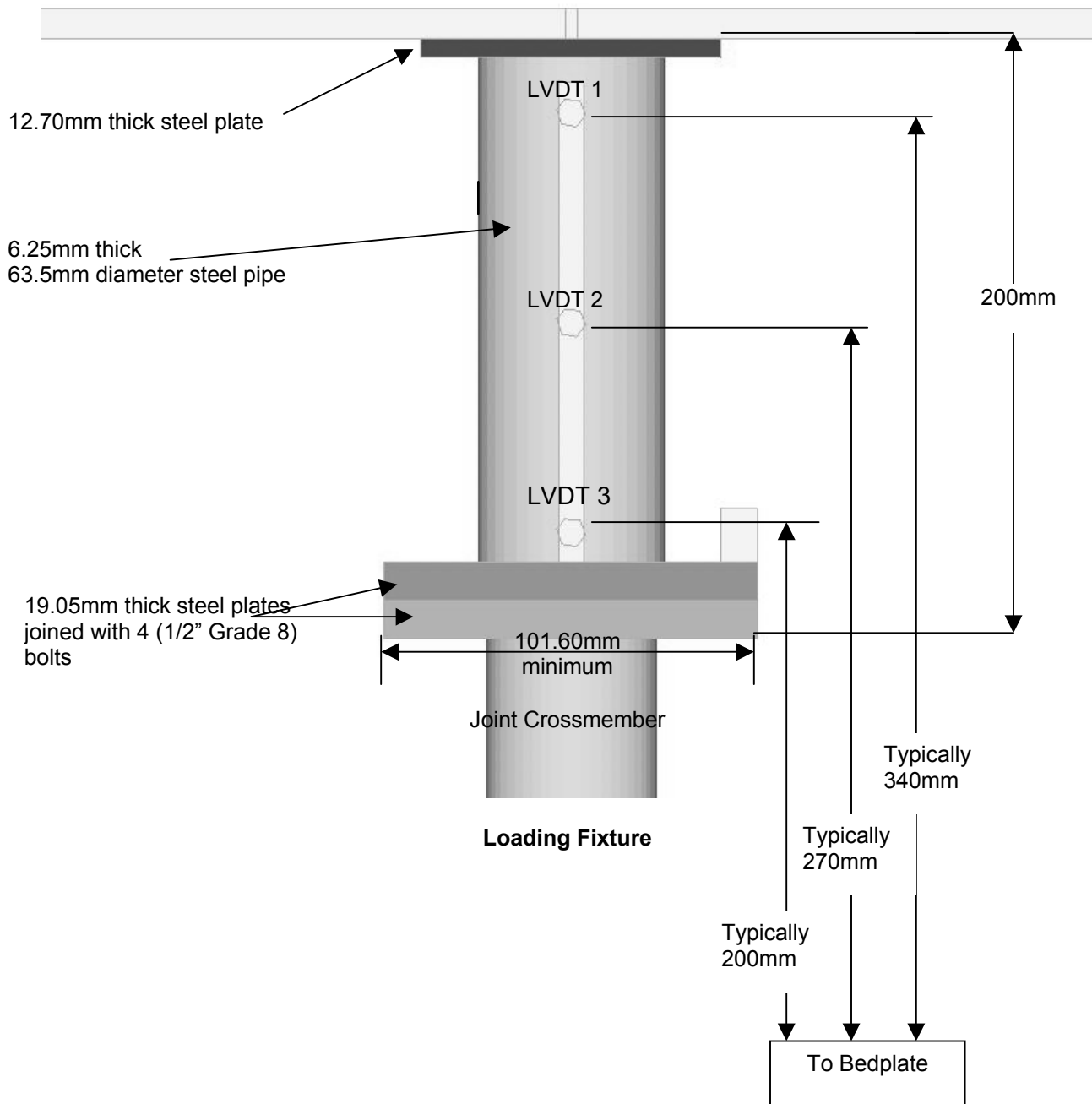Joint 5 Vertical Load Test vs. Analysis

APPENDIX C: TEST RESULTS

Joint 5 Torsion Load Test vs. Analysis

APPENDIX D: DIAGRAM OF JOINT IN TEST FIXTURE

F_T

F_T

F_T :Torsional Load Application Points

304.80mm

50.80mm

381.00mm

25.40mm thick Steel Plates

F_V :Vertical Load Application Points
$F_{F/A}$:Fore/Aft Load Application Points

F_V

$F_{F/A}$

$F_{F/A}$

F_V

3 LVDT's measuring Fore/Aft and Vertical Loadcases

2 LVDT's measuring Torsional Loadcase

End Plate Welded to Side Rail

4 bolts (1/2" Grade 8) Connecting End Plates and Fixture

End Plate Bolted to Fixture

Fixture Mounted to Bed Plate

APPENDIX D: DIAGRAM OF JOINT IN TEST FIXTURE

Loading Fixture with Fore/Aft and Vertical Loadcase LVDT Placement

12.70mm thick steel plate

LVDT 1

6.25mm thick
63.5mm diameter steel pipe

LVDT 2

200mm

LVDT 3

19.05mm thick steel plates
joined with 4 (1/2" Grade 8)
bolts

101.60mm
minimum

Joint Crossmember

Loading Fixture

Typically
340mm

Typically
270mm

Typically
200mm

To Bedplate

APPENDIX D: DIAGRAM OF JOINT IN TEST FIXTURE

Loading Fixture with Torsional Loadcase LVDT Placement

LVDT 1   152.4 mm   ₵   152.4mm   LVDT 3

LVDT 2
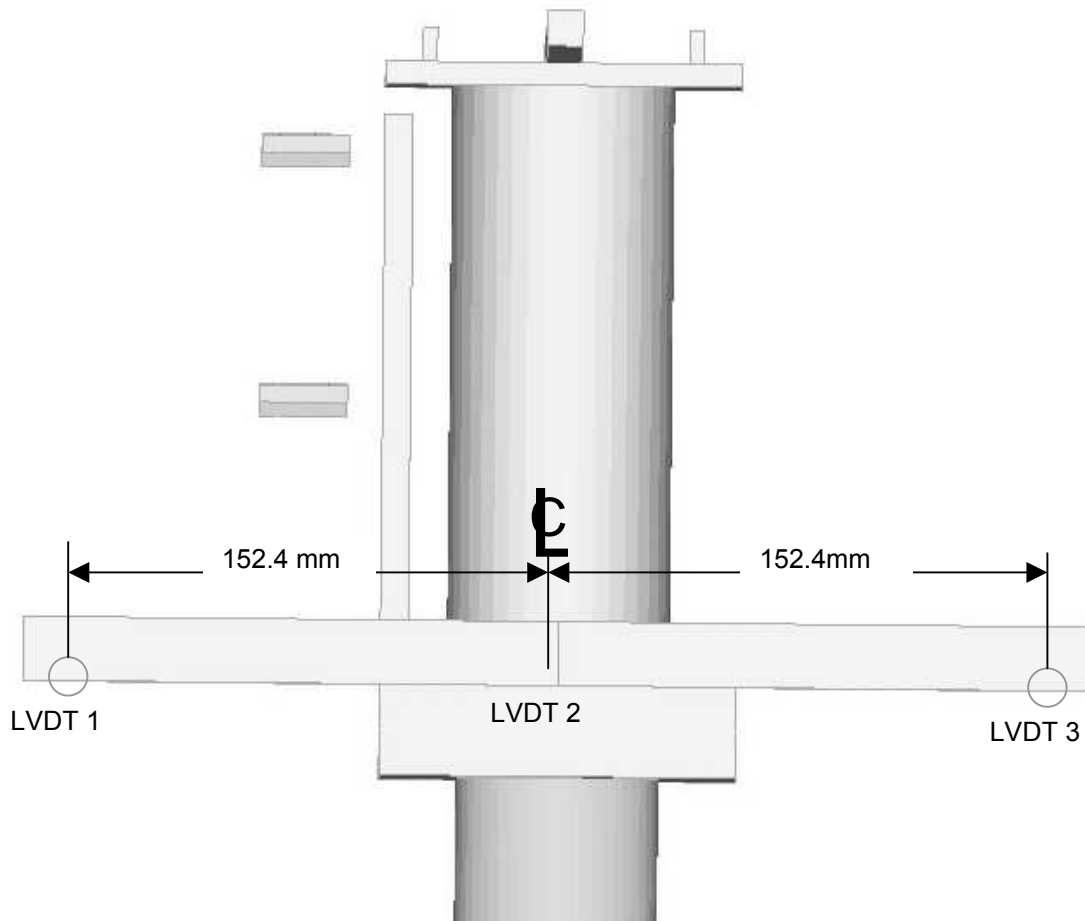
APPENDIX D: DIAGRAM OF JOINT IN TEST FIXTURE

Typical Test Setup of Vertical Load

Angle brackets mounted to bed plate

Test joint

Location of pneumatic cylinder for fore/aft loadcase
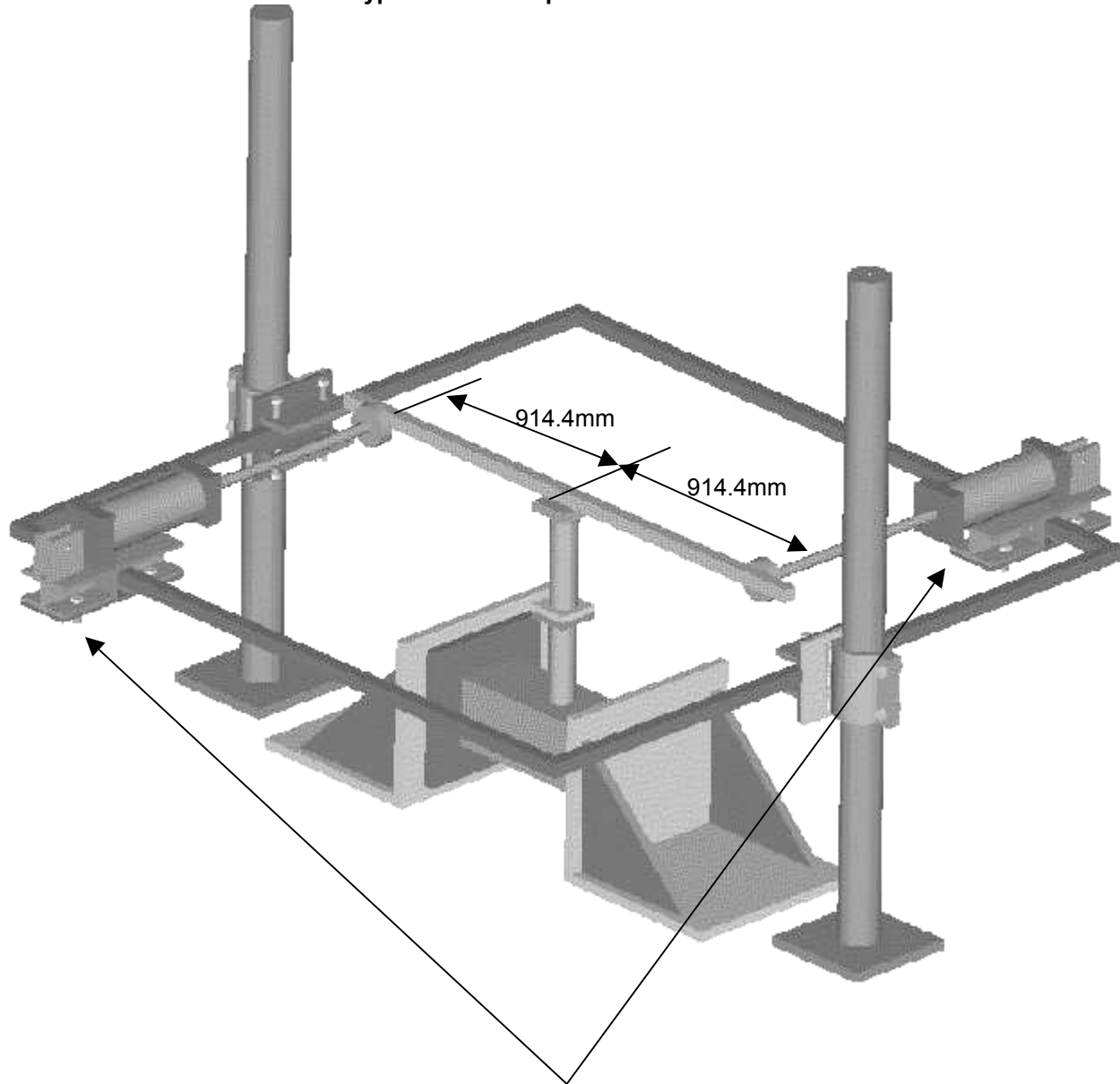
Pneumatic cylinder
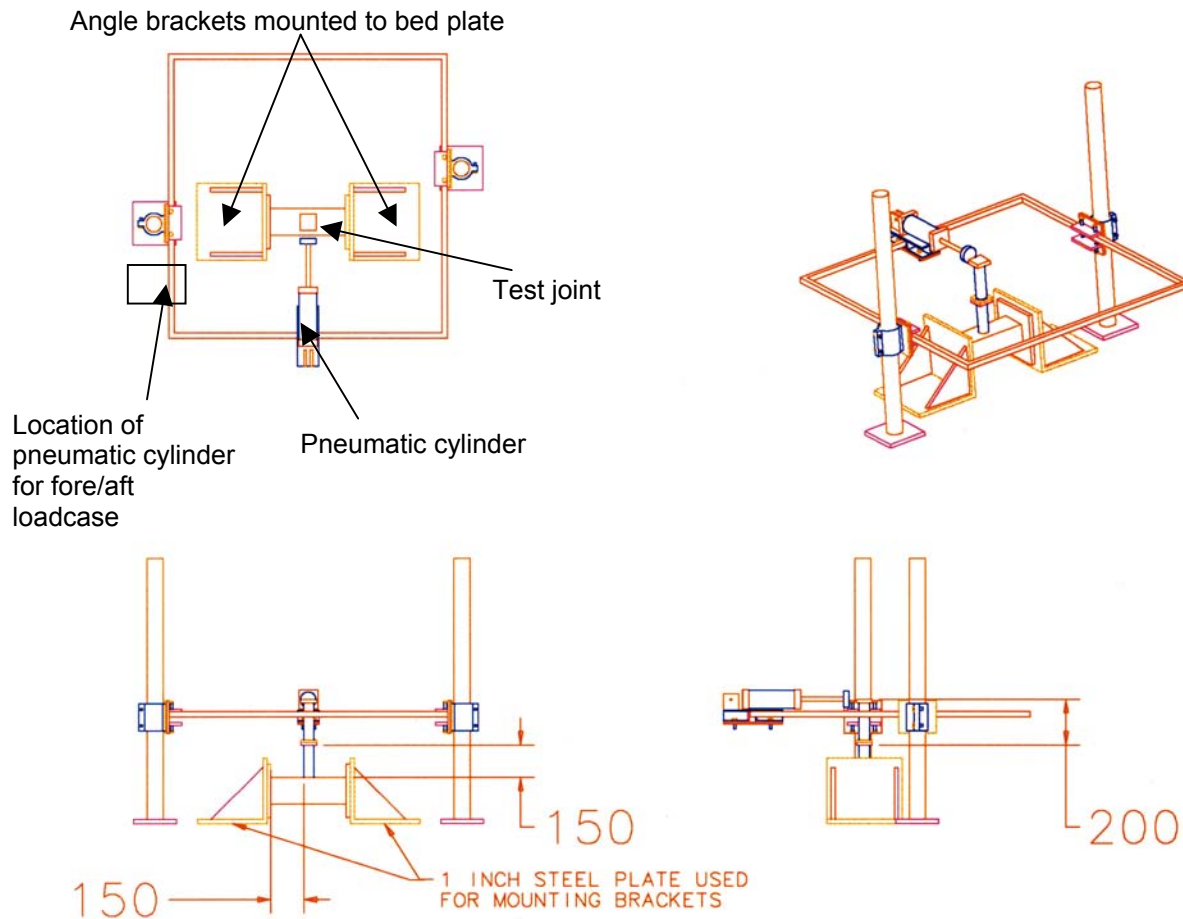
The fore/aft load would be similar with the pneumatic cylinder moved to the indicated location

APPENDIX D: DIAGRAM OF JOINT IN TEST FIXTURE

Typical Test Setup of Torsional Load

914.4mm

914.4mm

Pneumatic cylinders applying torsional load on joint